Myoblast Alignment and Fusion on Glyco-Biointerfaces with Micropatterned Geometries

プーサラ, ポーンティダ

https://doi.org/10.15017/1785445

出版情報：九州大学, 2016, 博士（農学）, 課程博士
バージョン：

Myoblast Alignment and Fusion on Glyco-Biointerfaces with Micropatterned Geometries

Pornthida Poosala

2016

Acknowledgments

This dissertation would not have been possible without the guidance and the help of several individuals who have in one way or another contributed and extended their valuable assistance in this complete study. First and foremost, I would like to express the deepest appreciation to my research supervisor, Professor Takuya Kitaoka for his constructive advice, serious direction and considerable encouragement throughout this work. Without his guidance and persistent help this dissertation would not have been possible. I also want to express my heartfelt thanks to Professor Takuya Kitaoka for his time and continuous support during the whole course of my work. At the same time, I wish to thank Associate Professor Hirofumi Ichinose for academic assistance and valuable opinions. I would also like to give my special thanks to Professor Yuji Tsutsumi for his critical reading of my PhD thesis.

I am also grateful to the Research Support Center, Research Center for Human Disease Modeling, Graduate School of Medical Sciences, Maidashi campus, Kyushu University for providing me many fruitful collaborations and for allowing me to use their machines.

Furthermore, my special thanks are due to all members of the Laboratory of Bioresources Chemistry, Kyushu University for their kind help and assistance. I owe my deepest gratitude to my friends who live in Fukuoka, Japan for all support and help to me. In addition, this thesis was partially supported by scholarship and contingencies from Japanese Government Monbukagakusho: MEXT International Doctor's program of Graduate School of Bioresource & Bioenvironmental Sciences for which I am very thankful. Finally, I owe my deepest gratitude to my family for their support in various aspects.

August, 2016

Pornthida Poosala

Abbreviations

AMPK	Adenosine monophosphate-activated protein kinase
BSA	Bovine serum albumin
C2C12	Mouse derived C2C12 myoblast cell
COSs	Chitooligosaccharides
DMEM	Dulbecco's modified Eagle's medium
DP	Degree of polymerization
ECM	Extracellular matrix
FAK	Focal adhesion kinase
FBS	Fetal bovine serum
GAPDH	Glyceraldehyde-3-phosphate dehydrogenase
GlcNAc	*N*-Acetyl-D-glucosamine
GlcNAc6	Chitohexaose
GlcNAc6-SAMs	Self-assembled monolayer of chitooligomers
GLUT4	Glucose transporter type 4
MRF	myogenic regulatory factors
MyoD	Myogenic differentiation 1
MyHC	Myosin heavy chain
PBS	Phosphate buffered saline
QCM	Quartz crystal microbalance
RhoA	Ras homolog gene family, member A

ROCK	Rho-associated protein kinase
RT-PCR	Real-time polymerase chain reaction
NMR	Nuclear magnetic resonance
NOS	Nitric oxide synthase
TCPS	Tissue culture polystyrene
TSC	Thiosemicarbazide
SAM	Self-assembly monolayer
XPS	X-ray photoelectron spectroscopy

List of Figures

List of Tables

Table of Contents

Chapter 2 Micropatterning and Cellular Alignment in Skeletal Muscle Cells 34

Chapter 3 Myoblasts fusion and Myotube Formation 70

Chapter 1

Chapter 1

Introduction

Glycobiology is fastly emerging as a primary field of interest in biomolecular and biomedical research. Once considered insignificant, glycans are intricately involved in many aspects of cellular processes and immunological systems, which open the possibility of exploiting them for therapeutic and diagnostic purposes. This alternative has given much attention due to its potential to regulate various physiological phenomena. In living systems, the complexity and heterogeneity of glycan structures serve as fundamental characteristics of glycoproteins, glycolipids, and other glycoconjugates, which are essential not only for supporting constituents of cell surfaces but also as ideal candidates for molecular recognition (Fig. 1-1). The diversity of these glycan has been shown to play pivotal roles in cellular recognition because of the high structural diversity of glycan chains. Their molecular diversity has given rise to an array of different derivatives, structures and characteristics through the specific structure of *N*- and *O*-linked carbohydrates, allowing to controls interesting aspects in biological functions. For instance, immune response and cell recognition, cell-cell interaction/signaling, cell adhesion mechanisms and including the modulation of cell–matrix interactions *via* carbohydrates-mediated protein interactions [1,2]. Furthermore, the complex glycan structures on cellular surfaces are capable of facilitating and response to inner or outer cellular environments, making them attractive new targets for interventions to treat pathological conditions in several diseases such as cancer, tumor progression and metastasis [3-8].

Recently, research and development tasks for carbohydrates are energetically being pushed forward. In particular, mono-/oligosaccharides have played crucial roles in *in vitro* applications as the predominant candidate for understanding biological phenomena *in vivo*. This is due to the fact that the structures of oligosaccharides and their monosaccharide constituents are found on cell

surface glycoproteins. As an example, the monosaccharide β-*N*-acetyl-glucosamine (*O*-GlcNAc) a potential regulator of cardiac metabolism through *O*-GlcNAcylation [9]. Others information suggest that oligomannose is responsible for regulating the efficiency in synapses in the adult brain and other neuropathological symptoms [10]. Moreover, the remodeling of cell membranes with complex polysaccharides such as glycosaminoglycans (GAGs) and heparan sulfate (HS) could provide a novel approach to control key cellular events in many aspects of stem cell biology and technology. For instance, engineered neurons which modified cell surfaces with specific sulfated glycosaminoglycans exhibited increased activation of neurotrophin-mediated signaling pathways and enhanced axonal growth [11]. Otherwise, heparan sulfate has been used as substrates to support the long-term propagation of multiple human embryonic stem cells (hES) and induced pluripotent stem cells (iPS) [12]. Based on research studies above, the functional biointerfaces of carbohydrates at cell interface that can promote a specific cell behavior is a promising way to study on how carbohydrates induce sustained effects on cellular signaling and function, which have an importance in a wide range of research fields, especially for bio-mimetic materials.

However, the scope of this thesis will be focused on the advanced concept of the combination of chitooligosaccharides (COSs) with tailored physical and *biofunctions* properties on micropatterns. COSs have a broad range of biological activities in various applications of the biomedical field due to its favorable biological properties, including its specific interaction with the extracellular matrix, resulting in the enhancement of cellular affinity, this represents a significant potential for biomolecular recognition processes [13-17]. The following section in this chapter will focus on the description of an overview of engineered biointerfaces in biomedical field, the relationship between cell and material that triggers cellular processes, the microtopographical features that were used in this study including fundamental characteristics of chitin and chitooligomers, are briefly discussed.

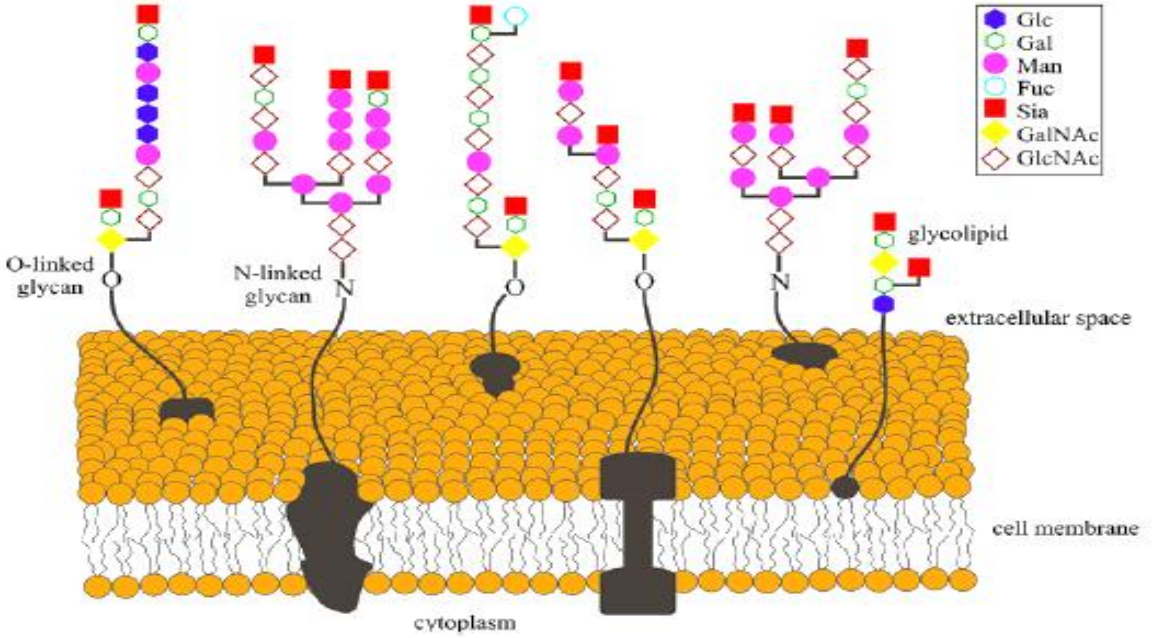

Fig. 1-1 Schematic illustration of carbohydrate heterogeneity found on a cell surface (Ghazarian, H.; Idoni, B.; Oppenheimer, S. B. A glycobiology review: Carbohydrates, lectins and implications in cancer therapeutics. *Acta Histochem.* **2011**, *113*, 236–247.)

1.1 Engineered biointerfaces in tissue engineering and regenerative medicine

Biointerfaces, boundary surfaces of cell membranes, have played essential roles in biological systems due to their unique interfacial properties having various influences on cell surfaces and cell environments which are surrounded by extracellular matrix (ECM). The extracellular matrix is a complex network of secreted proteins and polysaccharides, mainly produced and remodeled locally by the cells in the matrix as shown in Figure 1-2. The interactions of ECM components with cells are critical to the establishment and maintenance of tissues architecture in determining of cell shape during embryonic development [19,20]. *In vivo*, biointerfaces are closely involved in many aspects of biological phenomena, due to biomechanical properties of ECM enable to contribute the transmission intracellular signal transduction pathways to affect cell functions e.g. cell adhesion, cell–cell interaction, cell–cell singling and cellular recognition [21,22]. Many studies on biointerface materials for *in vivo* applications have been reported, but several problems still remain inconclusive in showing beneficial and safe uses in living systems because of biocompatibility. However, various research cases give various new ideas and concepts for studying biointerfaces in depth, in particular, focused on *in vitro* applications for biomedical engineering and regenerative medicine.

Regenerative medicine is a new field in science based on the combination of technology, stem cells engineering, and reconstructive surgery, aiming at the regeneration of natural and/or improved tissues [23]. A number of carbohydrate polymers have been used in tissue engineering and regenerative medicine applications because they have macromolecular properties similar to the ECM. They are hydrophilic polysaccharides that interact with cell surfaces *in vivo*, and thus they have been utilized as scaffolding materials [24]. Recently, the growing demand for using carbohydrates as a scaffold and the trend in smart biointerface materials have become increasingly popular for stem cell-based therapeutic applications. It has offered the possibility of exciting alternative treatments of current tissue engineering and regenerative medicine. For instance, artificial ECMs act as high-performance biomaterials for rebuilding skin tissues, bone remodeling, including heart and muscle regeneration (Fig. 1-2b). Besides, biomolecules (e.g. hormones, oligosaccharides, oligopeptides and oligonucleotides) embedded on these material surfaces could improve functional and interfacial properties. These interactions would be involved in dynamic attachment and detachment of cells cultured on material surfaces.

Furthermore, there is numerous literature published for appealing novel ideas that the interplay between physicochemical and biological features of either natural biopolymer or bioactive molecules motifs incorporation have also gained much attention in the field of tissue engineering. This is because it has been designed as a 3D scaffold which is composed of carbohydrate/carbohydrate, carbohydrate/protein or ideal bio-scaffold containing nanoparticles, resulting in the regulation of cell responses. For instance, cellulose-based nanocomposites can be used as scaffolds for vascular tissue engineering and skin regeneration [25,26]. Hybrid scaffolds of chitin/gelatin revealed potential ability to control mechanical properties for specific loading-bearing musculoskeletal tissues [27]. Hyaluronan and its derivatives can regulate the biological processes by mediating with cell surface receptors (e.g. CD44, RHAMM, ICAM-1), to enhance tissue growth and repair [28]. Or demonstrating the possibility of propagating human pluripotent stem cells and modulating cell adhesion as well as cell fate on material substrates through glycosaminoglycans (GAGs), which represents as carbohydrate-based stem cell markers [29,30]. Besides, monosaccharides such as ManNAc and neuraminic acid, have been increasingly used in neural tissue engineering, especially in nerve regrowth and spinal cord regeneration [31-33]. These findings suggested that glycan can provide an appropriate manner in many aspects of stem cell biology, coupled with increasing evidence that regulates cell fate and enhances the rate of tissue regeneration. Therefore, the biofunctional design of biointerfaces would provide a good promising way to breakthrough this critical situation of biomedical engineering and regenerative medicine, aiming at the *in vitro* applications of the biomimetic interactions between cultured cells and material surfaces [34-36].

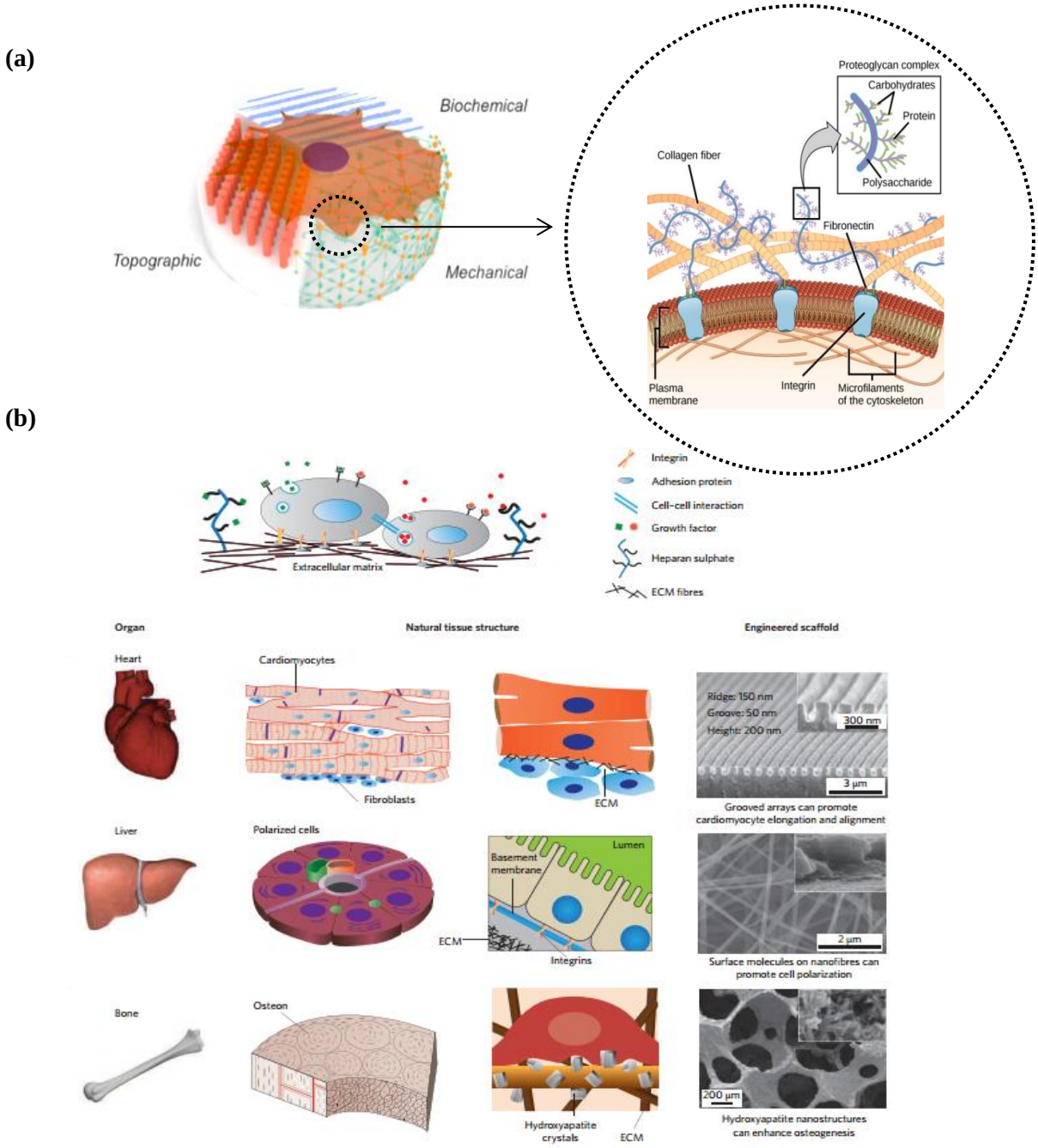

Fig. 1-2 Schematic illustration of extracellular matrix and the information provided to cells by the extracellular matrix (ECM). **a)** ECM fibers provide cells with topographical features that trigger morphogenesis. **b)** Illustrations of the cell/matrix interaction on ECM scaffold. (Ventre, M.; Netti, P. A. Engineering Cell Instructive Materials To Control Cell Fate and Functions through Material Cues and Surface Patterning. *ACS Appl. Mater. Interfaces* **2016**, acsami.5b08658)

1.2 Cell–material interactions

The nature of cell adhesion to substrate materials has a tremendous effect on cell function and tissue development, as it plays an integral role in cell communication and regulation by stimulating signals that regulate cell differentiation, cell cycle, cell migration, and cell survival [38]. In the field of tissue engineering, the understanding how cells interact and coordinate their behaviors on material surface is a crucial consideration of achieving in biomaterial design and development. In addition, the surface chemistry and topography of the material have also been shown to exhibit extraordinary effects on cell behavior [39,40]. Substrate stiffness is an example, plays an essential role in the regulation of cell function and gene expression through a variety of anchorage-dependent cells [41-44]. A vast amount of studies have shown that mammalian cells establish and maintain adhesive contacts with extracellular structures and adjacent cells through several types of adhesion receptors that are displayed on the cell surface. The process in which cells attach to a substrate can be described in 3 steps. Initially, adhesion receptors are assembled into clusters, then these transmembrane receptors are often linked to cytoskeletal structures (e.g. actin filaments, microtubules) and both anchor the cellular skeleton to extracellular structures and mediate the transmission of mechanical forces. Thirdly, regulatory proteins (protein kinases) are associated with receptor clusters and are responsible for controlling cluster stability and initiating signaling events that regulate cell proliferation and other functions regarding the biological and developmental consequences of cell adaptation to mechanical perturbations [45,46]. Therefore, understanding the mechanotransduction in tissue cell adhesion appears as an important step in numerous fields. The summary of adhesion molecules and their signal mechanotransduction that are involved in the study of cell-material interactions will be described in the subsection as follows.

1.2.1 Integrin

Integrins are heterodimeric transmembrane receptors, consist of α and β subunit [47,48]. Integrins play a crucial role in mediating cell adhesion to various types of ECM protein. Clustering of integrins at the interface of cell membrane not only provides stronger anchorage to the surface but also regulates intracellular signal transduction cascades that ultimately control differentiation, proliferation, and survival [49,50]. For instance, in the presence of integrin-mediated adhesion in activation of the G1 phase of the cell cycle and the Rho-family small GTPases, a regulatory convergence node dictates cytoskeletal assembly and organization of actin polymerization through

clustering of activated forms of signaling proteins such as focal adhesion kinase (FAK) [51-53]. Besides, mediating stable adhesion, integrins also play a crucial role in cellular motility by anchoring the actin cytoskeleton to the ECM in cell-matrix adhesions and regulate the expression of genes related to cell differentiation [54].

1.2.2 Focal adhesion

Focal adhesion is generally located near the periphery of the cell. Focal adhesions have been extensively studied in cultured cells because of its activity that enables to regulate cell adhesion. Generally, as sites of attachment between the cell and ECM, focal adhesions started binding to integrins, leading to the assembly of proteins on the intracellular side and subsequent building up a signaling complex to generate stress fibers in the cell. These stress fibers turn to promote bundles of actin filaments (Fig. 1-3).

The components of focal adhesions are diverse and include scaffolding molecules, GTPases, and enzymes such as kinases. Interestingly, the differences in specific type function of focal adhesion are dependent on a signaling cascade that involved in the RhoA small GTPase and the levels of protein components which induced assembly of focal adhesion [55]. For instance, focal complexes or small focal adhesions, are often regulated by Rac and Cdc42, and have been associated with cell migration [56] whereas maturation of adhesion structures is more likely to be found in cytoskeletal in which regulate the assembly of actin filament bundles *via* Rho activity [57,58]. Furthermore, the contractile properties of various cell types are associated with individual types and biomechanical properties of focal adhesion, including substrate stiffness [59,60]. Cells on a more rigid substrate have shown more stable focal adhesion [61]. For example, smooth muscle cells were found to migrate toward and accumulated on the stiff regions of the substrate [62].

Moreover, it is noteworthy that myosin type 2, a family of ATP-dependent motor proteins, drives changes in focal adhesion morphology and composition in a maturation process that is crucial for regulating adhesion dynamics and signaling guiding cell adhesion, migration and fate [63]. Myosin type 2 plays a role in muscle contraction and involvement in a wide range of other motility processes [64]. Regarding the mechanism of myosin type 2 to form focal adhesion, myosin activity drives stress fiber assembly and enhanced tension force. Those tension forces directly trigger integrins on cell membranes which in turns provide some signals through the adhesion complex, subsequently promote focal adhesion [65-68]. (Fig. 1-4)

1.2.3 Integrin-ligand binding and signal transduction

Integrin-ligand binding regarding the effects of cell-substrate interaction is influenced by various ligand properties and material properties of substrate. Such interactions initiate signaling cascades that mainly controll cell behaviors. At the cell–ECM interface, cells sense the physical properties of ECM by translating mechanical forces and deformations into biochemical signals. Interestingly, the focal adhesion components act as mechanical transducing devices, replaying changes in intra- and extracellular tension into signaling pathways [71]. The mechanosensitive feedback modulates the intracellular signaling pathways, which are activated by integrin binding. Such interaction has recently been implicated as playing a role in ECM-dependent changes in various cellular functions [72,73]. The relationship between substrate or ligand properties and cell function is illustrated in Figure 1-5.

Cell Adhesion Phases	Phase I	Phase II	Phase III
Schematic diagram of cell adhesion	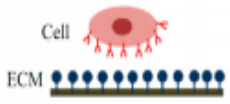	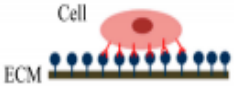	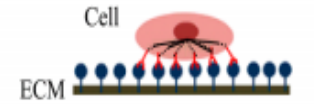
Schematic diagram of the transformation of cell shape	 Initial attachment	 Flattening	 Fully spreading and structural organization
Cell adhesion intervension	Electrostatic interaction	Integrin bonding	Focal adhesion
Adhesion stages	Sedimentation	Cell attachment	Cell spreading and stable adhesion

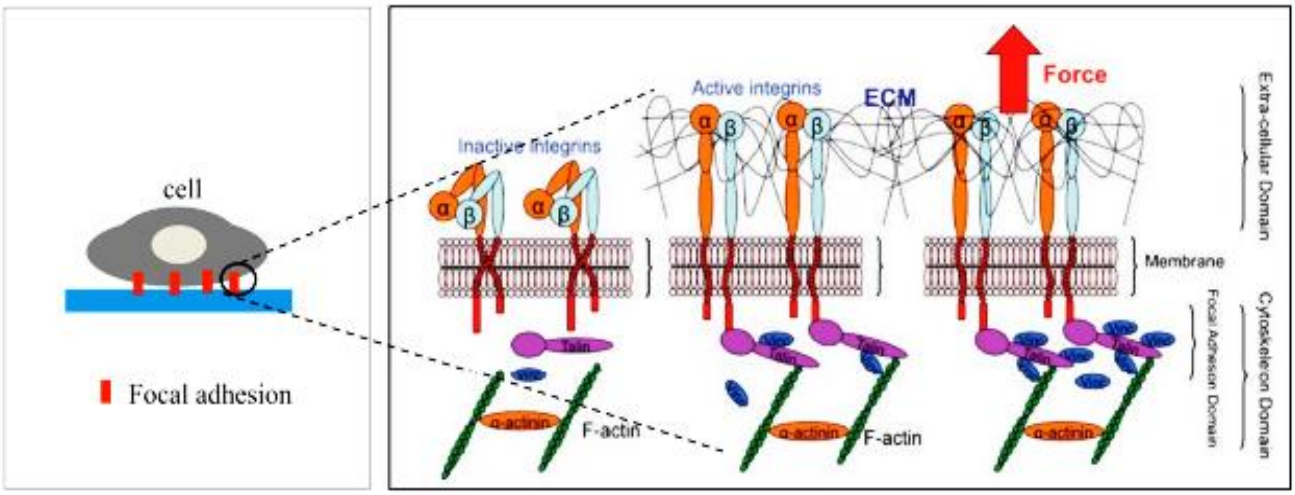

Fig. 1-3 Schematic representation of activated integrin and formation of ECM-integrin-cytoskeleton linkages in the focal adhesion site upon application of an external tensile load and evaluation in *in vitro* cell adhesion intervention and stages. (Khalili, A. A.; Ahmad, M. R. A Review of cell adhesion studies for biomedical and biological applications. *Int. J. Mol. Sci.* **2015**, *16*, 18149–18184.) and (Honarmandi, P.; Lee, H.; Lang, J. M.; Kamm, D. R. A microfluidic system with optical laser tweezers to study mechanotransduction and focal adhesion recruitment**.** *Lab Chip* **2011**, *11*, 684-694.)

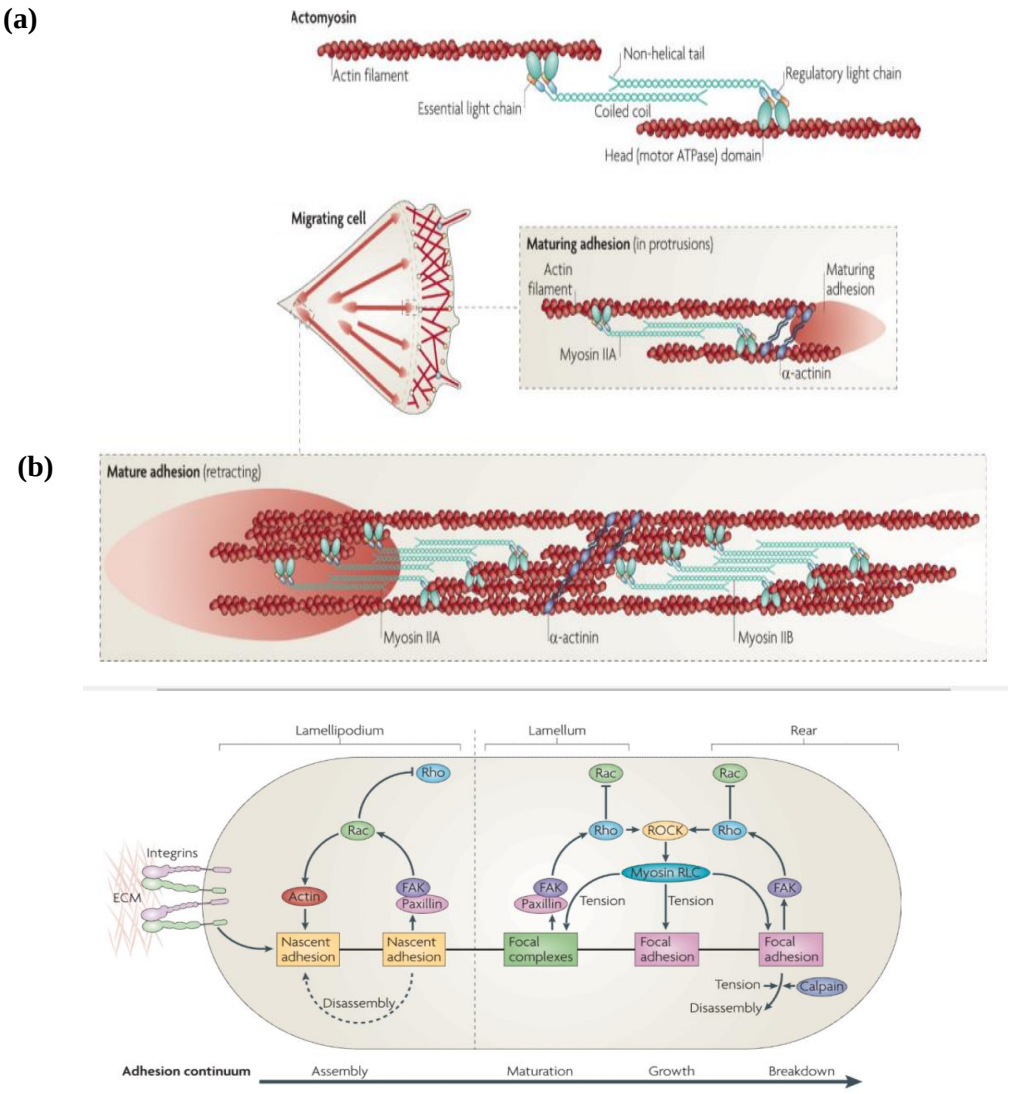

Fig. 1-4 Schematic illustration of myosin type 2 and the generation of adhesion maturation. **a)** Actin filaments cross-linked with myosin 2A. This leads to tension on the conformational sensitivity and clustering of adhesion molecules that are directly or indirectly associated with actin. **b)** Myosin type 2-generated tension sustains adhesion maturation by cross-linking and tension-induced conformational changes in various adhesion proteins. Adhesion maturation is accompanied by localized activation of Rho, perhaps through FAK-dependent recruitment of Rho pathway. Rho activation sustains the activation of myosin type 2 through the action of Rho-associated protein kinase (ROCK), which controls the kinases and phosphatases that regulate its regulatory light chain (RLC) phosphorylation. (Parsons, J. T.; Horwitz, A. R.; Schwartz, M. a Cell adhesion: integrating cytoskeletal dynamics and cellular tension. *Nat. Rev. Mol. Cell Biol.* **2010**, *11*, 633–643.)

1.2.4 Protein–glycan recognition

Glycan structures are known to be principal players in mediating the flow of information in cell–cell and cell–extracellular space communication. Recognition of glycoconjugates is informative factors responsible for cell development in multicellular organisms of the biological system. Those recognitions are frequently in the form of carbohydrate-protein interactions [75,76]. Carbohydrate–protein interactions are important for the initiation, maintenance and sustenance of a number of biological processes. Generally, these interactions are weak in affinities as compared to protein-protein interaction. This weak binding is unlikely to be of any biological significance, especially considering the high level of specificities with biological recognition processes. However, the low affinities are overcome through multivalent interactions, also known as cluster glycoside effect or multivalent effect, in which multiple copies of the ligands and receptors undergo sequential and/or simultaneous binding, resulting in increased binding affinity, which is required for biologically meaningful and potentially relevant in recognition process [77,78]. In this dissertation, glycoside clustering effect was the key factor to promote the cellular activities and responsiveness to the established micropatterns through carbohydrate-mediated specific recognition *via* receptors on the cell surface.

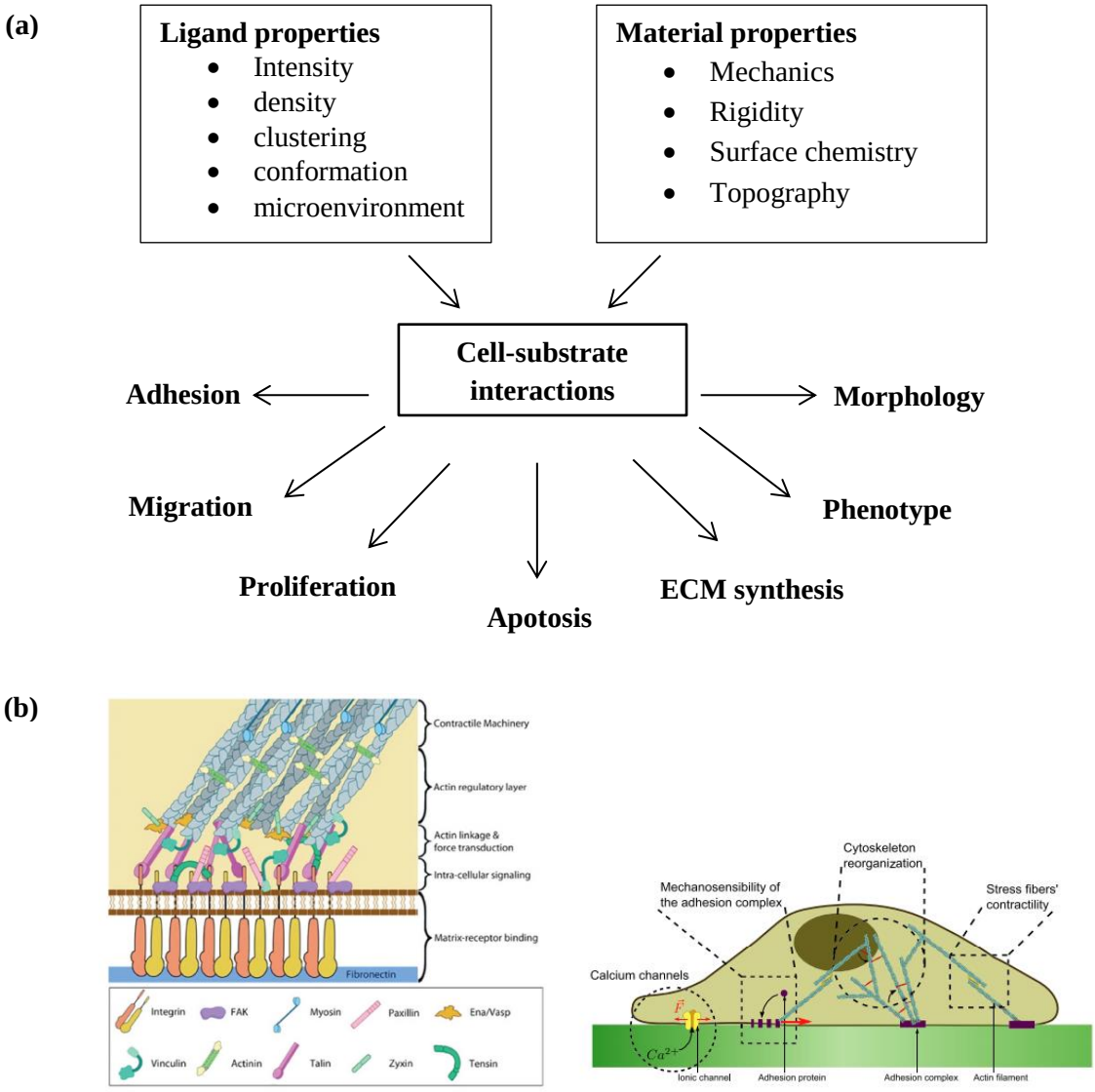

Fig. 1-5 Schematic representation of integrin-ligand binding regarding the effects of cell-substrate interaction. **a)** The interplay between ligand and material properties on cell behaviors. **b)** Schematic representation of focal adhesion (left) and the different mechanosensitive elements (right). Cells respond to the external stresses and applied stresses that modify internal signals through various mechanisms including assembly or disassembly of adhesion patches and actin remodeling. (Ladoux, B.; Nicolas, A. Physically based principles of cell adhesion mechanosensitivity in tissues. *Reports Prog. Phys.* **2012**, *75*, 116601.)

1.3 Microtopographical features

Currently, topographical features are being fabricated to mimic the tissue's native structural environment. Understanding the manner in which cells interact with their physical environment, it may be possible to control cellular behavior through the fabrication of substrates. In pursuit of understanding cell-material interactions, nano- and microfabrication technologies have been widely used to construct substrates [79]. Furthermore, these topographical features can be integrated with chemical stimuli to enhance manipulating cell behavior through cell–substrate interactions such as adhesion, morphology, migration, and differentiation [80-82]. In this section, some fabrication methods that have been used to fabricate carbohydrate patterns are presented.

1.3.1 Topography

Cells are capable of sensing topographic features in their surroundings. *In vivo*, cells are surrounded by the ECM which provids topographic, mechanical and biochemical stimuli at nano to micro scale. Topography is identified as a powerful tool to stimuli cell function, in particular, focusing on grooves and ridges. Cells react to ridges and grooves in the micrometer range largely by aligning along the structures, mediating through contact guidance [83]. Changes in substrate topographic and geometric features affect downstream cell behaviors such as adhesion, spreading, alignment, and migration, including cell survival and cell-cell interaction [84]. For example, increasing the surface roughness of topography has been shown to decrease proliferation of osteoblast whereas the proliferation of endothelial and smooth muscle cells is increased [85].

1.3.2 Self-assembled monolayer (SAMs)

General concepts of SAMs in various applications are rapidly growing. Accordingly, the designed SAMs provide unique characteristics, which tailor the interfacial properties of metals. The structures of SAMs are commonly ordered molecular assemblies that are formed by the spontaneous adsorption of organic molecules *via* specific affinities for transition metal surfaces [86]. There are a large number of articles reviewing various types of SAMs. However, alkanethiolates-SAMs have been a major used in term of the creation of synthetic biointerfaces that replicate chemical and physical aspects of the cellular microenvironment. Because, the formation of Au-S bonding on gold substrates through chemisorption of thiol groups exhibits strong intermolecular interactions, which allow rapid immobilization and stabilization of SAMs [87]. In addition, SAMs can be incorporated

with other biocomponents through chemical modifications, leading to fabricate the 2-dimensional (2D) or 3-dimensional (3D) nanoarchitectures on the substrates [88]. Hence, SAMs enable to be used as exceptional tools which provide an opportunity to gain a better understanding of interfacial phenomena, possibly leading to utilization in biological systems [89]. Especially, noteworthy is their abilities to probe molecular recognition at the interfaces and analysis of protein binding [90]. Oligo (ethylene glycol) alkanethiolate-SAMs have emerged as a predominant representative for the development and new investigation of biologically active ligands (peptides and carbohydrates) [91].

As mentioned before, self-assembled monolayers have very unique properties, which are widely used in the development of biological applications. The SAMs in living systems play significant roles in a wide variety of the biomolecular conformations. Recently, carbohydrate-terminated SAMs, protein-SAMs, and peptide-SAMs are increasingly becoming important for biological applications. The advantages of peptide building blocks for the formation of SAMs can be noticed toward several applications as biosensors, tissue engineering and the development of antibacterial agents, according to diverse nanostructures (nanotubes, nanospheres, nanofibrils, nanotapes) of short peptides.

In biological systems, self-assembled structures; the building blocks of peptide-SAMs, can be modified with a tripeptide recognition factor (RGD) which enhances cell regulation on ECMs [92]. Co-assembling peptide-SAMs, containing multiple ligands, can modulate human umbilical vein endothelial cells (HUVEC) behaviors [89]. Furthermore, the presence of ligands bound onto SAM surfaces represents an elegant study on dynamic SAMs, causing the selective releasing and attachment of chemical moieties on peptide motifs [93]. In addition, 3D scaffold of peptide-SAMs demonstrates that its structure can support the axonal regeneration of mouse neuronal cells and encapsulate living cells inside the 3D SAMs which have potentially been used over a wide range in biomedical applications [94].

On the other hand, carbohydrate-terminated SAMs have shown promising strong antifouling properties, which enable them to avoid nonspecific protein adsorption on material surfaces, leading to biomedical *in vivo* diagnostics and therapeutic applications [95]. Fyrnera et al. have proven that oligo (lactose)-based thiol SAMs showed higher protein fouling resistance than oligo (ethylene) glycols, a conventional polymer which is used as an excellent bio-inert polymer for resistance to cell attachment [96]. Therefore, these SAMs are not only to provide the design of biomimetic self-assembled monolayers for developing biological phenomena as cell proliferation but also to serve as essential carriers with efficient diagnosis functions, which are important in the field of biomedical.

1.4 Fundamental characteristics of chitin and chitooligomers

Chitin is the second most abundant natural biopolymer in the world after cellulose. The sources of chitin are found in a wide variety of species, not only in exoskeletons of arthropods (insects, arachnids, and crustaceans) but also in the internal structure of lower invertebrates (sponges, coelenterates, nematodes and mollusks) [97]. In addition, other potential sources for chitin production can be exploited from microorganisms, including the cell walls and structural membranes of fungi and bacteria as well as algae. In nature as structural polysaccharides, chitin has a resemblance to cellulose in chemical structure because of a linear homopolymer composed of a monosaccharide repeating unit. Cellulose is a linear β-(1–4)-linked polymer of D-glucopyranose units in the $^4C_1$ conformation. Chitin may be regarded as a cellulose derivative whose a 2-hydroxy group is substituted by an acetamido group, and thus the repeating unit is *N*-acetylglucosamine (GlcNAc). Chitin also has a β-1,4 glycosidic linkage. In addition, the different crystalline structures of chitin are well known in 3 categories, namely α-, β- and γ-forms. α-chitin form is generally the most abundant form found in nature, especially in crab and shrimp shells. This chitin structure shows an antiparallel chain packing, allowing the formation of numerous intra- and intermolecular hydrogen bonds, resulting in an immensely high tensile strength [97]. On the other hand, β-chitin form can be isolated from squid pens. The structure of β-chitin presents a parallel chain arrangement, resulting in loose packing structure which is more attractive in practical applications. Finally, the molecular conformation of γ-chitin is alternatively rearranged in both of antiparallel and parallel chains

1.4.1 Biological applications of chitin

Over past decades, the utilization of chitin has made a remarkable contribution to various applications from food processing to the medical and pharmaceutical industries in fields such as cosmetics, foods, supplements, textiles, membranes, films, binders, wound dressings and artificial implant materials have been marketed. Chitin has increasingly focused on its particular aspects for biomedical purposes due to its non-toxic, biodegradable and biocompatible properties. Acetylamino groups of chitin molecules have promising advantages for biological functions. Hence, it can serve as a potential candidate for practical applications in tissue engineering, biosensing and drug delivery systems [98,99]. For example, chitin-based scaffold materials promote versatile biological functions such as cell adhesion and cell migration. With an intriguing structure as a rigid scaffold material,

this excellent architecture appears to have great potential to be used in bone tissue engineering because of the strength, stability and rigidity. The interests in these unique mechanical and physical properties provide an ideal environment to fabricate biomimetic architectures such as ECMs which are found in native tissues *in vivo.*

Furthermore, chitin has been shown to accelerate healing and exhibit both greater biocompatibility *in vivo* and cytocompatibility *in vitro* [100]. Based on these properties, chitin is a great candidate material to be used as wound dressings. Khor and coworkers have reported that the utilization of chitin scaffolds can enhance the re-epithelialization during the proliferative phase in wound healing process, including diminished innate inflammatory responses as compared to that on of any commercial polyurethane-based film dressings [101]. In addition, many researches have focused on developing new antimicrobial materials to cure skin wounds, through the therapeutic intervention using noble metal nanoparticles/chitin composite scaffolds [102]. The advantage of chitin utilization, as previously mentioned is to be applied through specific recognition with various biomolecules, possibly available for a wide range of biomedical applications such as biosensors and drug delivery vehicles [103,104].

1.4.2 Chitooligomer and its derivatives

Chitooligosaccharides (COSs) can be obtained by polymer scission of long-chain chitin through several integrated techniques such as hydrolytic and enzymatic reactions. The degree of polymerization (DP) of COSs typically ranges from two to seven repeating units, which represent an interesting biological concept. However, deep understanding of the biological properties of chitooligomers has been insufficiently reported so far. Hence, many researchers have devoted themselves to studies on its biological effects. Recently, chitooligomers have been receiving increasing attention for medical applications due to their excellent biocompatibility. A large amount of literature has been published for chitin derivatives that enhance protective immunity against tumor metastasis in breast cancer, possibly *via* the inhibition of cancer-associated marker protein [105]. In addition, it is also applicable for improving therapeutic strategies in drug delivery systems such as anticancer drug carrier [106]. Furthermore, the modification of GlcNAc *via* β-*O*-linkage has an influence on myocardial cells, which are often used for the preliminary investigation of cardiac dysfunction [107,108]. Also, the nano-scale density of COSs chains clustered on a substrate can regulate cell behavior and responsiveness [109]. These beneficial advantages have been

partially attributed to biointerface functions, and would increase crucial understanding for cell regulation in *in vitro* applications.

Dissertation Overview

The overarching theme of this thesis is investigating how artificially-designed glyco-biointerfaces with micropatterned geometries can guide cell behavior and regulate cell function of the mammalian cell. In this dissertation, mouse-derived myoblast cells line C2C12 has been used to study cell alignment and cell fusion during myogenesis in skeletal muscle development.

Alignment is an important prerequisite for two- and three-dimensional cellular organization in various human tissues and *in vitro* cell culture applications. Orientation of C2C12 cells has a strong influence on their differentiation *in vitro* into multinucleated myotubes and allows for the structural anisotropy that contributes to muscle tissue functions, such as stretching and contraction. However, the spatial arrangement of these cells is limited by physical factors when they are cultured on polystyrene dishes, a significant potential obstacle to promoting cellular alignment and specific biological functions. In addition, the differentiation of C2C12 cells and myotube maturation *in vitro* require switching from growth medium to differentiation medium in order to decrease growth factors and slow cell proliferation, resulting in withdrawal from the cell cycle. Nevertheless, serum-free culture has been required for tissue engineering, to avoid immune rejection for *in vitro* applications. Thus, myoblast fusion into functionally-distinct myotubes to form *in vitro* skeletal muscle constructs under differentiation serum-free conditions still remains a challenge.

In this study, I successfully arranged C2C12 cells along micropatterned gold strips on which chitohexaose (GlcNAc6) was deposited *via* a vectorial chain immobilization approach. Cultured myoblasts on GlcNAc6-fixed patterns demonstrated the efficiency of myoblast fusion without requiring horse serum or any differentiation medium during cell culture and myotubes-like characteristics were observed. The micropatterned self-assembled monolayer of GlcNAc6 (GlcNAc6-SAMs) were successfully fabricated by a chemoselective modification with thiosemicarbazide (TSC), which enabled S–Au chemisorption to form the SAMs on a gold substrate in striped micropatterns. Two-dimensional flatted micropatterns were designed with a variety of different geometries (200, 500 and 1000 μm in width) using template mask and ion sputtering technique. Unidirectional alignment of C2C12 cells having GlcNAc6 receptors was clearly observed along the micropatterns at 7 day after culture, while those on the non-patterned surface exhibited a random orientation, indicating that the cultured cells had a flat morphology and irregular shapes on tissue culture polystyrene plates (TCPS) and GlcNAc6-free patterns. Decreasing striped pattern width increased cell attachment and proliferation, suggesting that the fixed GlcNAc6 and

micropatterns impacted cell growth behavior. I anticipated that such cellular alignment and drastic morphological alterations, possibly occurring through GlcNAc6-mediated receptors on myoblast surfaces, might offer a desirable microenvironment to drive downregulation *MyoD* prior to commitment to differentiated myoblast without requiring any differentiation medium. I found that reduced expression in *MyoD* caused by the upregulation of myogenin, which in turns myoblasts into multinucleated myotubes. The predominant effect was a stronger expression of *MyoD* and *myogenin* in C2C12 cells cultured on GlcNAc6-SAMs with certain patterns, particularly GlcNAc6-SAMs having a 500 μm in width. In addition, the role of focal adhesion kinase (FAK) mediates signals from integrins would play an important part in the initial activation of *MyoD* expression.

To further confirm these results, I examined the possible role of GlcNAc6 micropatterns in the behavior of C2C12 cells in early and late stage of myogenesis through mRNA expression of myosin heavy chain (MyHC) isoforms. MyHC plays important parts in several cellular processes that require force and translocation such as the major contractile proteins of cardiac and skeletal muscle. The difference in MyHC isoforms composition demonstrates three functionally distinct classes of fiber types (type 1, 2a and 2b). *MyHC* type 1 (*MyHC-1)* and *MyHC* type 2 (*MyHc-2*) have a fundamental role in processes that require cellular reshaping and movement, such as cell adhesion, cell migration and cell division, during skeletal muscle development and differentiation. Furthermore, they are dispensable for the assembly and disassembly of nascent adhesions where are connected to the actin cytoskeleton [110-112]. The role of *MyHc-2a* and *MyHc-2b* in modulating cell behavior and functions remains unclear and their mechanisms are not yet completely understood. However, there is a possibility that *MyHc-2* is associated with downstream effectors of numerous signaling pathways. Herein, the expression levels of *MyHc-2a* on all GlcNAc6-SAM patterns increased between day 3 and 5 of cell culture by eight-fold on GlcNAc6-SAM with narrow patterns and by five-fold on the wide pattern. Conversely, we observed no changes in the mRNA expression level of *MyHC-2b*. However, there was a slight increase in *MyHC-1* expression on the narrow pattern (200 μm) and wide pattern (1000 μm). These results suggest that cultured myoblasts on GlcNAc6-SAM patterns underwent differentiation with complicated changes in morphology and were subsequently able to drastically transform. Interestingly, the initial stage of myoblast-induced cell fusion seems likely to depend on *MyHc-2a* gene expression. The expression level of *MyHC-1* on the wider pattern (1000 μm) was higher than that on the narrow patterns between day 5 and 7 of cell culture; however, the level of *MyHC-2b* expression did not significantly change during myoblast development. Conversely, the narrow patterns showed higher expression of *MyHC-2b* and

consistently altered in the expression levels of both *MyHC* type 2 isoforms. In contrast to those muscle regulatory genes and *MyHCs*, *FAK* expression was not significantly affected by clustered carbohydrates or geometric patterns.

To compare the morphological changes of myotubes in the late stage of muscle differentiation, herein, myoblasts were cultured in differentiation serum-free and differentiation serum-containing media. Immunostaining at day 7 confirmed that the myoblasts were completely transformed into myotubes by fusion on GlcNAc6-SAM patterns under differentiation serum-free conditions, showing the long and thin appearance of myotubes. By contrast, control TCPS substrate promoted thicker myotubes with numerous branched structures when compared to those of GlcNAc6-SAM patterns. This indicated that more mature myotubes were found on the control substrate, due to the effect of differentiation media. However, these results revealed that GlcNAc6 oligomer-fixed geometries enhanced the fusion efficiency of myoblasts and greatly influenced the regulation of myotube formation without requiring any differentiation medium during cell culture, eventually leading to muscle contraction.

In addition, the main text of thesis will be divided into 6 parts. The chapter 1 will give a brief overview of trends of engineered biointerfaces in tissue engineering and briefly the fundamental characteristics of chitooligomers. Morphology and characterizations of the self-assembled monolayer of chitooligomer (GlcNAc6-SAMs) patterns such as the elemental analysis of the carbohydrate-functionalized on gold substrates were performed using X-ray photoelectron spectroscopy (XPS), quantitation of sugar density on gold substrate by quartz crystal microbalance (QCM) analysis will be discussed in chapter 2, including the influence of carbohydrate-functionalized surface geometries on the alignment and proliferation of C2C12 myoblast cells. Chapter 3 demonstrates the effect of GlcNAc6-SAM micropatterned substrates on gene expression in C2C12 cells during early and late stage of myogenesis using real-time polymerase chain reaction (RT-PCR). Two muscle-specific genes in a member of the muscle regulatory factor gene family (MRF), *MyoD* and *myogenin*, as well as myosin heavy chains were chosen. The biological characterizations of cultured C2C12 cells on GlcNAc6-SAMs and the efficiency of myoblast fusion to form multinucleated myotube without requiring any differentiation medium were included in this chapter. Chapter 4 presents the correlation between activation of Rho signaling pathway and parallel orientation of actin filaments in cultured myoblasts on GlcNAc6-SAMs patterns. Rho family plays crucial roles in the regulation of a wide range of cellular processes and the activation of downstream kinases, which make an impact on cellular mechanisms. In addition to the

aforementioned effects, the Rho activation would consequently have been introduced with the contractile activity of cells through contraction-stimulated glucose uptake. Therefore, the presences of spontaneous contractile activity in cultured myotubes on GlcNAc6-SAMs patterns will be described in chapter 5. The confirmation of these contractions could be investigated through glucose transporter type 4 (GLUT4) mRNA expression and glucose uptake. The general conclusion in chapter 6 will summarize the main findings from this work and suggestion for further investigations will also be addressed in order to improve a better understanding of how glyco-biointerfaces regulate the mammalian cell function.

References

1. Kleene, R.; Schachner, M. Glycans and neural cell interactions. *Nat. Rev. Neurosci.* **2004**, *5*, 195–208.
2. Fyrner, T.; Lee, H. H.; Mangone, A.; Ekblad, T.; Pettitt, M. E.; Callow, M. E.; Callow, J. A.; Conlan, S. L.; Mutton, R.; Clare, A. S.; Konradsson, P.; Liedberg, B.; Ederth, T. Saccharide-functionalized alkanethiols for fouling-resistant self-assembled monolayers: Synthesis, monolayer properties, and antifouling behavior. *Langmuir* **2011**, *27*, 15034–15047.
3. Rabinovich, G. A.; van Kooyk, Y.; Cobb, B. A. Glycobiology of immune responses. *Ann. N. Y. Acad. Sci.* **2012**, *1253*, 1–15.
4. Rademacher, T. W.; Parekh, R. B.; Dwek, R. A. Glycobiology. *Annu Rev Biochem.* **1988**, *57*, 785-838
5. Tateno, H.; Uchiyama, N.; Kuno, A.; Togayachi, A.; Sato, T.; Narimatsu, H.; Hirabayashi, J. A novel strategy for mammalian cell surface glycome profiling using lectin microarray. *Glycobiology* **2007**, *17*, 1138–1146.
6. Priatel, J. J.; Chui, D.; Hiraoka, N.; Simmons, C. J.; Richardson, K. B.; Page, D. M.; Fukuda, M.; Varki, N. M.; Marth, J. D. The ST3Gal-I sialyltransferase controls CD8+ T lymphocyte homeostasis by modulating O-glycan biosynthesis. *Immunity* **2000**, *12*, 273–283.
7. Lau, K. S.; Dennis, J. W. N-Glycans in cancer progression. *Glycobiology* **2008**, *18*, 750–760.
8. Dennis, J. W.; Granovsky, M.; Warren, C. E. Glycoprotein glycosylation and cancer progression. *Biochim. Biophys. Acta - Gen. Subj.* **1999**, *1473*, 21–34.
9. Darley-Usmar, V. M.; Ball, L. E.; Chatham, J. C. Protein O-linked ß-N-acetylglucosamine: A novel effector of cardiomyocyte metabolism and function. *J Mol Cell Cardiol.* **2012**, *52*, 538–549.
10. Matus, A.; De Petris, S.; Raff, M. C. Mobility of concanavalin A receptors in myelin and synaptic membranes. *Nature New Biol.* **1973**, *244*, 278–280.
11. Pulsipher, A.; Griffin, M. E.; Stone, S. E.; Brown, J. M.; Hsieh-Wilson, L. C. Directing Neuronal Signaling through Cell-Surface Glycan Engineering. *J. Am. Chem. Soc.* **2014**, *136*, 6794–6797.
12. Joseph, R. K.; Lingyin, L.; Paul, J. W.; Marian, S. P.; Kiessling, L. L. A defined

glycosaminoglycan-binding substratum for human pluripotent stem cells. **2010**, *7*, 989–994.

13. Gu, X.; Ding, F.; Yang, Y.; Liu, J. Construction of tissue engineered nerve grafts and their application in peripheral nerve regeneration. *Prog. Neurobiol.* **2011**, *93*, 204–230.
14. Freier, T.; Koh, H. S.; Kazazian, K.; Shoichet, M. S. Controlling cell adhesion and degradation of chitosan films by N-acetylation. *Biomaterials* **2005**, *26*, 5872–5878.
15. Hu, N.; Wu, H.; Xue, C.; Gong, Y.; Wu, J.; Xiao, Z.; Yang, Y.; Ding, F.; Gu, X. Long-term outcome of the repair of 50 mm long median nerve defects in rhesus monkeys with marrow mesenchymal stem cells-containing, chitosan-based tissue engineered nerve grafts. *Biomaterials* **2013**, *34*, 100–111.
16. Jiang, M.; Cheng, Q.; Su, W.; Wang, C.; Yang, Y.; Cao, Z.; Ding, F. The beneficial effect of chitooligosaccharides on cell behavior and function of primary schwann cells is accompanied by Up-regulation of adhesion proteins and neurotrophins. *Neurochem. Res.* **2014**, *39*, 2047–2057.
17. Sunasee, R.; Narain, R. Glycopolymers and Glyco-nanoparticles in Biomolecular Recognition Processes and Vaccine Development. *Macromol. Biosci.* **2013**, *13*, 9–27.
18. Ghazarian, H.; Idoni, B.; Oppenheimer, S. B. A glycobiology review: Carbohydrates, lectins and implications in cancer therapeutics. *Acta Histochem.* **2011**, *113*, 236–247.
19. Rozario, T.; Desimone, D. W. The Extracellular Matrix In Development and Morphogenesis: A Dynamic View. *Dev Biol.* **2010**, *341*, 126–140.
20. Brown, N. H. Extracellular matrix in development: Insights from mechanisms conserved between invertebrates and vertebrates. *Cold Spring Harb. Perspect. Biol.* **2011**, *3*, 1–14.
21. Chen, S. S.; Fitzgerald, W.; Zimmerberg, J.; Kleinman, H. K.; Margolis, L. Cell-Cell and Cell-Extracellular Matrix Interactions Regulate Embryonic Stem Cell Differentiation. *Stem Cells* **2007**, *25*, 553–561.
22. Hansen, N. U. B.; Genovese, F.; Leeming, D. J.; Karsdal, M. A. The importance of extracellular matrix for cell function and in vivo likeness. *Exp. Mol. Pathol.* **2015**, *98*, 286–294.
23. Hosseinkhani, H.; Hong, P. Da; Yu, D. S. Self-assembled proteins and peptides for regenerative medicine. *Chem. Rev.* **2013**, *113*, 4837–4861.
24. Piskin, E. Biodegradable polymers in medicine. *Degradable polymers* **2002**, 343–355.
25. Pooyan, P.; Kim, I. T.; Jacob, K. I.; Tannenbaum, R.; Garmestani, H. Design of a cellulose-based nanocomposite as a potential polymeric scaffold in tissue engineering. *Polym. (United Kingdom)* **2013**, *54*, 2105–2114.

26. Raghavendra, G. M.; Jayaramudu, T.; Varaprasad, K.; Sadiku, R.; Ray, S. S.; Mohana Raju, K. Cellulose-polymer-Ag nanocomposite fibers for antibacterial fabrics/skin scaffolds. *Carbohydr. Polym.* **2013**, *93*, 553–560.
27. Sarem, M.; Moztarzadeh, F.; Mozafari, M. How can genipin assist gelatin/carbohydrate chitosan scaffolds to act as replacements of load-bearing soft tissues? *Carbohydr. Polym.* **2013**, *93*, 635–643.
28. Collins, M. N.; Birkinshaw, C. Hyaluronic acid based scaffolds for tissue engineering - A review. *Carbohydr. Polym.* **2013**, *92*, 1262–1279.
29. Du, J.; Yarema, K. J. Carbohydrate engineered cells for regenerative medicine. *Adv. Drug Deliv. Rev.* **2010**, *62*, 671–682.
30. Lutolf, M. P.; Hubbell, J. a Synthetic biomaterials as instructive extracellular microenvironments for morphogenesis in tissue engineering. *Nat. Biotechnol.* **2005**, *23*, 47–55.
31. Srinivasa-Gopalan, S.; Adrienne, L.; Kevin, J. Y. Sialic acid and the central nervous system: Perspectives onbiological functions, detection, imaging methods and manipulation. *CNS Neurol Disord Drug Targets* **2006**, *5*, 425–440.
32. Büttner, B.; Kannicht, C.; Schmidt, C.; Löster, K.; Reutter, W.; Lee, H.-Y.; Nöhring, S.; Horstkorte, R. Biochemical engineering of cell surface sialic acids stimulates axonal growth. *J. Neurosci.* **2002**, *22*, 8869–8875.
33. Collins, B. E.; Fralich, T. J.; Itonori, S.; Ichikawa, Y.; Schnaar, R. L. Conversion of cellular sialic acid expression from N-acetyl- to N-glycolylneuraminic acid using a synthetic precursor, N-glycolylmannosamine pentaacetate: inhibition of myelin-associated glycoprotein binding to neural cells. *Glycobiology* **2000**, *10*, 11–20.
34. Sun, T.; Qing, G.; Su, B.; Jiang, L. Functional biointerface materials inspired from nature. *Chem. Soc. Rev.* **2011**, *40*, 2909–2921.
35. Langer, R.; Tirrell, D. a Designing materials for biology and medicine. *Nature* **2004**, *428*, 487–492.
36. Shmulewitz, A.; Langer, R.; Patton, J. Convergence in biomedical technology. *Nat. Biotechnol.* **2006**, *24*, 277–277.
37. Ventre, M.; Netti, P. A. Engineering Cell Instructive Materials To Control Cell Fate and Functions through Material Cues and Surface Patterning. *ACS Appl. Mater. Interfaces* **2016**, acsami.5b08658.
38. Huang, S.; Ingber, D. E. The structural and mechanical complexity of cell-growth control.

Nat. Cell Biol. **1999**, *1*, E131–8.

39. Flemming, R.; Murphy, C.; Abrams, G.; Goodman, S.; Nealey, P. Effects of synthetic micro-and nano-structured surfaces on cell behavior. *Biomaterials* **1999**, *20*, 573–588.
40. Curtis, A.; Wilkinson, C. Topographical control of cells. *Biomaterials* **1997**, *18*, 1573–1583.
41. Engler, A. J.; Griffin, M. A.; Sen, S.; Bnnemann, C. G.; Sweeney, H. L.; Discher, D. E. Myotubes differentiate optimally on substrates with tissue-like stiffness: Pathological implications for soft or stiff microenvironments. *J. Cell Biol.* **2004**, *166*, 877–887.
42. Kong, H. J.; Polte, T. R.; Alsberg, E.; Mooney, D. J. FRET measurements of cell-traction forces and nano-scale clustering of adhesion ligands varied by substrate stiffness. *Proc. Natl. Acad. Sci. U. S. A.* **2005**, *102*, 4300–4305.
43. Romer, L. H.; Birukov, K. G.; Garcia, J. G. N. Focal adhesions: Paradigm for a signaling nexus. *Circ. Res.* **2006**, *98*, 606–616.
44. Balaban, N. Q.; Schwarz, U. S.; Riveline, D.; Goichberg, P.; Tzur, G.; Sabanay, I.; Mahalu, D.; Safran, S.; Bershadsky, a; Addadi, L.; Geiger, B. Force and focal adhesion assembly: a close relationship studied using elastic micropatterned substrates. *Nat. Cell Biol.* **2001**, *3*, 466–472.
45. Wang, Y.-K.; Chen, C. S. Cell adhesion and mechanical stimulation in the regulation of mesenchymal stem cell differentiation. *J. Cell. Mol. Med.* **2013**, *17*, 823–832.
46. Lotfi, M.; Nejib, M.; Naceur, M. Cell Adhesion to Biomaterials : Concept of Biocompatibility. *Adv. Biomater. Sci. Biomed. Appl.* **2013**, 207–240.
47. Schwartz, M. A. Integrins and extracellular matrix in mechanotransduction. *Cold Spring Harb. Perspect. Biol.* **2010**, *2*, 1–13.
48. Giancotti, F. G.; Ruoslahti, E. Integrin Signaling. **1999**, *285*, 1028–1032.
49. Chen, Q.; Lin, T. H.; Der, C. J.; Juliano, R. L. Integrin mediated activation of mitogen activated protein (MAP) or extracellular signal related kinase kinase (MEK) and kinase is independent of Ras. *J.B.C.* **1996**, *271*, 18122–18127.
50. Renshaw, M. W.; Ren, X.-D.; Schwartz, M. A. Growth factor activation of MAP kinase requires cell adhesion. *EMBO J.* **1997**, *16*, 5592–5599.
51. Mettouchi, A.; Klein, S.; Guo, W.; Lopez-Lago, M.; Lemichez, E.; Westwick, J. K.; Giancotti, F. G. Integrin-specific activation of Rac controls progression through the G1 phase of the cell cycle. *Mol. Cell* **2001**, *8*, 115–127.
52. Danen, E. H. J.; Yamada, K. M. Fibronectin, integrins, and growth control. *J. Cell. Physiol.*

2001, *189*, 1–13.

53. Assoian, R. K.; Schwartz, M. A. Coordinate signaling by integrins and receptor tyrosine kinases in the regulation of G1 phase cell-cycle progression. *Curr. Opin. Genet. Dev.* **2001**, *11*, 48–53.
54. Menko, A. S.; Boettiger, D. Occupation of the extracellular matrix receptor, integrin, is a control point for myogenic differentiation. *Cell* **1987**, *51*, 51–57.
55. Wozniak, M. A.; Modzelewska, K.; Kwong, L.; Keely, P. J. Focal adhesion regulation of cell behavior. *Biochim. Biophys. Acta* **2004**, *1692*, 103–119.
56. Nobes, C. D.; Hall, a Rho, rac, and cdc42 GTPases regulate the assembly of multimolecular focal complexes associated with actin stress fibers, lamellipodia, and filopodia. *Cell* **1995**, *81*, 53–62.
57. Ridley, A. J.; Hall, A. The small GTP-binding protein rho regulates the assembly of focal adhesions and actin stress fibers in response to growth factors. *Cell* **1992**, *70*, 389–399.
58. Chrzanowska-Wodnicka, M.; Burridge, K. Rho-stimulated Contractiliry Drives the Formation of Stress Fibers and Focal Adhesions. *J. Cell Biol.* **1996**, *133*, 1403–1415.
59. Geiger, B.; Spatz, J. P.; Bershadsky, A. D. Environmental sensing through focal adhesions. *Nat. Rev. Mol. Cell Biol.* **2009**, *10*, 21–33.
60. Doyle, A. D.; Wang, F. W.; Matsumoto, K.; Yamada, K. M. One-dimensional topography underlies three-dimensional fi brillar cell migration. *J. Cell Biol.* **2009**, *184*, 481–490.
61. Lo, C. M.; Wang, H. B.; Dembo, M.; Wang, Y. L. Cell movement is guided by the rigidity of the substrate. *Biophys. J.* **2000**, *79*, 144–152.
62. Wong, J. Y.; Langer, R.; Ingber, D. E. Electrically conducting polymers can noninvasively control the shape and growth of mammalian cells. *Proc. Natl. Acad. Sci. U. S. A.* **1994**, *91*, 3201–3204.
63. Stricker, J.; Beckham, Y.; Davidson, M. W.; Gardel, M. L. Myosin II-Mediated Focal Adhesion Maturation Is Tension Insensitive. *PLoS One* **2013**, *8*, e70652.
64. Parsons, J. T.; Horwitz, A. R.; Schwartz, M. a Cell adhesion: integrating cytoskeletal dynamics and cellular tension. *Nat. Rev. Mol. Cell Biol.* **2010**, *11*, 633–643.
65. Puklin-Faucher, E.; Sheetz, M. P. The mechanical integrin cycle. *J Cell Sci* **2009**, *122*, 179–186.
66. Vicente-Manzanares, M.; Koach, M. A.; Whitmore, L.; Lamers, M. L.; Horwitz, A. F. Segregation and activation of myosin IIB creates a rear in migrating cells. *J. Cell Biol.* **2008**, *183*, 543–554.

67. Schwartz, M. a The Force Is with Us. *Science.* **2009**, *323*, 588–589.
68. Pasapera, A. M.; Schneider, I. C.; Rericha, E.; Schlaepfer, D. D.; Waterman, C. M. Myosin II activity regulates vinculin recruitment to focal adhesions through FAK-mediated paxillin phosphorylation. *J. Cell Biol.* **2010**, *188*, 877–890.
69. Khalili, A. A.; Ahmad, M. R. A Review of cell adhesion studies for biomedical and biological applications. *Int. J. Mol. Sci.* **2015**, *16*, 18149–18184.
70. Honarmandi, P.; Lee, H.; Lang, J. M.; Kamm, D. R. A microfluidic system with optical laser tweezers to study mechanotransduction and focal adhesion recruitment**.** *Lab Chip* **2011**, *11*, 684-694
71. Geiger, B.; Bershadsky, A.; Pankov, R.; Yamada, K. M. Transmembrane crosstalk between the extracellular matrix--cytoskeleton crosstalk. *Nat. Rev. Mol. Cell Biol.* **2001**, *2*, 793–805.
72. Riveline, D.; Zamir, E.; Balaban, N. Q.; Schwarz, U. S.; Ishizaki, T.; Narumiya, S.; Kam, Z.; Geiger, B.; Bershadsky, A. D. Focal contacts as mechanosensors: Externally applied local mechanical force induces growth of focal contacts by an mDia1-dependent and ROCK-independent mechanism. *J. Cell Biol.* **2001**, *153*, 1175–1185.
73. Giannone, G.; Dubin-Thaler, B. J.; D??bereiner, H. G.; Kieffer, N.; Bresnick, A. R.; Sheetz, M. P. Periodic lamellipodial contractions correlate with rearward actin waves. *Cell* **2004**, *116*, 431–443.
74. Ladoux, B.; Nicolas, A. Physically based principles of cell adhesion mechanosensitivity in tissues. *Reports Prog. Phys.* **2012**, *75*, 116601.
75. Lee, Y. Biochemistry of carbohydrate-protein interaction. *FASEB J. 1992, 6*, 3193–3200.
76. Schnaar, R. L. Glycans and glycan-binding proteins in immune regulation: A concise introduction to glycobiology for the allergist. *J. Allergy Clin. Immunol.* **2015**, *135*, 609–615.
77. Jayaraman, N.; Maiti, K.; Naresh, K. Multivalent glycoliposomes and micelles to study carbohydrate-protein and carbohydrate-carbohydrate interactions. *Chem. Soc. Rev.* **2013**, *42*, 4640–4656.
78. Jayaraman, N. Multivalent ligand presentation as a central concept to study intricate carbohydrate-protein interactions. *Chem. Soc. Rev.* **2009**, *38*, 3463–3483.
79. Nikkhah, M.; Edalat, F.; Manoucheri, S.; Khademhosseini, A. Engineering microscale topographies to control the cell-substrate interface. *Biomaterials* **2012**, *33*, 5230–5246.
80. Dent, E. W.; Gertler, F. B. Cytoskeletal Dynamics and Review Transport in Growth Cone Motility and Axon Guidance. *Neuron* **2003**, *40*, 209–227.

81. Haga, H.; Irahara, C.; Kobayashi, R.; Nakagaki, T.; Kawabata, K. Collective movement of epithelial cells on a collagen gel substrate. *Biophys. J.* **2005**, *88*, 2250–2256.

82. Friedl, P. Prespecification and plasticity: Shifting mechanisms of cell migration. *Curr. Opin. Cell Biol.* **2004**, *16*, 14–23.

83. Rorth, P. Whence Directionality: Guidance Mechanisms in Solitary and Collective Cell Migration. *Dev. Cell* **2011**, *20*, 9–18.

84. Andalib, M. N.; Dzenis, Y.; Donahue, H. J.; Lim, J. Y. Biomimetic substrate control of cellular mechanotransduction. *Biomater. Res.* **2016**, *20*, 11.

85. Lee, S. J.; Choi, J. S.; Park, K. S.; Khang, G.; Lee, Y. M.; Lee, H. B. Response of MG63 osteoblast-like cells onto polycarbonate membrane surfaces with different micropore sizes. *Biomaterials* **2004**, *25*, 4699–4707.

86. Brandon, G. G.; Sujata, K. B. Tissue scaffold surface patterning for clinical applications**.** *Biotechnol. J.* **2013**, *8*, 73–84.

87. Briand, E.; Salmain, M.; Compère, C.; Pradier, C. M. Immobilization of Protein A on SAMs for the elaboration of immunosensors. *Colloids Surfaces B Biointerfaces* **2006**, *53*, 215–224.

88. Stevenson, M. D.; Piristine, H.; Hogrebe, N. J.; Nocera, T. M.; Boehm, M. W.; Reen, R. K.; Koelling, K. W.; Agarwal, G.; Sarang-Sieminski, A. L.; Gooch, K. J. A self-assembling peptide matrix used to control stiffness and binding site density supports the formation of microvascular networks in three dimensions. *Acta Biomater.* **2013**, *9*, 7651–7661.

89. Zhao, Y.; Zeng, H.; Nam, J.; Agarwal, S. Fabrication of skeletal muscle constructs by topographic activation of cell alignment. *Biotechnol. Bioeng.* **2009**, *102*, 624–631.

90. Bishop, A. R.; Nuzzo, R. G. Self-assembled monolayers: recent developments and applications. *Curr. Opin. Colloid Interface Sci.* **1996**, *1*, 127.

91. Herbert, C. B.; McLernon, T. L.; Hypolite, C. L.; Adams, D. N.; Pikus, L.; Huang, C. C.; Fields, G. B.; Letourneau, P. C.; Distefano, M. D.; Hu, W. S. Micropatterning gradients and controlling surface densities of photoactivatable biomolecules on self-assembled monolayers of oligo(ethylene glycol) alkanethiolates. *Chem. Biol.* **1997**, *4*, 731–737.

92. Yousaf, M. N.; Houseman, B. T.; Mrksich, M. Using electroactive substrates to pattern the attachment of two different cell populations. *Proc. Natl. Acad. Sci. U. S. A.* **2001**, *98*, 5992–5996.

93. Smith, R. K.; Lewis, P. A.; Weiss, P. S. Patterning self-assembled monolayers. *Prog. Surf. Sci.* **2004**, *75*, 1–68.

94. Hosseinkhani, H.; Hong, P. Da; Yu, D. S. Self-assembled proteins and peptides for regenerative medicine. *Chem. Rev.* **2013**, *113*, 4837–4861.

95. Li, S.; Yang, D.; Tu, H.; Deng, H.; Du, D.; Zhang, A. Protein adsorption and cell adhesion controlled by the surface chemistry of binary perfluoroalkyl/oligo(ethylene glycol) self-assembled monolayers. *J. Colloid Interface Sci.* **2013**, *402*, 284–290.

96. Fyrner, T.; Ederth, T.; Aili, D.; Liedberg, B.; Konradsson, P. Synthesis of oligo(lactose)-based thiols and their self-assembly onto gold surfaces. *Colloids Surf. B. Biointerfaces* **2013**, *105*, 187–193.

97. Merzendorfer, H. The cellular basis of chitin synthesis in fungi and insects: Common principles and differences. *Eur. J. Cell Biol.* **2011**, *90*, 759–769.

98. Tokura, S.; Tamura, H. Chitin and Chitosan. Comprehensive Glycoscience **2007**, *2*, 449–475.

99. Sudheesh Kumar, P. T.; Srinivasan, S.; Lakshmanan, V.-K.; Tamura, H.; Nair, S. V.; Jayakumar, R. β-Chitin hydrogel/nano hydroxyapatite composite scaffolds for tissue engineering applications. *Carbohydr. Polym.* **2011**, *85*, 584–591.

100. Jayakumar, R.; Chennazhi, K. P.; Srinivasan, S.; Nair, S. V.; Furuike, T.; Tamura, H. Chitin scaffolds in tissue engineering. *Int. J. Mol. Sci.* **2011**, *12*, 1876–1887.

101. Yusof, N. L. B. M.; Wee, A.; Lim, L. Y.; Khor, E. Flexible chitin films as potential wound-dressing materials: wound model studies. *J. Biomed. Mater. Res. A* **2003**, *66*, 224–232.

102. Singh, R.; Singh, D. Chitin membranes containing silver nanoparticles for wound dressing application. *Int. Wound J.* **2014**, *11*, 264–268.

103. Kittle, J. D.; Wang, C.; Qian, C.; Zhang, Y.; Zhang, M.; Roman, M.; Morris, J. R.; Moore, R. B.; Esker, A. R. Ultrathin chitin films for nanocomposites and biosensors. *Biomacromolecules* **2012**, *13*, 714–718.

104. Suginta, W.; Khunkaewla, P.; Schulte, A. Electrochemical Biosensor Applications of Polysaccharides Chitin and Chitosan. *Chem. Rev.* **2012**, *113*, 5458–5479.

105. Libreros, S.; Garcia-Areas, R.; Shibata, Y.; Carrio, R.; Torroella-Kouri, M.; Iragavarapu-Charyulu, V. Induction of proinflammatory mediators by CHI3L1 is reduced by chitin treatment: Decreased tumor metastasis in a breast cancer model. *Int. J. Cancer* **2012**, *131*, 377–386.

106. Yuichi, O.; Koji, N.; Tatsuro, O. In vivo and in vitro antitumor activity of CM-chitin immobilized doxorubicins by lysosomal digestible tetrapeptide spacer groups. *J. Bioact. Compat. Polym.*1995, *10*, 223–234.

107. Lunde, I. G.; Aronsen, J. M.; Kvaløy, H.; Qvigstad, E.; Sjaastad, I.; Tønnessen, T.; Christensen, G.; Grønning-Wang, L. M.; Carlson, C. R. Cardiac O-GlcNAc signaling is increased in hypertrophy and heart failure. *Physiol. Genomics* **2012**, *44*, 162–72.

108. Ngoh, G. A.; Facundo, H. T.; Zafir, A.; Jones, S. P. O-GlcNAc signaling in the cardiovascular system. *Circ. Res.* **2010**, *107*, 171–185.

109. Yuka, Y.; Takuya, K. Tailoring hybrid glycol-nanolayers composed of chitohexaose and cellohexaose for cell culture applications. *J. Mater. Chem.* **2011**, *21*, 11150–11158.

110. Swailes, N. T.; Colegrave, M.; Knight, P. J.; Peckham, M. Non-muscle myosins 2A and 2B drive changes in cell morphology that occur as myoblasts align and fuse. *J Cell Sci* **2006**, *119*, 3561–3570.

111. Horwitz, A. R. Non-muscle myosin II takes centre stage in cell adhesion and migration. *Nat. Rev. Mol. Cell Biol.* **2009**, *10*, 778–790.

112. Alexandrova, A. Y.; Arnold, K.; Schaub, S.; Vasiliev, J. M.; Meister, J. J.; Bershadsky, A. D.; Verkhovsky, A. B. Comparative dynamics of retrograde actin flow and focal adhesions: Formation of nascent adhesions triggers transition from fast to slow flow. *PLoS One* **2008**, *3*, 1–9.

Chapter 2

Chapter 2

Micropatterning and Cellular Alignment in Skeletal Muscle Cells

Skeletal muscle has a complex hierarchical structure which is responsible for controlling voluntary movement and maintenance of body structure. Skeletal muscle fibers are surrounded by connective tissue and are rearranged into fascicles which contain thousands of individual muscle cells known as myocytes. The physical fiber dimensions are several centimeters in length and the fibers are roughly cylindrical in cross-section, having the thickness of approximately 50-150 micrometers (μm). Dissected single fibers are called myofibers, which are composed of several small bundles of myofibrils. These myofibrils exhibit a distinctive banding pattern when is viewed under a microscope due to their arrangement in longitudinally repeating unit structures of sarcomeres. The major cytoplasmic proteins on sarcomeres are highly ordered and consist of actin and myosin, which are also well known as thin and thick filaments, respectively (Fig. 2-1). These fibers are remarkable to generate muscle contraction through strong cross-bridge binding cycles, which are triggered by the activation of calcium ions (Ca^{2+}) and ATP [1].

Skeletal muscle tissue engineering holds promise for the treatment of a variety of muscle diseases, e.g., muscular dystrophy [2]. The process of new muscle formation requires that quiescent mononucleated muscle precursor cells become activated, proliferate, differentiate, and fuse together to form multinucleated myotubes [3]. The proliferation of skeletal myoblasts is governed by the upregulation of basic helix-loop-helix transcriptional activators of the myogenic regulatory factors (MRF) such as MyoD and Myf5. These proliferated myoblasts must withdraw

from the cell cycle to become terminally differentiated myoblasts that express late MRFs, myogenin, and MRF4. The cells subsequently express muscle structural protein myosin heavy chain (MyHC) and muscle creatine kinase (MCK), and fuse to form multinucleated myotubes [3,4]. Several distinct approaches are currently being investigated to therapeutically mediate the muscle regenerative process, including injection of growth factors, [5] gene therapy,[6] and the delivery of exogenous cells [7].

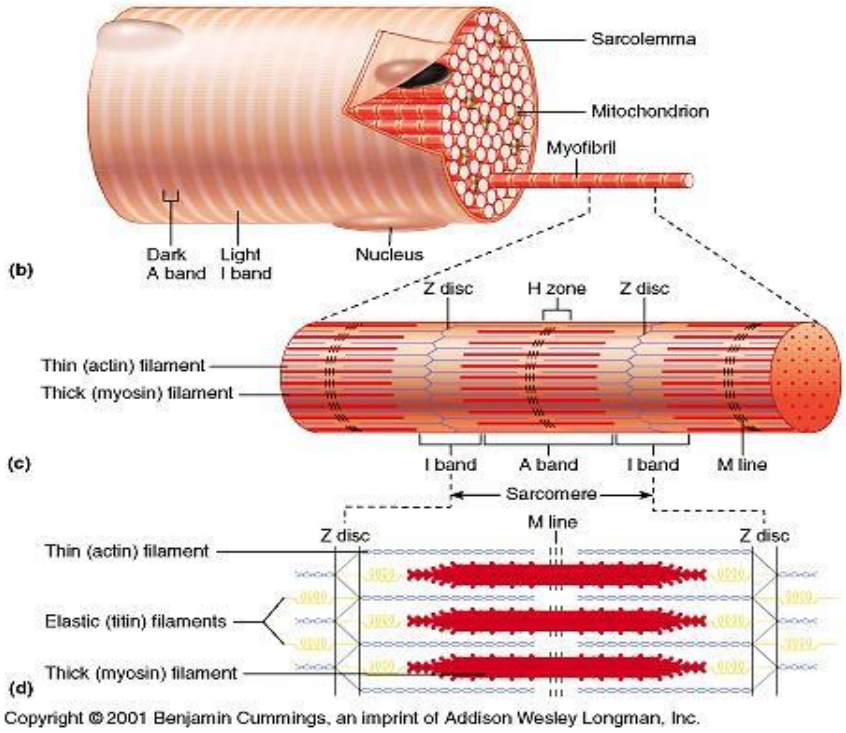

Fig. 2-1 The structure of skeletal muscle. (James F. Thompson. Individual lecture and lab course information. Chapter 09: Sliding filament mechanism)

2.1 Mouse-derived myoblast C2C12 cells

Myoblast cell (C2C12 cell) is a type of embryonic progenitor cells which are formed in the myogenesis process. They have the potential to differentiate into muscle cells through forming of multinucleated myotubes. The myoblast fusion phenomenon is unique and predominantly found only in the formation of skeletal muscle fibers and does not occur ordinarily in other cell types [9,10]. C2C12 cells were originally obtained using the protocol of Yaffe and Saxel through isolated and cultured cells from thigh muscle of adult C3H mice after a crush injury [11].

Cell adhesions play important roles in a myriad of biological processes, particularly in cell motility, and cell-cell recognition including the determination of cell fate, as described in chapter 1. They provide an interactive interface between cells and ECM surfaces through cell adhesion molecules (CAMs). CAMs are proteins uniformly distributed on cell surfaces as transmembrane receptors, which can be involved in cell communication and signal transduction. Additionally, CAMs are typically given as 5 classes; cadherins, the immunoglobulin (Ig) superfamily, selectins, mucins and integrins (Fig. 2-2).

Integrins, as cell-cell adhesion molecules, are a major family of cell surface receptors that are responsible for anchoring cells to ECMs. The integrins are heterodimer molecules containing α and β subunits, which are necessary for adhesive binding. Recent studies have shown that a wide variety of integrins stimulate various activities in biological phenomena such as gene expression, cell proliferation and differentiation in embryonic development. Moreover, integrin-mediated signaling has influence on several critical cellular processes, whose intracellular signal pathways are pursuable to generate specific proteins. These proteins are involved in cell locomotion, cell migration and contractility of muscle cells (e.g. cytoskeletal protein, stress fiber, focal adhesion and actin filament) [12-14]. Furthermore, specific proteins of muscles could be regulated by gene expression, especially in the myogenic regulatory factors (MRFs) family. MRFs are proteins, consisting of 4 genes namely Myo-D, Myf-5, MRF-4 and myogenin, which are expressed during muscle differentiation processes [15].

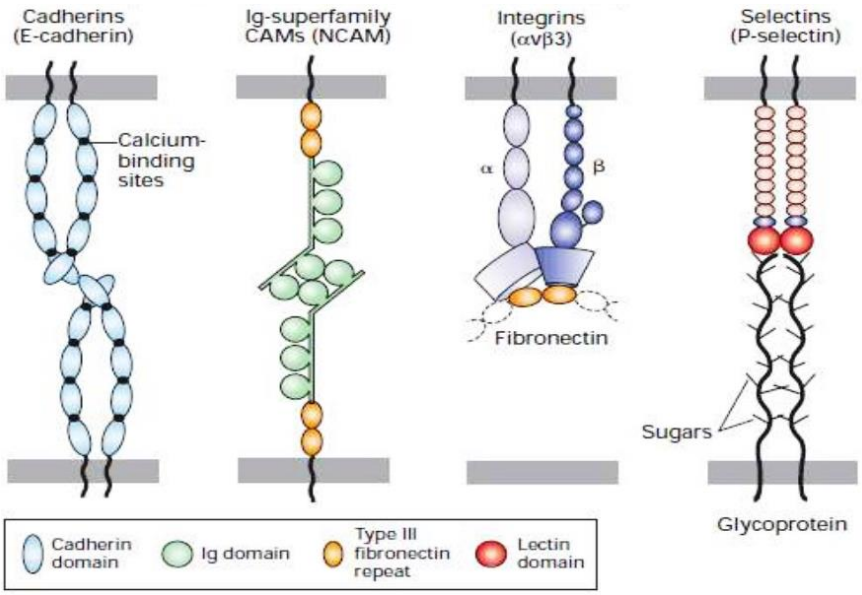

Fig. 2-2 Illustration of specific proteins inside cell. (http://www.slideshare.net/aljeirou/adhesion-molecules)

2.2 Cellular alignment and micropatterning

Cellular alignment is an important in tissue engineering and regenerative medicine due to various advantages that can generate and transform tissue monolayers to three-dimensional structures. Engineered micropatterns can provide two- and three-dimensional complex and dynamic microenvironment for individual cells or multicellular arrangements resulting in the potential to control cell morphology and cell behavior [16]. Consequently, cellular micropatterning has become a useful method in fundamental studies to investigate in cell-material interactions. Furthermore, some literature has been reported that cellular micropatterning has a potential for the treatment of muscular dysfunction. This is due to the geometrical cues of substrates can significantly influence the differentiation process of C2C12 skeletal myoblasts [17]. However, skeletal muscle generation *in vitro* still remains limited due to difficulty in cellular alignment. Thus, the alignment of cells is required to mimic the highly organized structures of skeletal muscle *in vitro*. For example, Powell et al. reported that they achieved the creation of human bio-artificial muscles by culturing skeletal muscle cells in a collagen/matrigel matrix *via* parallel arrangements of myofibers [18]. In addition, micropatterned topography demonstrated that the alignment of myotubes can be controlled through polymer microfibers [19,20].

Micropatterning techniques have been explored to better control cell behavior since the 1970s. Later, Takezawa et al. and Yamada et al. discovered in 1990 that spatial topology of a thermo stimuli-responsive polymer, poly (*N*-isopropylacrylamide), is able to control the attachment of cells on surface without using enzymatic or mechanical procedures [21]. Recently, patterning has been used extensively in biomaterial engineering and has provided beneficial aspects for a variety of fundamental research in biotechnology, especially in cell biology. Several literatures sources reported that the alignment phenomena of cells were associated with topographical cues. However, the abilities to control cell adhesion and cell alignment on surfaces are difficult due to many different biological parameters in the regulation of cellular development. In addition, these results affect multicellular organization, leading to critical impact on cellular responses. Hence, micropatterning techniques are being increasingly used for investigating cell physiology, cell function and cell alignment toward *in vitro* applications [22,23].

In general, patterning techniques can be tailored on various sizes, ranging from nanometer scales to several micrometers through diverse techniques such as photolithography, soft-lithography, microcontact printing (μCP), microfluidic patterning and laminar flow patterning [24]. In addition, the generation of 3D micropatterning demonstrated more appropriate architecture for modulating cellular alignment and their physiological microenvironment than 2D micropatterning, and allows us to fabricate the biomimetic structures analogous to *in vivo* bioarchitectures [25]. For instance, switchable surfaces as 3D micropatterning structures enabled us to mimic dynamic models of motile cells on surfaces (Fig. 2-3). Many studies published lately have displayed that the dimensional geometries of patterning exposures to provide more valuable benefits toward the commitment of stem cell fate and mechanism. Kilian et al. reported that human mesenchymalstem cells (hMSC) can promote their differentiation into specific phenotypes through different types of pattern geometries [22]. In addition, the differentiation and alignment on topological patterning have influence not only on stem cell behavior but also several other types of cells such as myoblast cell (Fig. 2-4 and 2-5) [26]. Hence, micropatterning techniques have led to drastic enhancements in the development of today's tissue engineering applications. Interestingly, patterning techniques not only affect cell behaviors, notably cell growth and cell differentiation but also regulate fundamental cell fates. These advantages are important for controlling cell morphology, spatial arrangement and cell functions, leading to the reconstitution of tissue-like conditions for *in vitro* cell culture applications [27]. Particularly in co-culture systems, patterning allows the manipulation of cell–cell interaction, realizing regenerative medicines.

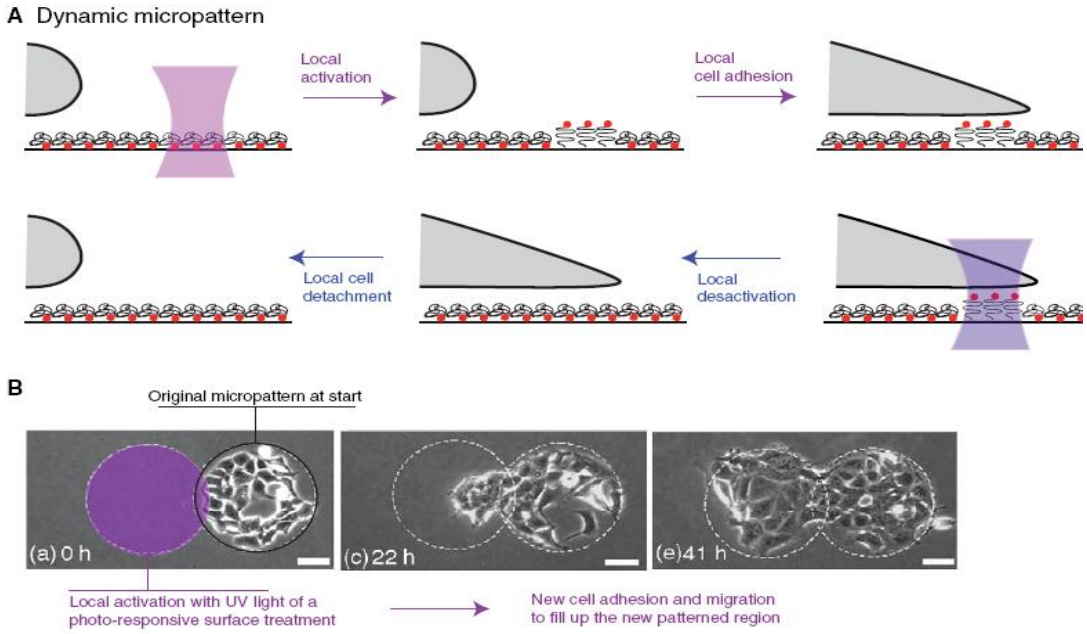

Fig. 2-3 The three dimensional structure of the cell microenvironment on dynamic or switchable surfaces. (Falconnet, D.; Csucs, G.; Michelle Grandin, H.; Textor, M. Surface engineering approaches to micropattern surfaces for cell-based assays. *Biomaterials* **2006**, *27*, 3044–3063)

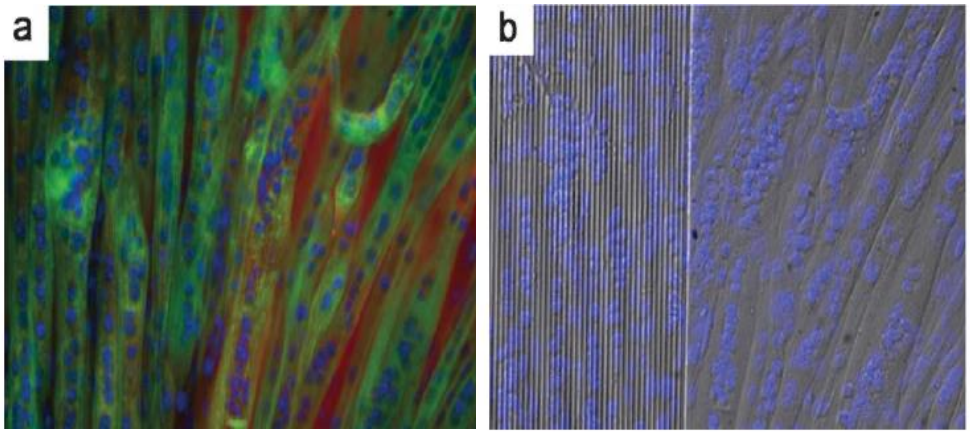

Fig. 2-4 Representative of immunofluorescence images of **a)** myotube alignment and actin filament staining, **b)** C2C12 cell nuclei stained under different surface topographies. Myosin heavy chain marked by red fluorescence, actin filament (green) and nuclei (blue) (Zhao, Y.; Zeng, H.; Nam, J.; Agarwal, S. Fabrication of skeletal muscle constructs by topographic activation of cell alignment. *Biotechnol. Bioeng.* **2009**, *102*, 624–631)

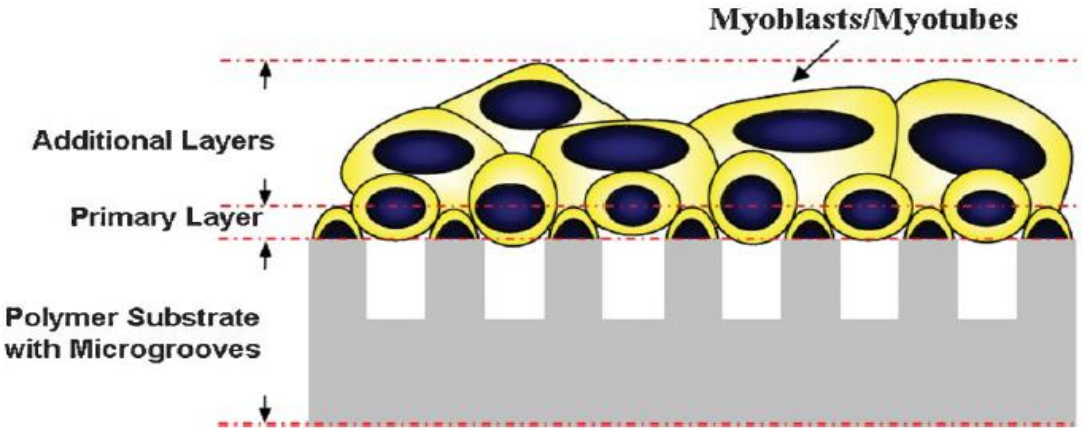

Fig. 2-5 Schematic drawing of topographically activated muscular tissue fabrication. The microgrooves showed primary layers of skeletal myotubes, which serve as a seed layer to affect the growth and differentiation of additional cell layers. Three-dimensional muscle like tissues with organized structures are formed (Zhao, Y.; Zeng, H.; Nam, J.; Agarwal, S. Fabrication of skeletal muscle constructs by topographic activation of cell alignment. *Biotechnol. Bioeng.* **2009**, *102*, 624–631)

2.3 Objective and achievements in the dissertation

Carbohydrates have played an important role in regulating diverse biological processes such as cell–cell communications and immunological responses as well as physiological phenomena. In living systems, structural heterogeneity of glycans on cell membrane surfaces plays a key factor not only to prevent undesirable non-specific adhesion of proteins but also to induce many aspects of the carbohydrate-protein interactions. Such interactions are very weak in spite of playing a significant role in various biological processes such as cell signaling and cell responsiveness including controllable cellular alignment.

A variety of carbohydrate scaffolds in tissue engineering have rapidly become a major point of interest challenge due to the possibility of controlling cellular functions in in vitro applications. Yoshiike et al. have recently reported that clustering of cello/chitohexoase hybrid on gold nanolayer demonstrated unique properties that the sugar-clustering state affected cytochrome P450 activity of human liver cells (HepG2) [31]. These results indicated that using carbohydrate-fixed nanolayers could regulate cellular alignment and control cellular biofunctions, which is of great importance for 3D scaffold microarchitectures (Fig. 2-6). On the other hand, free polysaccharides coated on surfaces showed apparent non-adhesion of cells, eventually being floated on the surfaces. (Fig. 2-6b) In addition, it has been reported that various artificially-designed glyco-biointerfaces, such as self-assembled monolayers (SAMs) of chitin/chitosan, hyaluronan, cellulose and its derivatives, which were vertically formed on gold (Au) surfaces, demonstrating desirable biocompatibility and leading to good cell adhesion and enhancing cell proliferation. [28-31].

My Ph.D. thesis work, I propose a new conceptual idea for controlling mouse-derived myoblast C2C12 cell alignment as well as regulating myoblasts fusion through clustered sugar functional groups, *N*-acetyl-D-glucosamine (GlcNAc), of chitooligomer-SAMs on rectangular striped gold micropatterns. In living systems, skeletal muscle cells are required to stand in a unidirectional orientation in order to exhibit their biological and mechanical properties. However, in general *in vitro* applications, these cells are scattered on tissue culture plates (TCPS), showing a similar morphology to epidermal cells. In addition, a greater understanding of microenvironmental cues is required to drive muscle formation. Such understanding has not yet been achieved, though recent studies fabricated an aligned architecture similar to that of native muscle using synthetic

polymers, such as a thermoresponsive poly(*N*-isopropylacrylamide) (PNIPAAm) [32] and soft poly(dimethylsiloxane) (PDMS) micropatterning [28]. A limitation of these materials is that they have no specific interaction with the cell surface to promote directional alignment and myogenesis regulation, both key factors for myoblast proliferation and differentiation. To mimic the highly-organized structure of skeletal muscles *in vitro*, various approaches should be investigated. In order to overcome those drawbacks, therefore, ultimate goals of this research are 1) to fabricate novel-concept biomimetic glyco-architecture for enhancing various biomolecular and cellular interactions (Fig. 2-7), 2) to modulate the physiological behavior of cellular orientation and biological functions on the glyco-clustered biointerfaces, and 3) to apply for *in vitro* biofunctional cell cultures.

Herein, as-prepared glyco-SAMs architecture was formed by site-selective modification of the reducing end groups of chitooligomers with thiosemicarbazide (TSC). This chapter, the influences of carbohydrate-functionalized surface geometries on the alignment and proliferation of C2C12 myoblast cells will be presented. In addition, the determination of self-assembly behavior of GlcNAc6 to form glyco-SAM architectures by quartz crystal microbalance (QCM) analysis and the biological characterizations of cultured C2C12 cells on GlcNAc6-SAMs with different geometries were investigated with regard to their initial adhesion, alignment, morphology, and early stage of cell differentiation by examining mRNA expression levels for myogenesis and bioassays. In depth details on chemical characterizations, cell assay and immunofluorescence analysis for biological characterizations will be shown in materials and method of chapter 2 and chapter 3. I expect that glyco-designed architecture can provide a new insight into a broad range of biofunctional design in advanced cell engineering as well as regenerative medicine and various life sciences and technology.

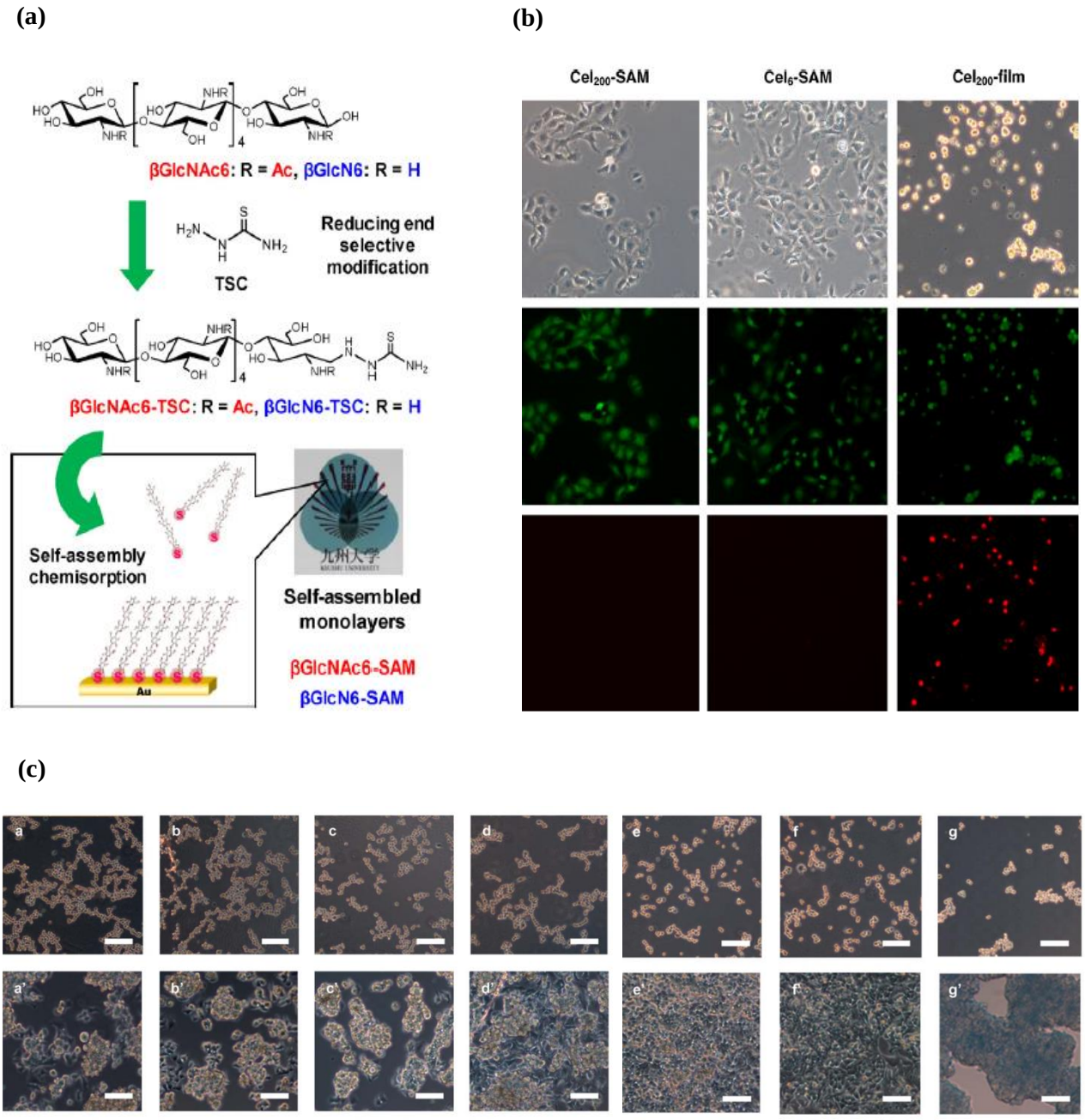

Fig. 2-6 a) Schematic illustration of the derivatization of cello-/chitohexaose with TSC and spontaneous self-assembly of carbohydrates on gold nanolayer substrate. (Yoshiike, Y.; Yokota, S.; Tanaka, N.; Kitaoka, T.; Wariishi, H. Preparation and cell culture behavior of self-assembled monolayers composed of chitohexaose and chitosan hexamer. *Carbohydr. Polym.* **2010**, *82*, 21–27). **b)** Microscopic images of IAR-20 cells cultured on various cellulose-SAM substrates (culture time: 24 h) Phase contrast micrographs (Top). Fluorescence micrographs of live and dead cells stained (Middle and bottom). (Yokota, S.; Kitaoka, T.; Wariishi, H. Biofunctionality of self-assembled nanolayers composed of cellulosic polymers. *Carbohydr. Polym.* **2008**, *74*, 666–672).

c) Microscopic images of HepG2 cell morphology, after 3 h (a–g) and 120 h (a'–g') incubation, on the hybrid nanolayers of βGlcNAc6 and βGlc6 with varying molar proportions of βGlcNAc6: 100% (a, a'), 61% (b, b'), 46% (c, c'), 8% (d, d') and 0% (e, e'). Control; TCPS (f, f') and commercial tissue culture scaffold for spheroid formation (g, g'). The scale bars correspond to 100 µm. (Yoshiike, Y.; Kitaoka, T. Tailoring hybrid glyco-nanolayers composed of chitohexaose and cellohexaose for cell culture applications. *J. Mater. Chem.* **2011**, *21*, 11150–11158)

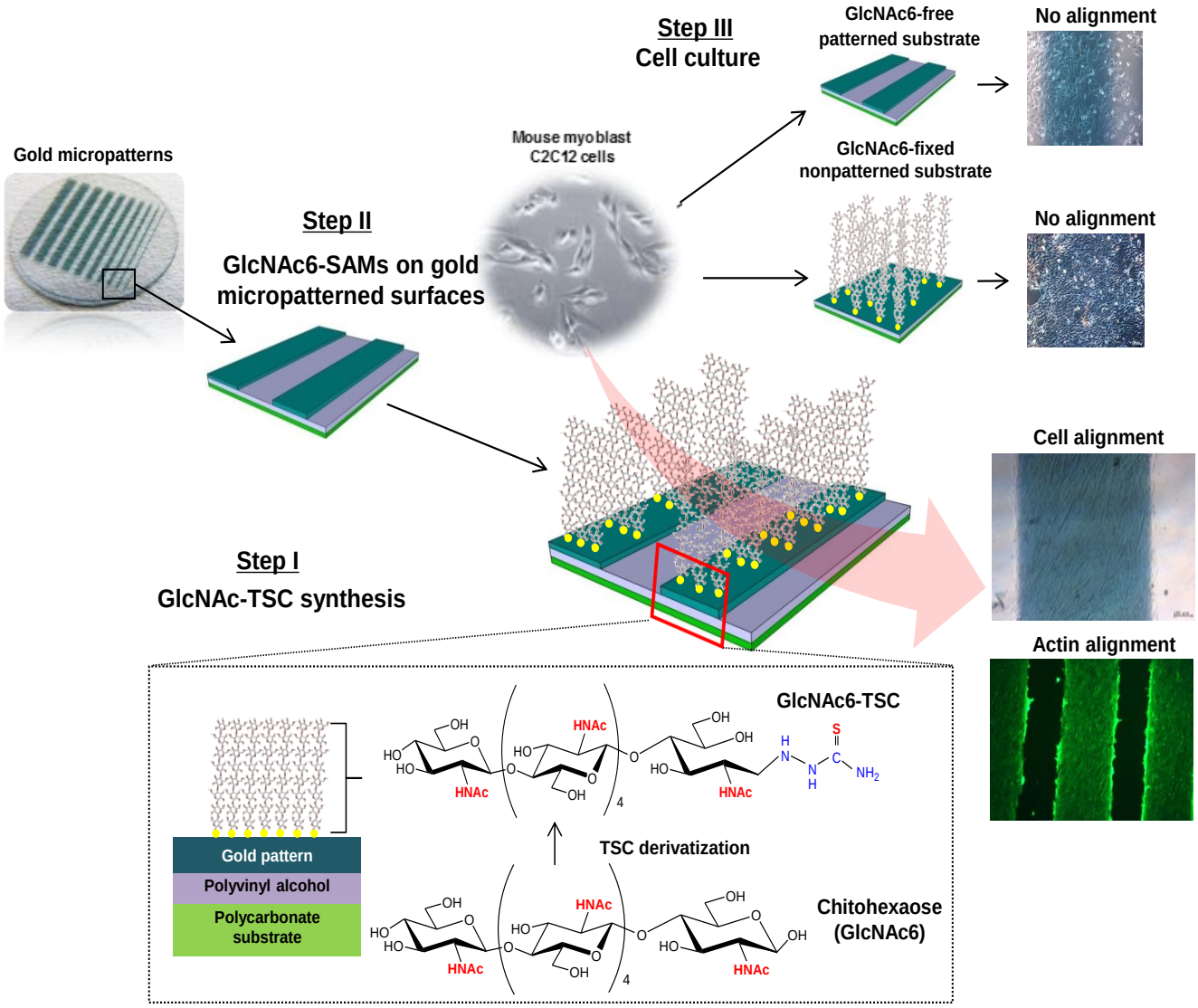

Fig. 2-7 Schematic illustration of the preparation of GlcNAc6-SAMs with micropatterns and myoblast cell alignment through a specific interaction with glyco-receptors on cell surfaces.

2.4 Materials and Method

2.4.1 Materials

Commercially pure α-chitin powder, isolated from crab shells (Katakura Chikkarin, Tokyo, Japan), was hydrolyzed to a chitooligomer mixture and purified by the gel filtration separation (Cellufine GCL-25, JNC Corporation, Tokyo, Japan) to obtain chitohexoase (GlcNAc6). Thiosemicarbazide (TSC, Wako Pure Chemical Industries, Osaka, Japan), sodium cyanoborohydride ($NaBH_3CN$, Sigma-Aldrich, St. Louis, MO, USA) and polyvinyl alcohol (PVA, MW 2000 Da, Kishida Chemical, Osaka, Japan) were used as received. The immortalized mouse muscle myoblast cell line C2C12 (ATCC-CRL1772™, ATCC, Manassas, VA, USA) was grown under standard conditions with Dulbecco's Modified Eagle's Medium (DMEM, Life Technologies, Tokyo, Japan) supplemented with 10% fetal bovine serum (FBS, Biowest, Nuaillé, France). Trypsin-ethylenediaminetetraacetic acid (EDTA, Invitrogen, Tokyo, Japan) solution, 0.4% trypan blue solution (Invitrogen), phosphate buffered saline (PBS, Nissui Pharmaceutical, Tokyo, Japan), phalloidin-Alexa Fluor®488 conjugate (Lonza, Walkersville, MD, USA), and molecular biology grade Triton® X-100 (EMD Biosciences, San Diego, CA, USA) were used for biological assays. Tissue culture polystyrene (TCPS) dishes and TCPS plates (24-well) were purchased from Sumitomo Bakelite Co. Ltd. Tokyo (Japan). The water used in this study was purified with a Milli-Q system (Sartorius Stedim Biotech, Bohemia, NY, USA). Unless otherwise indicated, all chemicals were reagent grade and were used without further purification.

2.4.2 Preparation of micropatterned glyco-SAMs on gold surfaces

GlcNAc6 fractions were obtained by acid hydrolysis of chitin and gel filtration as described in Section 2.4.1 Purified GlcNAc6 was site-selectively modified at its reducing end group with 1 M TSC through reductive amination with 2 M $NaBH_3CN$ with stirring at 70 °C for 48 h, as illustrated in Figure 2-7. Unreacted GlcNAc6 and impurities were removed by precipitating the product in methanol, followed by centrifugation (5439 *g*, Tomy MX-301, Tokyo, Japan) at room temperature for 15 min; in this manner, the precipitate was washed seven times in methanol. GlcNAc6-TSC powder was obtained by freeze-drying the final pellet.

Polycarbonate substrates (PC; diameter 15 mm, thickness 0.5 mm) were immersed in solution (containing 1% (*w*/*v*) PVA, 5% (*v*/*v*) ethyl acetate and 20% (*v*/*v*) ethanol) at room temperature for 1 h and then air-dried. Gold micropatterns, with a typical discrete width (200, 500, and 1000 μm), were ion sputtered (VPS-020, ULVAC Inc. Miyazaki, Japan, current 10 mA, 3 min, 1.5 mPa) with gold on bioinert PVA-treated transparent PC substrates using template masks (Microtech Laboratory, Kanagawa, Japan). In this manner, ultraflat (approximately 30 nm thickness) gold (Au) micropatterns were obtained. The striped Au micropatterns were immersed in a 1 M aqueous solution of GlcNAc6-TSCs, fixing polymers on the micropatterns through S-Au chemisorption and leading to the formation of SAMs on a gold surface. Preparation of micropatterned GlcNAc6-SAMs and the general procedure for cell culture on the GlcNAc6-immobilized gold micropatterns are illustrated in Figure 2-7.

2.4.3 Characterization of micropatterned glyco-SAMs

2.4.3.1 NMR analysis

TSC modification of carbohydrates was determined by ^{1}H-NMR spectroscopy (JNM-AL 400, JEOL Ltd., Tokyo, Japan). GlcNAc6-TSC (20 mg) was dissolved in 750 μL deuterium oxide in a 5-mm capillary NMR tube. ^{1}H NMR chemical shifts were expressed in ppm; a standard sodium 3-trimethylsilylpropane sulfonate (TSP) was included. The chemical shifts of the anomeric protons in chitohexoase at 5.20 and 4.55–4.65 ppm correspond to the α- and β-anomers, respectively, at each reducing end. Axial protons at internal C1 positions were assigned at 3.2–4.2 ppm [34,35]. Acetyl and ring protons appear at 2.02–1.98 and 3.74–3.92 ppm, respectively [35]. The integrated intensities of the signals were used to estimate the degree of polymerization of the chitooligomer.

2.4.3.2 Quartz crystal microbalance analysis (QCM)

Quantitation of carbohydrate-TSC molecules chemisorbed on the gold surfaces was performed with a QCM apparatus (AFFINIXQ, Initium Inc., Tokyo, Japan) with a 27 MHz AT-cut crystal resonator. The frequency changes of the sensor chip were monitored by injecting dilute aqueous solutions of GlcNAc6-TSC (1 mM) at 25 °C. The injection was repeated until the frequency reached equilibrium. The approximate amounts of chemisorbed carbohydrates on the QCM chip were calculated using Sauerbrey's Equation (1) as described in our previous study [31]:

$$\Delta F = \frac{f_0 \Delta M \times 6.022 \times 10^{23}}{(M_w)A} \quad (1)$$

In Equation (1), ΔF is the final frequency change and f_0 is the resonant frequency. ΔM, the mass change, indicates the amount of carbohydrates adsorbed on the QCM chip (1 Hz = 30 pg). M_W is the molecular weight of the carbohydrate-TSC (1310.5 Da). The Au electrode surface area, A, of the quartz probe is 4.9 mm^2.

2.4.3.3 X-ray photoelectron spectroscopy (XPS)

Elemental analysis of the carbohydrate-TSC molecules absorbed on the gold surfaces was performed with an AXIS-HSi XPS apparatus (Shimadzu/Kratos Co. Ltd., Kyoto, Japan). XPS measurements were performed at 12 kV and 10 mA with a monochromatic Al *K*α X-ray source (1486.6 eV) with the analyzing chamber pressure maintained below 0.5 μPa during the measurements. The pass energy and step width were set at 40 and 0.05 eV, respectively. The binding energies for all spectra were referenced to the C1s signal (reduced C–C band) at 285.0 eV. [36].

2.4.5 Cell culture assays and microscopic observations

C2C12 myoblast cells were cultured in DMEM supplemented with 10% (*v*/*v*) FBS. Unattached cells were removed by washing with PBS. Gold substrate was placed in a 24 well-plate and sterilized with ultraviolet light prior to cell seeding. Each cell suspension (0.5 mL, 5.0 × 10^4 cells·mL^{-1}) was seeded on each gold substrate with 0.5 mL of cell culture medium. Samples were incubated for one, three, five, and seven days at 37 °C in an atmosphere of 95% air and 5% CO_2. Cells began to adhere within 24 h and were confluent at days 7. The number of viable cells was measured with an automated cell counter (TC 20TM, Bio-Rad Laboratories, Inc., Philadelphia, PA, USA) after treating them with a 0.4% trypan blue solution. Cell behaviors and morphologies were observed under a phase-contrast microscope (Leica DMI 4000B microscope, Wetzlar, Germany).

2.4.6 Biological characterization

2.4.6.1 F-actin staining

Alignment of actin filaments was visualized by fluorescence staining for F-actin. Cultured cells were rinsed twice in pre-warmed PBS, fixed with 3.7% formaldehyde for 10 min and permeabilized with 0.1% Triton® X-100 in PBS for 5 min. Fixed cells were pre-incubated with 1% bovine serum albumin in PBS for 20 min to block non-specific protein binding and to enhance fluorescence intensity. Filamentous actin was stained with Alexa Fluor®488-conjugated phalloidin according to manufacturer's protocol. Images of stained sections were acquired using a Leica DMI 4000B microscope.

2.4.6.2 RNA extraction and quantitative real-time polymerase chain reaction (RT-PCR)

Total RNA was isolated from cell preparations using ISOGEN (Nippon Gene Co., Ltd., Toyama, Japan) according to the manufacturer's instructions. The purity and concentration of each RNA preparation was assessed using a NanoDrop™ 1000 spectrophotometer and Experion (Bio-Rad Laboratories Inc., Hercules, CA, USA), consisting of a 20 ng cDNA template, 10 µM of forward and reverse primers, and fast in 10 µL of SYBR Green Master Mix (Applied Biosystems™, Life Technologies, New York, NY, USA). The primer sequences of each gene, *MyoD*, *Myogenin*, and *FAK* was designed by the primer 3 plus software and blasted in the NCBI PubMed primer blast software. Forward primer: 5′ CCGTGTTCCTACCCCCAATG 3′ and reverse primer: 5′ AAGCCCAGCTCTCCCCATA 3′ for *GAPDH*, and forward primer: 5′ TACAGTGGCGACTCAGATGC 3′ and reverse primer: 5′ CACTGTAGTAGGCGGTGTCG 3′ for *MyoD*, and forward primer: 5′ GTGCCCAGTGAATGCAACTC 3′ and reverse primer: 5′ GCAGATTGTGGGCGTCTGTA 3′ for *myogenin*, and forward primer: 5′ ACAGACAAAGGCTGCAATC 3′, and reverse primer: 5′ GCACCAGCGATTTTGAGTTG 3′ for *FAK*. Amplification and quantification of mRNA were performed at 95 °C for 20 s, followed by 3 s at 95 °C, and 30 s at 60 °C for 40 cycles. After amplification, a melting curve analysis was performed to verify amplification product specificity. The relative expression levels of targeted genes were calculated and normalized by subtracting the corresponding *GAPDH* threshold cycle (CT) values and using the ΔΔCT comparative method [37]. PCR products were separated on 2%

agarose gels, stained with ethidium bromide and photographed under UV light to confirm the single amplicon.

2.4.7 Statistical analysis

Bioassay results for individual samples were independently performed in triplicate using GraphPad Prism version 6.0 software (GraphPad Software, Inc., La Jolla, CA, USA). Data are expressed as means ± standard error of the mean (SEM). Statistical differences between two groups were evaluated using an independent samples *t*-test. Statistical significance is indicated by *p*-values of: * $p < 0.05$, ** $p < 0.01$, *** $p < 0.001$ and **** $p < 0.0001$.

2.5 Results and Discussion

2.5.1 Self-assembly immobilization of chitooligomers on micropatterned gold surfaces

The strategy for chitohexaose-SAM (GlcNAc6-SAM) formation on Au substrates involved site-chemoselective conjugation, by which the reducing end group of GlcNAc6 was anchored to the Au surface after the TSC modification at its reducing terminus (Fig. 2-7). This was expected to expose the carbohydrate ligands (nonreducing end groups) aligned vertically to the substrate top surfaces. The NMR spectra (Fig. 2-8) showed the presence and absence of anomeric proton peaks at each reducing end in unmodified and TSC-modified samples, respectively. The average degree of polymerization (DP) of hydrolyzed chitooligomer, determined based on the integral ratios of internal H-1/(H-1α + H-1β), was calculated to be six, a polymer size referred to as chitohexoase. These results showed that the C1-terminal aldehyde of the GlcNAc6 pyranose ring was successfully modified with TSC to form an open ring [31]. Moreover, XPS spectra (Fig. 2-9) revealed that the carbon elements of the GlcNAc6 residues showed three different binding energy shifts. The glyco-biointerfaces exhibited characteristic bands at 286.7 and 288.1 eV, corresponding to C–O and C=O bonds, respectively, which can be assigned to unique structures of hydroxyl C–OH and acetal (O–C–O)/acetamido (CH_3C=O) groups in the chitooligomer molecules (Fig. 2-9a). In contrast, the C1s spectrum of the carbohydrate-free substrates showed a weak peak at 285.0 eV, attributed to the C–C/C–H contaminants on the bare Au surface (Fig. 2-9b). In addition, the carbon signal intensity shifted to a slightly lower binding energy because of formation of SAMs of GlcNAc6-TSC on the gold surfaces *via* specific thiolate anchoring [38,39]. After the appearance of the Au4f peak, the carbohydrate-SAM layer was very thin, less than 10 nm [31].

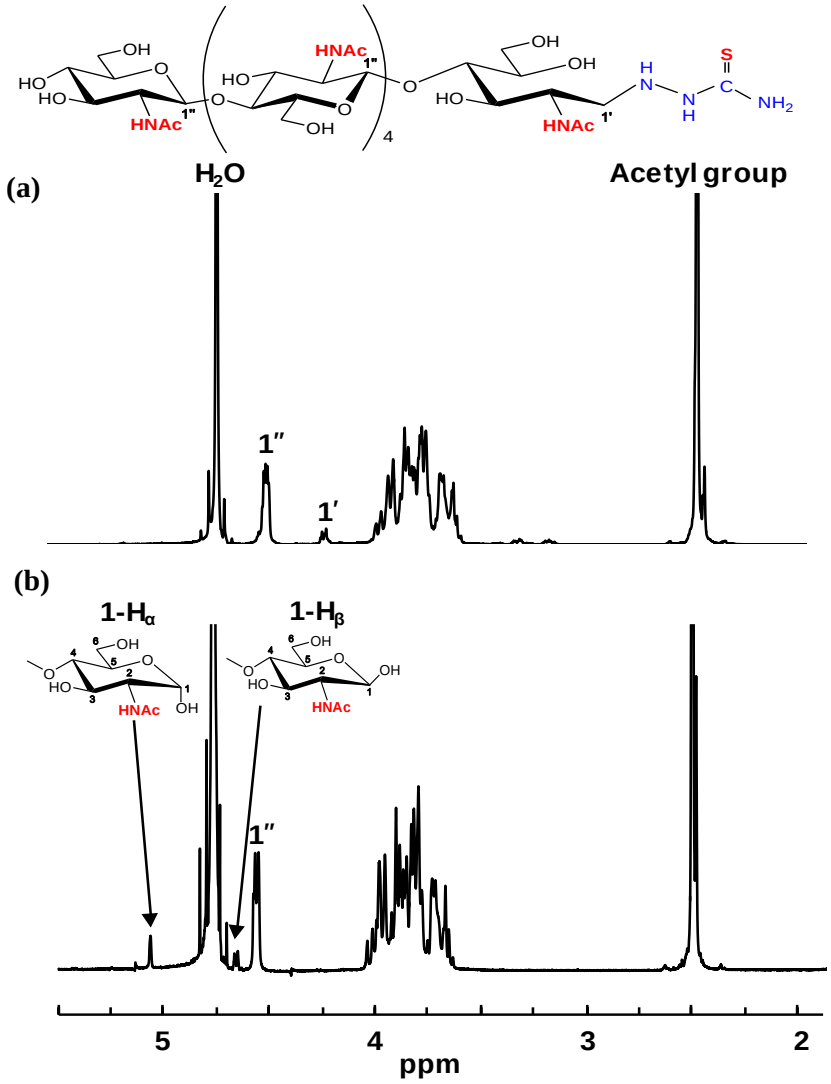

Fig. 2-8 ^{1}H NMR spectra of GlcNAc6 with **a)** or without **b)** TSC derivatization.

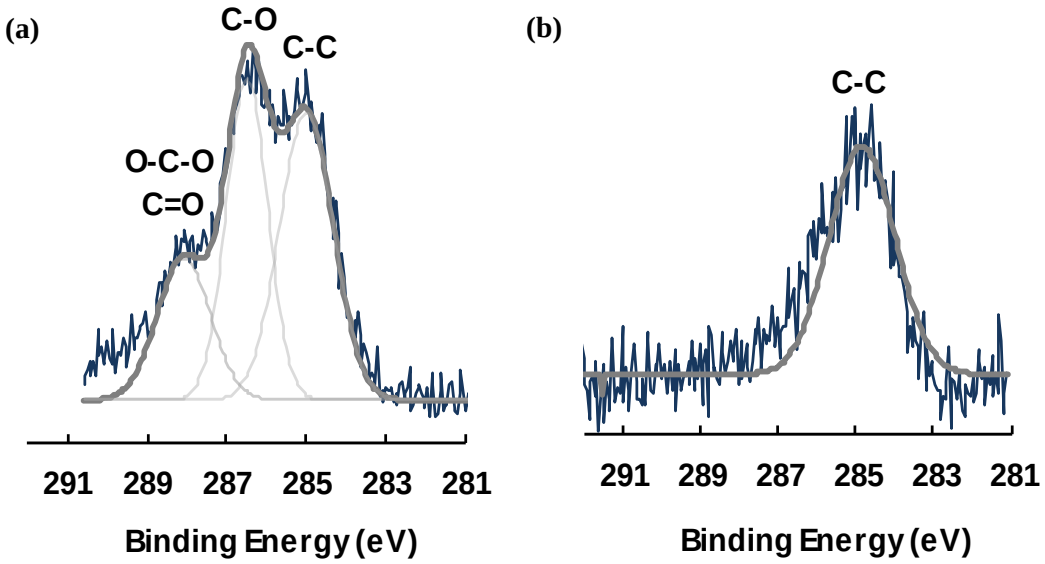

Fig. 2-9 High-resolution XPS spectra of **a)** GlcNAc6-immobilized and **b)** GlcNAc6-free Au surfaces.

2.5.2 Surface analysis and sugar densities of micropatterned glyco-SAMs

The chemisorption of carbohydrate-TSC molecules on the Au-coated quartz crystal of the QCM apparatus was evaluated by the steady decrease in QCM frequencies (Fig. 2-10). After the first injection of the sugar-TSC solution, the QCM frequency first decreased rapidly and, subsequently, declined gradually upon repeated sample injections. This indicated that the carbohydrate-TSC molecules were strongly adsorbed on the Au electrode surface. The control experiment (pure GlcNAc6 without TSC) displayed a minimal significant drop in frequency after sample injections. The correlation between the change in frequencies of QCM profiles and sugar density was quantified using the Sauerbrey equation as shown in Table 1. The amount of sugar on Au patterns was 0.68 chains nm^{-2}, meaning a high sugar density similar to that previously reported, 0.65 chains nm^{-2} [31], whereas TSC-free GlcNAc6 exhibited no significant adsorption. Therefore, the TSC presumably acted as an anchor, immobilizing the reducing end group of GlcNAc6 to the gold surfaces.

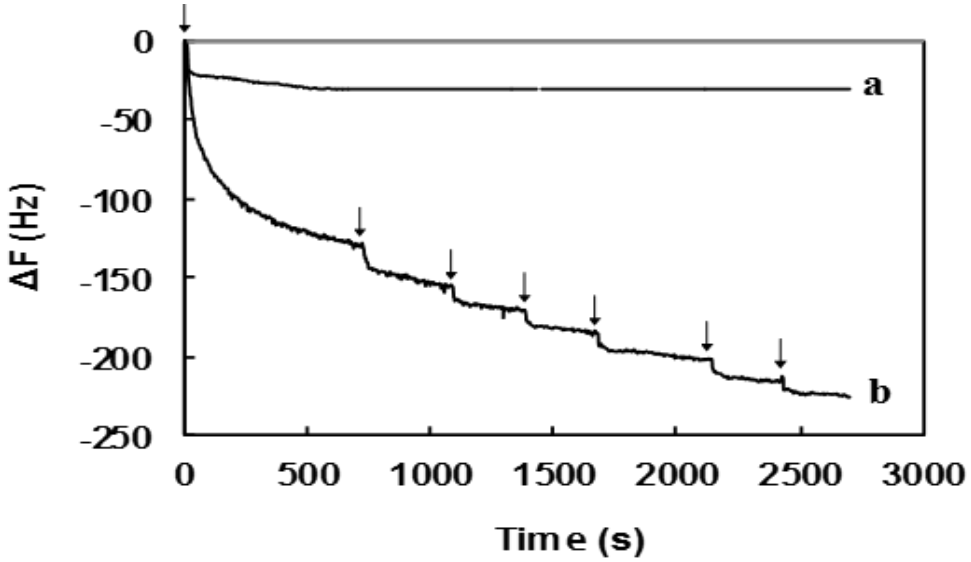

Fig. 2-10 QCM profiles for spontaneous chemisorption of **a**) TSC-free GlcNAc6 and **b**) GlcNAc6-TSCs on a gold surface. Arrows indicate sample injection.

Table 1. Sugar density of GlcNAc6-TSC molecules immobilized on gold surfaces.

Sample	**QCM Data**		**GlcNAc6**
	ΔF (Hz)	**Mass (ng)**	**Density (Chains nm^{-2})**
Pure GlcNAc6	−30.7	0.92	0.09
GlcNAc6-TSC	−225.5	6.77	0.68

2.5.3 Cell morphology and behavior influenced by micropatterning of chitooligomers

Two different geometries, denoted as micropatterned and non-patterned GlcNAc6-SAMs, were selected for testing as functional scaffolds for engineering parallel-aligned myoblast cells, determining attachment and spreading of individual cells (Fig. 2-11). The cells adhered to all substrates after 24 h initial seeding. Significant differences in cell morphology were observed after 3–7 days. As predicted, cells adhered on GlcNAc6-SAM micropatterns showed evidence of cell alignment, while those on the non-patterned surfaces exhibited a random orientation, indicating that the cultured cells had a flat morphology and irregular shapes on TCPS and GlcNAc6-free Au patterns (Fig. 2-11a). Over a period of culture days, the morphology of myoblasts changed during their alignment on micropatterned GlcNAc6-SAMs, with cells becoming elongated (Fig. 2-11b), as denoted by the white arrows. From these results, I hypothesized that the unidirectional immobilization of chitohexaose was critical to promoting cell organization, possibly through carbohydrate-protein interactions occurring during their alignment. I further proposed that alignment in response to glyco-SAMs patterns *via* nonreducing end groups occurred through crosstalk between adherent cells involving protein binding sites and GlcNAc receptors on the C2C12 cell surface [40-42]. This would suggest that cell-cell interactions play an auxiliary role as cells become confluent and can enhance cellular alignment [43]. Some research has reported that, in cell cultures, confluence is the determining factor for achieving cell alignment, though the detailed mechanisms of improving myoblast alignment through cell–cell interactions remain unknown [44]. I examined the direction of alignment of the self-organized myoblasts, appearing as highly aligned microconstructs along the edges of the striped Au surfaces of my designed GlcNAc6-SAM micropatterns (Fig. 2-11b). Once cells began aligning on the edges, the entire micropatterned surface became covered with cells after seven days in culture. The cell bundles were densely and unidirectionally aligned on the GlcNAc6-SAM patterns. Interestingly, these alignments were similar to those formed by muscle cells *in vivo*. Another important observation was that F-actin filaments were arranged in parallel in cells cultured on GlcNAc6-SAM micropatterns (Fig. 2-12). This result indicated that the glyco-patterns could regulate carbohydrate-mediated signaling *via* F-actin anchoring of cell-substrates, potentially guiding actin alignment. The actin filament is closely associated with activation of integrin receptors at focal adhesion sites, which are important

mediators of signals initiated by adhesion molecules [45-47]. Actin filaments are also involved in cell motility across a surface and in the contractile assemblies of muscle fibers. Existence of contractile assemblies is considered to require a unique property of muscle tissues. I observed preliminary evidence of actin formation aligned in parallel to the micropatterns of glyco-SAMs five days after myoblast differentiation, as indicated by fluorescent staining of F-actin with phalloidin. Actin filament formation was also observed in cells cultured on commercial polystyrene and glyco-free substrates but without any evidence of a specific cellular orientation. Here, I highlighted the possibility of direct association between bioactive oligosaccharides and cell surface receptors *via* carbohydrate-protein interactions, without the need for serum stimulation to enhance cell adhesion at an initial stage. Then, cells straightforwardly attached onto the GlcNAc6-SAM micropatterns and changed their morphology.

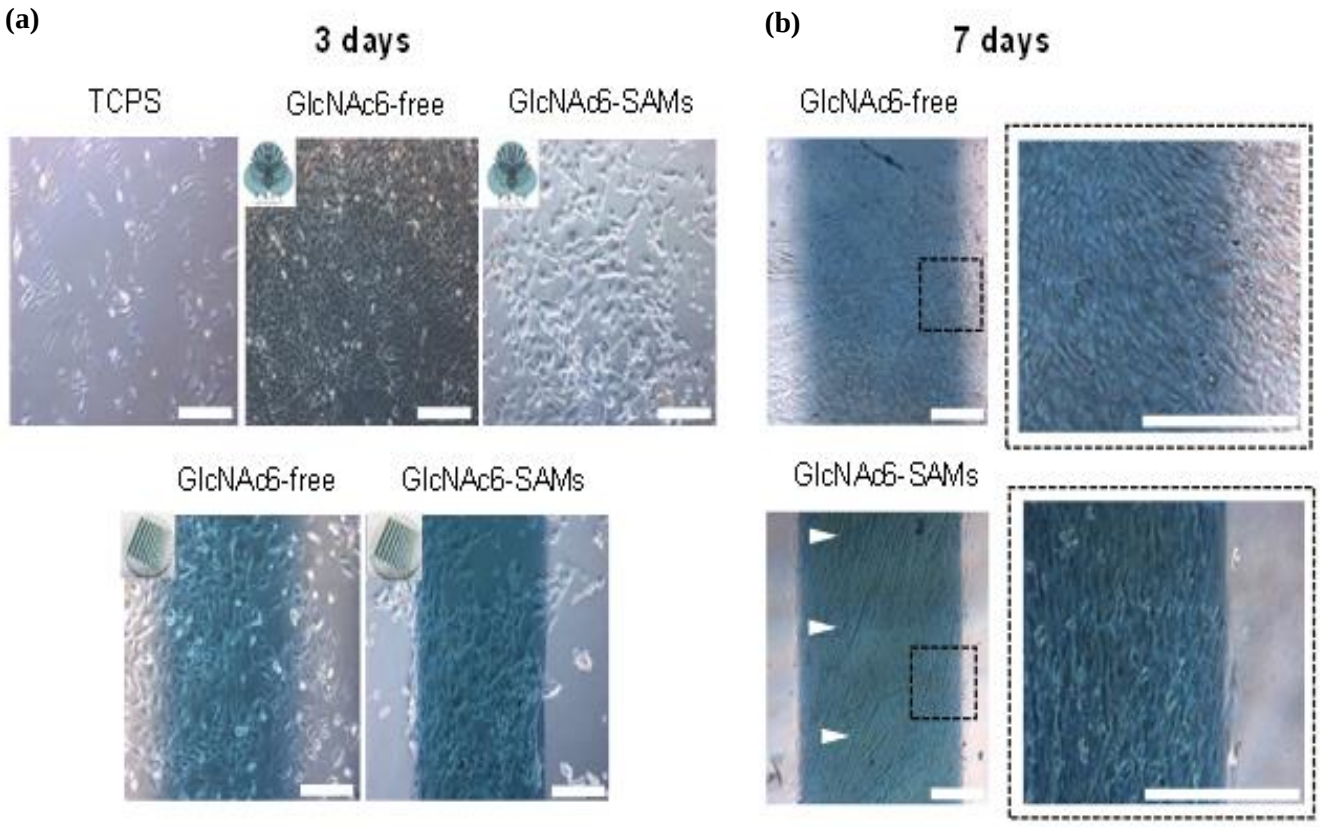

Fig. 2-11 Representative phase-contrast microscopic images of mouse myoblast C2C12 cells **a)** three days and **b)** seven days after cell seeding on GlcNAc6-SAMs and GlcNAc6-free, with and without gold micropatterned substrates. The alignment of cultured cells was clearly dependent on GlcNAc6-SAM patterns, demonstrating a densely packed cellular assembly with the outermost cells along the edge of gold micropatterns, as shown in a dashed box. The white arrows indicated the elongated myoblasts. Scale bars correspond to 200 μm.

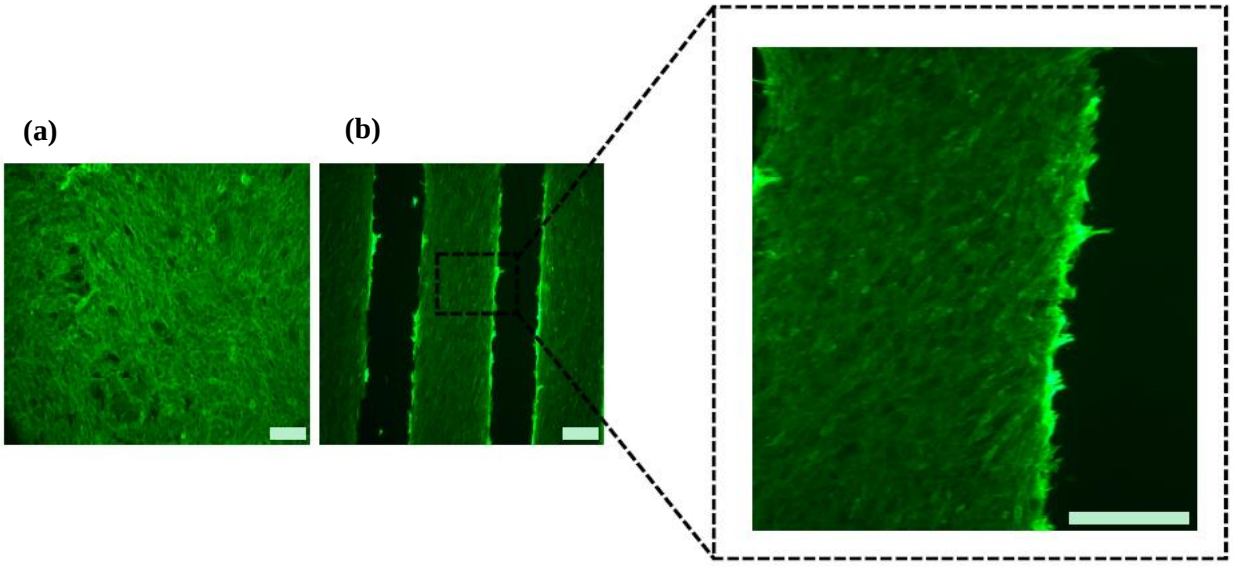

Fig. 2-12 Fluorescent images showing arrangement of actin filaments after five days culture of C2C12 cells on **a)** TCPS substrates or **b**) micropatterned GlcNAc6-SAM. Actin filaments were stained with phalloidin (green) and the characteristic morphology of densely packed bundles of actin filaments was clearly evident in cells cultured on micropatterned GlcNAc6-SAM, as shown in a dashed box. Scale bars correspond to 200 μm.

2.5.4 Effect of micropattern width on gene expression in C2C12 cells

The ability of GlcNAc6-SAM micropatterned substrates to control cell behaviors was investigated with different substrate geometries. C2C12 cells were successfully cultured and were always unidirectionally aligned on all glyco-substrates. I further observed that cells achieved the highest proliferation rates when cultured on narrower patterns, possibly because of the restricted substrate area. However, increasing the pattern width to 1000 μm resulted in overlapping of neighboring cells into interspacing areas between the GlcNAc6-SAM patterns. This suggested that the surface area of each pattern had a substantial effect on biological responses, such as myogenic cell differentiation. To address this possibility, I investigated mRNA expression, using RT-PCR, in cells cultured on GlcNAc6-SAM substrates with or without patterns. In this experiment, total RNA was collected from the exclusive area on GlcNAc6-SAMs to eliminate artifacts from gene expression induced by adjacent cells. The representative patterns were characterized by determining restriction patterns in widths of 200, 500, and 1000 μm. The predominant effect was a stronger expression of *MyoD* and *myogenin* in C2C12 cells cultured on GlcNAc6-SAMs with certain patterns. In particular, expression of these genes after three days was higher on GlcNAc6-SAM patterns having a 500 μm width than on those on non-patterned substrates or those with widths of 200 or 1000 μm (Fig. 2-13), possibly because of the presence of enough aligned cells to begin the differentiation. Clearly, after five days' culture, expression of muscle regulator genes was decreased with only trace amounts of these mRNAs detectable (Fig. 2-13b). These results were consistent with reports that the time when cultured cells have reached confluence and are ceasing proliferation represents the early stages of myogenic differentiation of myoblasts into myotubes [48-50]. I anticipated that such cellular alignment and drastic morphological alterations, possibly occurring through GlcNAc-mediated receptors on myoblast surfaces, might offer a desirable microenvironment to drive downregulation of *myogenin via* multiple intracellular signaling pathways. Such pathways are implicated in reduced transcriptional activity of the *myogenin* gene prior to commitment to differentiated myoblasts during terminal differentiation, though the molecular mechanisms by which *myogenin* controls muscle cell differentiation are still unclear. At this stage, the preliminary results may indicate that the clustering of carbohydrate oligomers had an effect not only on cell morphology and orientation, but also on dynamic activation and/or deactivation of *myogenin*. Notably, expression of the *myogenin* gene increased again after seven days in culture, possibly indicating distinct developmental stages during

myogenesis. This finding was consistent with the substantial rearrangement of myoblasts and their recognition of neighboring cells following their rigorously controlled alignment on GlcNAc6-SAM patterns (Fig. 2-13b). In contrast to that of muscle regulatory genes, *FAK* expression was not significantly affected by clustered carbohydrates or geometric patterns (Fig. 2-13a–c). I believed that GlcNAc6-SAM patterns would play an essential role in the integrin/FAK signaling pathway, which has been shown to be required for myoblast differentiation, especially for cell migration and myotube formation through cell fusion. Skeletal muscle generally expresses many integrin subunits in developmentally regulated patterns, including the integrin β1 subunit and several integrin α subunits [51,52]. Thus, I assumed that integrin activation would impact myoblast differentiation and orientation upon integrin binding to GlcNAc6 clusters. However, at some point myoblast differentiation would be indirectly inhibited by integrin due to downregulation of *MyoD* expression. I further examined the influence of clustered carbohydrates on muscle-specific transcriptional regulation. Interestingly, expression of these targeted genes was significantly higher in cells on GlcNAc6-SAM patterns, compared with those on GlcNAc6-free patterns (Fig. 2-14). It was reported that myoblasts on micropatterned PDMS films were well organized and were promoted to fuse along the direction of the microgrooves, but these micropatterned substrates did not significantly affect cytoskeletal markers at the transcriptional or protein levels [53]. This suggested that clustered carbohydrates more effectively facilitated cell alignment and biological responses of myoblast C2C12 cells by providing underlying topographical cues. Despite glyco–clustered effects may influence the expression level of each targeted gene, in the meantime, cell morphology regulated by the pattern widths also influence the gene expression. There is an ambiguous point that GlcNAc6-SAM pattern with widths of 200 μm revealed the well-aligned cells, however, the gene expression level of targeted genes was not much different among all the patterned substrates. This would be the consequence of cell-cell interaction that proliferated cells were too tight, resulted in decreased expression of genes. Nevertheless, findings represent only one of many steps needed to reach an understanding of the numerous biological signaling pathways involved in muscle regeneration. Other biomechanical aspects requiring further investigation include examining late-stage differentiation markers such as myosin heavy chain (MyHC) and troponin T and evaluating contractile properties of these cellular structures by electrical stimulation. I believe that the glyco-SAMs patterns established in my study will prove useful in future research to clarify skeletal muscle development for *in vitro* applications. Next in the chapter 3, the effect of GlcNAc6-SAM patterns on myoblasts fusion and myotube formation will be discussed.

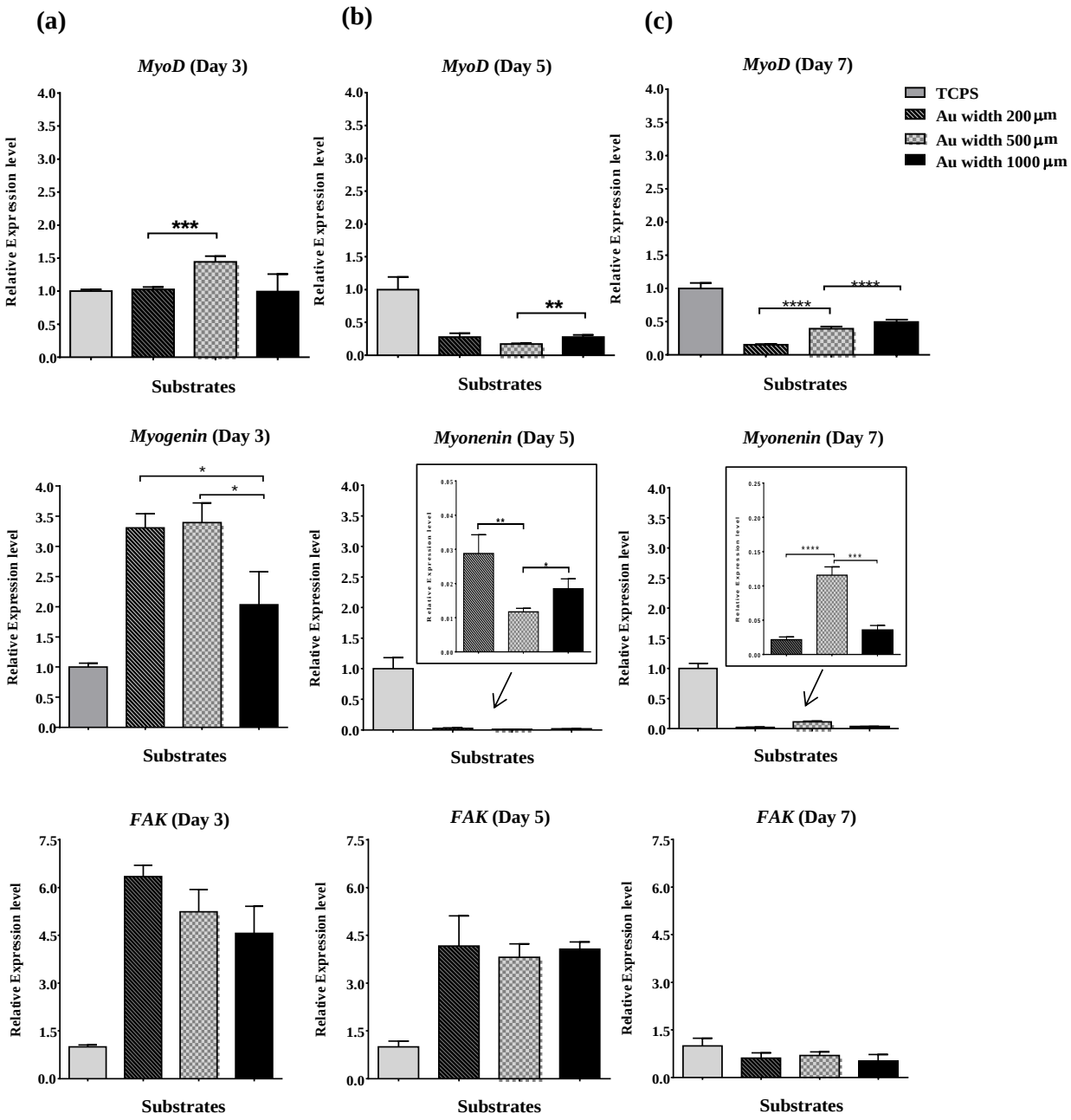

Fig. 2-13 Effects of micropattern geometries on gene expression in myoblasts. RT-PCR analysis of genes associated with myogenesis of myoblast C2C12 cells, including *MyoD*, *myogenin* and *FAK*, on micropatterned GlcNAc6-SAMs, were observed after **a**) three days; **b**) five days; and **c**) seven days of culture. Values are means ± standard error of mean. Statistically significant differences (n = 9 per sample); * $p < 0.05$; ** $p < 0.01$; *** $p < 0.001$ and **** $p < 0.0001$, by t-test.

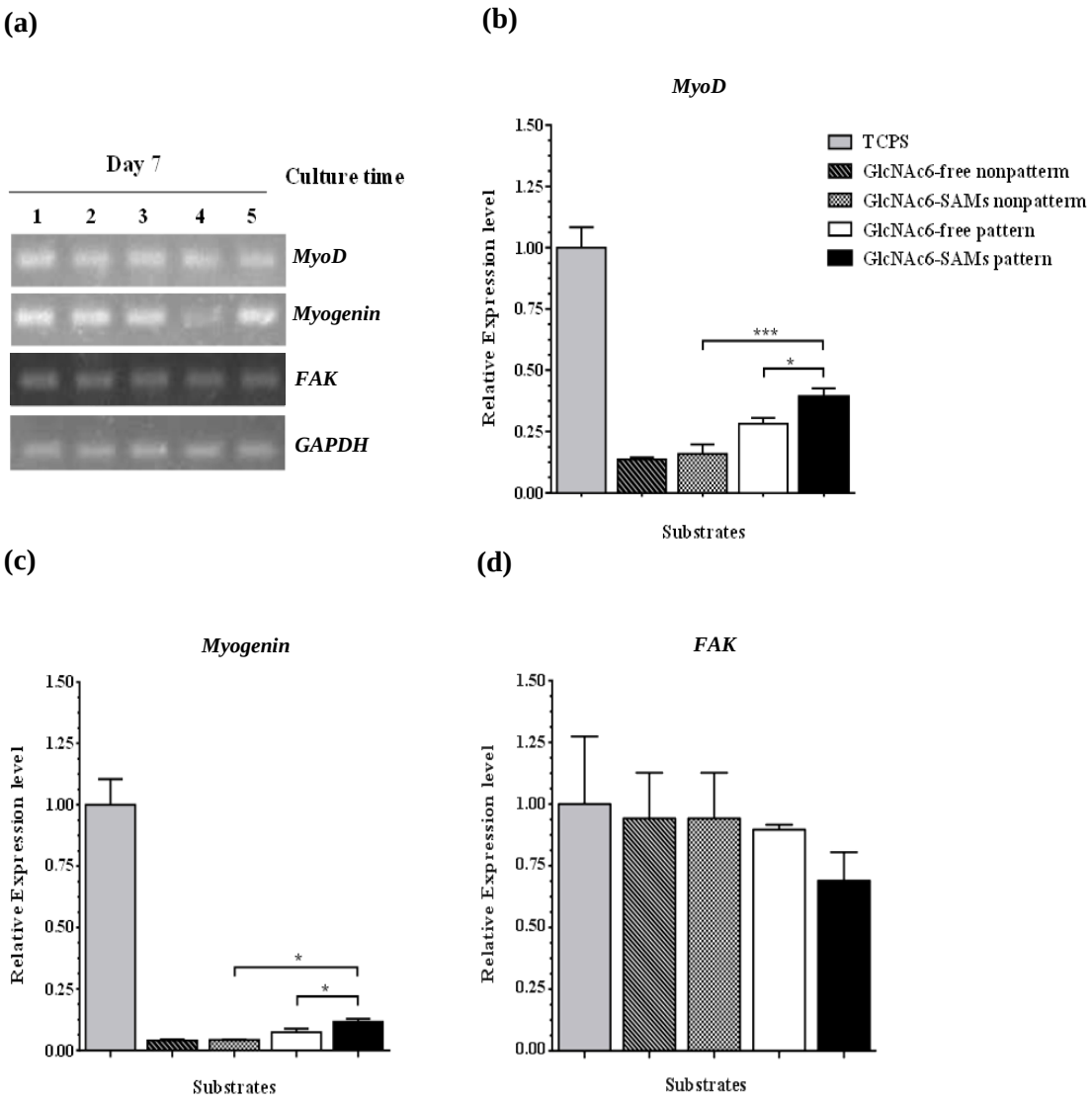

Fig. 2-14 Comparison of gene expression on micropatterns with and without GlcNAc6-SAMs after seven days' culture. The regulation of myogenin genes in myoblast C2C12 cells was detected using RT-PCR. **a**) PCR products were analyzed on a 2% agarose gel by ethidium bromide staining. Band intensities are presented, normalized to GAPDH. Lane 1, TCPS; Lane 2, GlcNAc6-free nonpatterns; Lane 3, GlcNAc6-SAMs nonpatterns; Lane 4, GlcNAc6-free pattern (500 μm); Lane 5, GlcNAc6-SAMs pattern (500 μm); **b**–**d**) Individual mRNA expression profiles in myoblast C2C12 cells on the different substrates.

2.6 Summary

Chitooligomer-SAM micropatterns on a transparent Au-coated polycarbonate surface were successfully fabricated by site-selective TSC-modification of chitohexaose at its reducing end, followed by S–Au chemisorption on the Au surface. Myoblast cells initially exhibited an apparently random attachment on these glyco-SAMs but gradually demonstrated unidirectional alignment along the micropatterned lines, after seven days in culture adopting an appearance similar to that of muscle cells *in vivo.* The underlying effects of micro-topographical patterns consisting of nonreducing ends of GlcNAc6 oligomers provide crucial insights into regulation of myoblast morphology and function, possibly involving carbohydrate-protein interactions. Controlled micropatterning for cell culture systems, based on our findings, represents a significant advance for future tissue engineering applications of glyco-biointerfaces.

References

1. Gordon, a M.; Homsher, E.; Regnier, M. Regulation of Contraction in Striated Muscle. *Physiol Rev*. **2000** *80*, 853-924.
2. Bach, A.D.; Beier, J.P.; Stern-Staeter, J.; Horch, R.E. Skeletal muscle tissue engineering. *J Cell Mol Med*. 2004, 8, 413-422.
3. Grounds, M. D.; White, J. D.; Rosenthal, N.; Bogoyevitch, M. A. The Role of Stem Cells in Skeletal and Cardiac Muscle Repair. **2002**, *50*, 589–610.
4. C Chargé, S. B. P.; Rudnicki, M. a Cellular and molecular regulation of muscle regeneration. *Physiol. Rev.* **2004**, *84*, 209–238.
5. Andres, V.; Walsh, K. Myogenin expression, cell cycle withdrawl, and phenotypic differentiation are temproarily seperable events that precede cell fusion upon myogenesis. *J. Cell Biol.* **1996**, *132*, 657–666.
6. Miller, K. J.; Thaloor, D.; Matteson, S.; Pavlath, G. K. Hepatocyte growth factor affects satellite cell activation and differentiation in regenerating skeletal muscle. *Am. J. Physiol. Cell Physiol.* **2000**, *278*, C174–C181.
7. Dean, D.A. Non viral gene transfer to skeletal, smooth, and cardiac muscle in living animals. *Am J Physiol Cell Physiol*. **2005**, *289*, C233–C245.
8. Beauchamp, J. R.; Morgan, J. E.; Pagel, C. N.; Partridge, T. A. Dynamics of myoblast transplantation reveal a discrete minority of precursors with stem cell-like properties as the myogenic source. *J. Cell Biol.* **1999**, *144*, 1113–1121.
9. Berendse, M.; Grounds, M. D.; Lloyd, C. M. Myoblast structure affects subsequent skeletal myotube morphology and sarcomere assembly. *Exp. Cell Res.* **2003**, *291*, 435–450.
10. Clark, P.; Dunn, G. A.; Knibbs, A.; Peckham, M. Alignment of myoblasts on ultrafine gratings inhibits fusion in vitro. *Int. J. Biochem. Cell Biol.* **2002**, *34*, 816–825.
11. Yaffe, D.; Saxel, O. Serial passaging and differentiation of myogenic cells isolated from dystrophic mouse muscle. *Nature* **1977**, *270*, 725–727.
12. Giancotti G.F, M. F. Integrin-mediated adhesion and signalling in tumorigenesis. *Biochim. Biophys. Acta* **1994**, *1198*, 47–64.
13. Schwartz, M. A.; Ingber, D. E. Integrating with integrins. *Mol Biol Cell* **1994**, *5*, 389–393.
14. Seller, Z. Cellular Adhesion and Adhesion Molecules. *Turkish J. Biol.* **2001**, *25*, 1–15.

15. Morfologiche, S.; Motorie, S.; Carlo, U. C 2 C 12 murine myoblasts as a model of skeletal muscle development: morpho-functional characterization. **2004**, 223–233.
16. Isenberg, B. C.; Backman, D. E.; Kinahan, M. E.; Jesudason, R.; Suki, B.; Stone, P. J.; Davis, E. C.; Wong, J. Y. Micropatterned cell sheets with defined cell and extracellular matrix orientation exhibit anisotropic mechanical properties. *J. Biomech.* **2012**, *45*, 756–761.
17. Bajaj, P.; Reddy, B. Jr.; Millet, L.; Wei, C.; Zorlutuna, P.; Bao, G.; Bashir, R. Patterning the differentiation of C2C12 skeletal myoblasts. ***Integr. Biol.,*** **2011**, ***3***, 897–909.
18. Badie, N.; Bursac, N. Novel micropatterned cardiac cell cultures with realistic ventricular microstructure. *Biophys. J.* **2009**, *96*, 3873–3885.
19. Santos, E.; Hernández, R. M.; Pedraz, J. L.; Orive, G. Novel advances in the design of three-dimensional bio-scaffolds to control cell fate: Translation from 2D to 3D. *Trends Biotechnol.* **2012**, *30*, 331–341.
20. Miller, J. S.; Stevens, K. R.; Yang, M. T.; Baker, B. M.; Nguyen, D.-H. T.; Cohen, D. M.; Toro, E.; Chen, A. a.; Galie, P. a.; Yu, X.; Chaturvedi, R.; Bhatia, S. N.; Chen, C. S. Rapid casting of patterned vascular networks for perfusable engineered three-dimensional tissues. *Nat. Mater.* **2012**, *11*, 768–774.
21. Ito, Y. Surface micropatterning to regulate cell functions. *Biomaterials* **1999**, *20*, 2333–2342.
22. Théry, M. Micropatterning as a tool to decipher cell morphogenesis and functions. *J. Cell Sci.* **2010**, *123*, 4201–4213.
23. Wen-Wen, L.; Zhen-Ling, C.; Xing-Yu, J. Methods for cell micropatterning on two-dimensional surfaces and their applications in biology. *Fenxi Huaxue/ Chinese J. Anal. Chem.* **2009**, *37*, 943–949.
24. Ross, A. M.; Lahann, J. Surface engineering the cellular microenvironment via patterning and gradients. *J. Polym. Sci. Part B Polym. Phys.* **2013**, *51*, 775–794.
25. Falconnet, D.; Csucs, G.; Michelle Grandin, H.; Textor, M. Surface engineering approaches to micropattern surfaces for cell-based assays. *Biomaterials* **2006**, *27*, 3044–3063.
26. Zhao, Y.; Zeng, H.; Nam, J.; Agarwal, S. Fabrication of skeletal muscle constructs by topographic activation of cell alignment. *Biotechnol. Bioeng.* **2009**, *102*, 624–631.

27. Brandon, G. G.; Sujata, K. B. Tissue scaffold surface patterning for clinical applications. *Biotechnol. J.* **2013**, *8*, 73–84.
28. Yoshiike, Y.; Yokota, S.; Tanaka, N.; Kitaoka, T.; Wariishi, H. Preparation and cell culture behavior of self-assembled monolayers composed of chitohexaose and chitosan hexamer. *Carbohydr. Polym.* **2010**, *82*, 21–27.
29. Yokota, S.; Kitaoka, T.; Wariishi, H. Biofunctionality of self-assembled nanolayers composed of cellulosic polymers. *Carbohydr. Polym.* **2008**, *74*, 666–672.
30. Tanaka, N.; Yoshiike, Y.; Yoshiyama, C.; Kitaoka, T. Self-assembly immobilization of hyaluronan thiosemicarbazone on a gold surface for cell culture applications. *Carbohydr. Polym.* **2010**, *82*, 100–105.
31. Yoshiike, Y.; Kitaoka, T. Tailoring hybrid glyco-nanolayers composed of chitohexaose and cellohexaose for cell culture applications. *J. Mater. Chem.* **2011**, *21*, 11150–11158.
32. Takahashi, H.; Nakayama, M.; Itoga, K.; Yamato, M.; Okano, T. Micropatterned thermoresponsive polymer brush surfaces for fabricating cell sheets with well-controlled orientational structures. *Biomacromolecules* **2011**, *12*, 1414–1418.
33. Yoshiike, Y.; Yokota, S.; Tanaka, N.; Kitaoka, T.; Wariishi, H. Preparation and cell culture behavior of self-assembled monolayers composed of chitohexaose and chitosan hexamer. *Carbohydr. Polym.* **2010**, *82*, 21–27.
34. Kobayashi, S.; Makino, A.; Matsumoto, H.; Kunii, S.; Ohmae, M.; Kiyosada, T.; Makiguchi, K.; Matsumoto, A.; Horie, M.; Shoda, S.I. Enzymatic polymerization to novel polysaccharides having a glucose-*N*-acetylglucosamine repeating unit, a cellulose-chitin hybrid polysaccharide. *Biomacromolecules* **2006**, *7*, 1644–1656.
35. Ihara, H.; Hanashima, S.; Tsukamoto, H.; Yamaguchi, Y.; Taniguchi, N.; Ikeda, Y. Difucosylation of chitooligosaccharides by eukaryote and prokaryote α1,6-fucosyltransferases. *Biochim. Biophys. Acta* **2013**, *1830*, 4482–4490.
36. Gross, T.; Lippitz, A.; Unger, W.E.S. Chemical and elemental depth profiling of very thin organic layers by constant kinetic energy XPS: A new Synchrotron XPS analysis strategy. *Anal. Chem.* **2012**, *84*, 5984–5991.
37. Livak, K.J.; Schmittgen, T.D. Analysis of relative gene expression data using real-time quantitative PCR and the 2(-Delta Delta C(T)) Method. *Methods* **2001**, *25*, 402–408.

38. Fyrner, T.; Ederth, T.; Aili, D.; Liedberg, B.; Konradsson, P. Synthesis of oligo(lactose)-based thiols and their self-assembly onto gold surfaces. *Colloids Surf. B Biointerfaces* **2013**, *105*, 187–193.
39. Liu, S.; Wang, K.; Du, D.; Sun, Y.; He, L. Recognition of glycoprotein peroxidase via Con A-carrying self-assembly layer on gold. *Biomacromolecules* **2007**, *8*, 2142–2148.
40. Walgren, J.L.E.; Vincent, T.S.; Schey, K.L.; Buse, M.G. High glucose and insulin promote *O*-GlcNAc modification of proteins, including alpha-tubulin. *Am. J. Physiol. Endocrinol. MeTab.* **2003**, *284*, E424–E434.
41. Fujita, T.; Furukawa, S.; Morita, K.; Ishihara, T.; Shiotani, M.; Matsushita, Y.; Matsuda, M.; Shimomura, I. Glucosamine induces lipid accumulation and adipogenic change in C2C12 myoblasts. *Biochem. Biophys. Res. Commun.* **2005**, *328*, 369–374.
42. Ogawa, M.; Sakakibara, Y.; Kamemura, K. Requirement of decreased O-GlcNAc glycosylation of Mef2D for its recruitment to the myogenin promoter. *Biochem. Biophys. Res. Commun.* **2013**, *433*, 558–562.
43. Vaz, R.; Martins, G.G.; Thorsteinsdóttir, S.; Rodrigues, G. Fibronectin promotes migration, alignment and fusion in an *in vitro* myoblast cell model. *Cell Tissue Res.* **2012**, *348*, 569–578.
44. Grigola, M.S.; Dyck, C.L.; Babacan, D.S.; Joaquin, D.N.; Hsia, K.J. Myoblast alignment on 2D wavy patterns: Dependence on feature characteristics and cell–cell interaction. *Biotechnol. Bioeng.* **2014**, *111*, 1617–1626.
45. Weber, G.F.; Menko, A.S. Actin filament organization regulates the induction of lens cell differentiation and survival. *Dev. Biol.* **2006**, *295*, 714–729.
46. Ting, H.J.; Chang, C. Actin associated proteins function as androgen receptor coregulators: An implication of androgen receptor's roles in skeletal muscle. *J. Steroid Biochem. Mol. Biol.* **2008**, *111*, 157–163.
47. Galli, C.; Piemontese, M.; Lumetti, S.; Ravanetti, F.; Macaluso, G.M.; Passeri, G. Actin cytoskeleton controls activation of Wnt/β-catenin signaling in mesenchymal cells on implant surfaces with different topographies. *Acta Biomater.* **2012**, *8*, 2963–2968.
48. Yaffe, D.; Feldman, M. The formation of hybrid multinucleated muscle fibers from myoblasts of different genetic origin. *Dev. Biol.* **1965**, *11*, 300–317.

49. Kim, J.A.; Shon, Y.H.; Lim, J.O.; Yoo, J.J.; Shin, H.I.; Park, E.K. MYOD mediates skeletal myogenic differentiation of human amniotic fluid stem cells and regeneration of muscle injury. *Stem Cell Res. Ther.* **2013**, doi:10.1186/scrt358B
50. Wood, W.M.; Etemad, S.; Yamamoto, M.; Goldhamer, D.J. MyoD-expressing progenitors are essential for skeletal myogenesis and satellite cell development. *Dev. Biol.* **2013**, *384*, 114–127.
51. Dudek, S.M.; Chiang, E.T.; Camp, S.M.; Guo, Y.; Zhao, J.; Brown, M.E.; Singleton, P.; Wang, L.; Desai, A.; Arce, F.T.; *et al*. Focal adhesion kinase signaling regulates the expression of caveolin 3 and 1 integrin, genes essential for normal myoblast fusion. *Mol. Biol. Cell* **2010**, *21*, 4042–4056.
52. Keselowsky, B.G.; Collard, D.M.; Garcia, A.J. Integrin binding specificity regulates biomaterial surface chemistry effects on cell differentiation. *Proc. Natl. Acad. Sci. USA* **2005**, *102*, 5953–5957.
53. Huang, N.F.; Lee, R.J.; Li, S. Engineering of aligned skeletal muscle by micropatterning. *Am. J. Transl. Res.* **2010**, *2*, 43–55.
54. James F. Thompson. Individual lecture and lab course information. Chapter 09: Sliding filament mechanism. http://www.apsubiology.org/anatomy/2010/2010_Exam_Reviews/Exam_3_Review/CH_09_Sliding_Filament_Mechanism.htm)
55. Share and Discover Knowledge on LinkedIn SlideShare. http://www.slideshare.net/aljeirou/adhesion-molecules

Chapter 3

Chapter 3

Myoblasts fusion and Myotube formation

One important aspect of myogenic differentiation in mammalian cells is the generation of multinucleate muscle fibers through the fusion of myoblasts. There are several roles that involved in mammalian myoblast fusion process such as the recruitment of specific cell-surface proteins between fusion partners and some signaling pathways that activate myogenic differentiation program including the geometrically-confined topography substrates. In this chapter, I provided new insight into direct stimulation of myoblast cell fusion by incorporating chitohexaose (hexa-*N*-acetyl-D-glucosamine (GlcNAc6)) oligomers in microtopographical cues, to promote the differentiation of myoblasts under culture conditions without the addition of horse serum or any other differentiation media. C2C12 cells were preferentially aligned along the chitohexaose patterns (GlcNAc6-SAMs) and demonstrated myotube-like characteristics. The GlcNAc6-SAMs, containing six *N*-acetyl-D-glucosamine (GlcNAc) residues, may be attractive for practical engineering of customized muscle-like tissue architectures. I anticipated that the parallel alignment of myoblasts would consequently facilitate cell fusion by promoting the contractile activity of cells through contraction-stimulated glucose uptake and regulation of glucose transporter 4 (GLUT4), a major glucose transporter, which has been identified and is predominantly expressed in C2C12 myoblasts [1] (this part will be discussed in chapter 5). Additionally, results revealed that GlcNAc6-SAM patterns enhanced the relative mRNA expression level of myosin heavy chain isoforms (MyHCs). Thus, in this study, I demonstrated that established carbohydrate-functionalized surface geometries enable the formation of robust myotubes from myoblasts without adding any differentiation culture medium. These findings are a crucial step toward tissue engineering and may have a great therapeutic potential in the future.

3.1 Myoblasts development process

Myoblast fusion is an indispensable step in the cell maturation process during the development and regeneration of adult skeletal muscular cells. At the cellular level, the fusion process of myoblasts is mainly involved in two characteristic stages: the phenotypic conversion and the subsequent transformation into multinucleated myotubes. Initially, the alignment of myoblasts was identified as critical for myoblast fusion *via* migration, recognition and rearrangement of the actin cytoskeleton at contact sites between two myogenic cells and the material surfaces. Then, membrane fusion occurs, leading to myoblast-myoblast fusion, which promotes the formation of nascent myotubes. Finally, growth of muscle fibers is accomplished by nuclei acceleration and the formation of more mature myotubes [2-5]. In addition a number of signaling molecules and pathways have been involved in the activation of fusion-competent myoblasts that regulate primary myoblast fusion, which results in nascent myotubes. Additional signaling molecules are then recruited, which lead to fusion of additional mononucleated myoblasts with nascent myotubes. Major signaling molecules involved in primary and secondary myoblast fusion based on experimental evidence are depicted in the upper line and specific myogenic markers expressed at different stages in cells of myogenic lineage during myogenesis are noted along the bottom as shown in Figure 3-1.

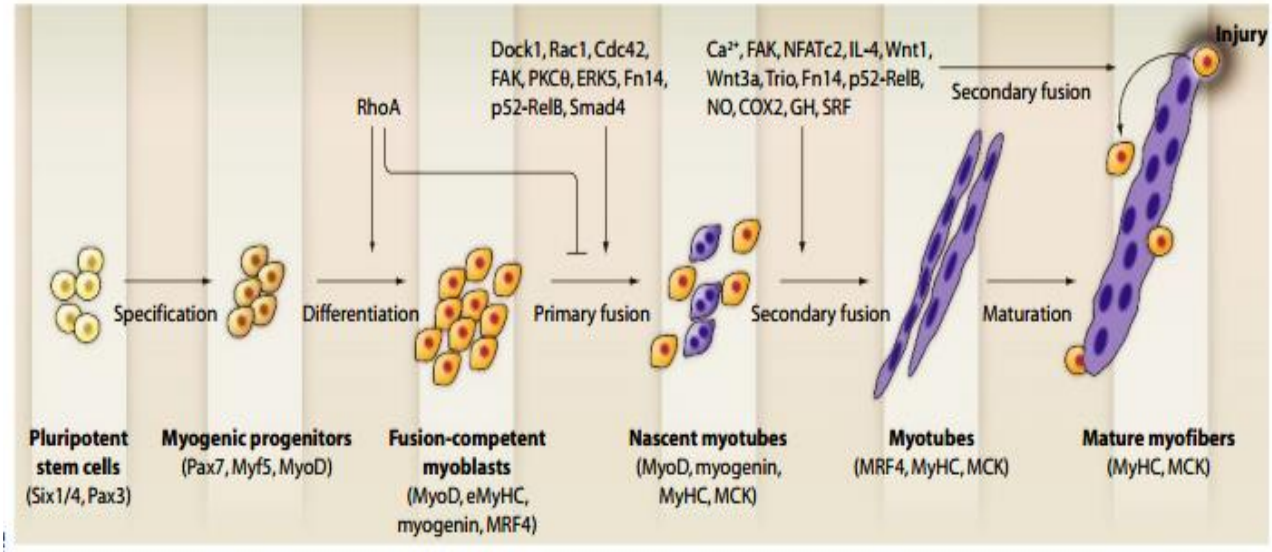

Fig. 3-1 The roles of different signaling molecules in primary and secondary myoblast fusion during myogenesis. (Hindi, S.M.; Tajrishi, M.M.; Kumar, A. Signaling mechanisms in mammalian myoblast fusion. *Sci. Signal.* **2013**, *6*, re2, doi:10.1126/scisignal.2003832)

3.2 Myotube formation

The differentiation of skeletal myoblasts (C2C12; a mouse myoblast cell line) and myotube maturation *in vitro* require switching from growth medium to differentiation medium, to decrease growth factors and slow cell proliferation, resulting in withdrawal from the cell cycle. Consequently, cell differentiation is promoted, and muscle-specific gene expression is initiated [6,7]. Over the past decade, serum-free culture has been required for tissue engineering, to avoid immune rejection for *in vitro* applications. Many studies have been reported that cells were treated under either serum-free or differentiation serum-free conditions [8–10]. Stevenson *et al.* [11] have shown that the cessation of feeding of myotubes in cell culture by starvation without media and serum replenishment resulted in the formation of significantly thinner myotubes and subsequent reduction in diameter, leading to rapid atrophy compared to control cells. Starvation atrophy in myotubes is presumed to be involved in the generation of reactive oxygen species, including changes in the transcription profiles [11]. Therefore, achieving direct stimulation of myoblast differentiation and fusion on the substrate in culture with growth serum medium without any addition of differentiation factors would be a promising progress in the development of functional muscles for *in vitro* applications. In addition, many studies have revealed that signaling pathways regulate various transcription factors and have provided significant information on the molecular mechanisms of cell fusion by the cooperative crosstalk of the core signal transduction machinery of each pathway [12–15] (Fig. 3-2). The understanding of these pathways has deepened through biomolecular interactions, occurring at cell-surface receptors *via* intracellular domain-associated signaling or adaptor proteins inside the cells. Furthermore, numerous types of natural bioactive molecules, which are immobilized on cell culture scaffolds, can immensely affect myoblast functions, particularly encouraging myotube formation and contractibility [16–19]. *In vitro*, the physicochemical properties of cell culture scaffold materials have been implicated to assist in mimicking the three-dimensional microenvironment conditions and represented the attainable goals of controlling cell behaviors and cell responses. The geometrically-confined topography at the micro- and nano-scale features influences the enhancement of myoblast fusion into myotubes by affecting the reorganization of the cytoskeleton and focal adhesion kinase (FAK) [20–22].

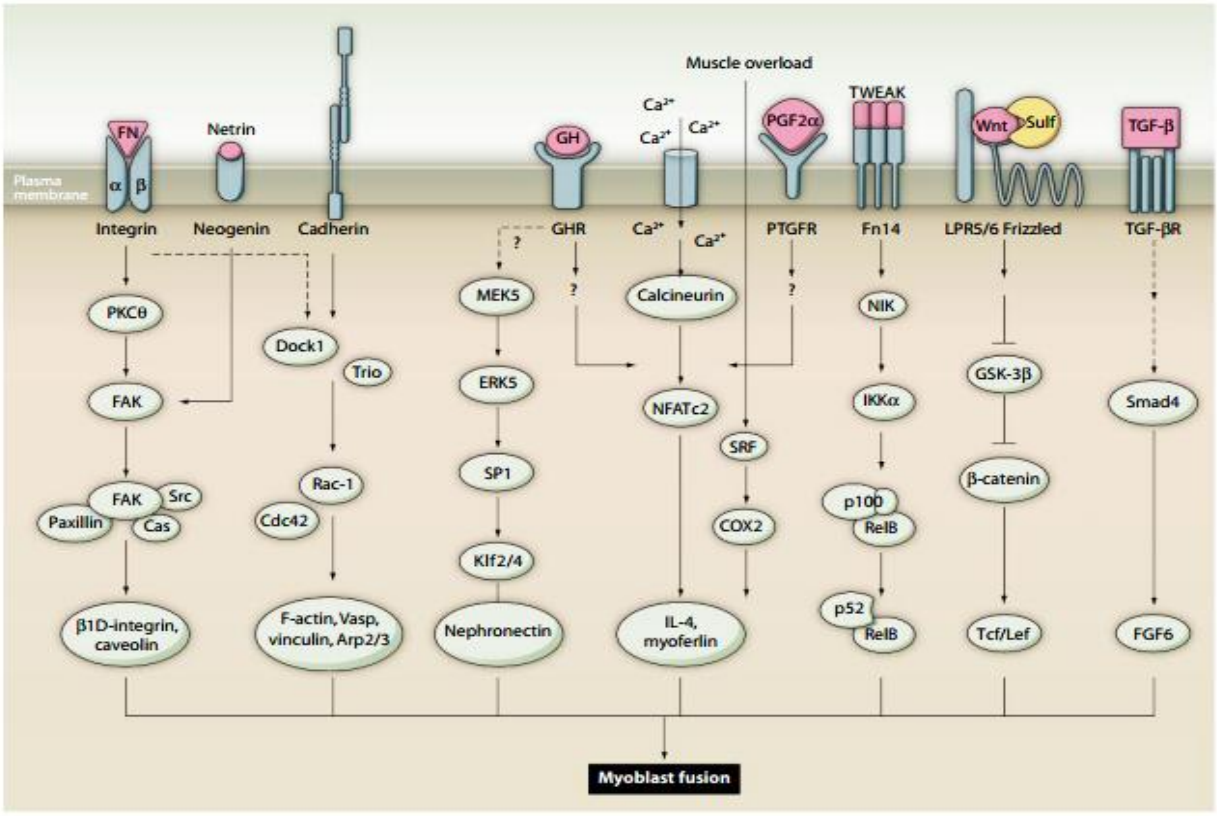

Fig. 3-2 The signaling mechanisms that stimulate myoblast fusion. (Hindi, S.M.; Tajrishi, M.M.; Kumar, A. Signaling mechanisms in mammalian myoblast fusion. *Sci. Signal.* **2013**, *6*, re2, doi:10.1126/scisignal.2003832)

3.3 Myosin heavy chain and its isoforms

The skeletal muscle comprises approximately 40% of the body mass and functions to empower body movements, including the regulation of systemic energy metabolism [23,24]. The skeletal muscle is mainly composed of myofibers, and myofiber composition in each muscle is heterogeneous, containing a mixture of slow and fast type myofibers [25]. These fiber phenotypes are first established during embryonic development by intrinsic myogenic control mechanisms and later changes in response to hormonal and neural influences [26]. The molecular mechanisms of the heterogeneity and plasticity of muscle fibers have been investigated through several signaling pathways which mediated the emergence of specific muscle phenotypes [27-30]. One main criterion to classify myofiber is based on myosin heavy chain (MyHC) isoforms expression. MyHCs are characterized as regulators that lead to a major change in cell membrane transformation during the late stage of myogenic differentiation, contributing to variations in contractile dynamic characteristics in myoblasts [31-33]. The characterization of MyHC isoforms can be divided as type 1 and type 2. The different isoform of MyHC can modulate the different type of muscle fibers by mean of MyHC type 1 generates slow-twitch type of muscle fiber, which is mostly found in cardiac muscles [34]. Otherwise, MyHC type 2 regulates fast-twitch type, which can be further divided into three isoforms such as 2A, 2B and 2C [35]. MyHC-2A and MyHC-2B are present in most cells, whereas MyHC-2C is not widely expressed and may have a role in cancer cells [36]. In addition, MyHC type 2 also bundles actin filaments owing to its actin-binding properties, which are responsible for skeletal muscle contraction [37,38].

3.4 Materials and Method

3.4.1 Materials

Materials are used in this experiment as described in chapter 2 section 2.4.1

3.4.2 Synthesis and fabrication of carbohydrate-functionalized monolayers on gold micropatterns

Briefly, chitohexaose (GlcNAc6) was prepared by acid hydrolysis and subsequently confirmed by chemical characterization as reported in our previous study [39]. Two-dimensional flattened micropatterns were designed with various intrinsic widths (200, 500 and 1000 μm), using template masks (Microtech Laboratory, Kanagawa, Japan). The patterned substrates were immersed in 1.0 M aqueous solution of chitohexaose conjugated with thiosemicarbazide (GlcNAc6-TSC) prior to subsequent initiation of cell culture. The formation of carbohydrate self-assembled monolayers (GlcNAc6-SAMs) was reproducibly achieved on gold micropattern surfaces using site selective conjugation with TSC at their reducing end groups, subsequent to depositing on the micropatterns through thiol chemisorption.

3.4.3 Cell culture assay

Mouse-derived C2C12 myoblasts were cultured in complete media consisting of DMEM supplemented with 10% FBS. Substrates were sterilized with ultraviolet (UV) light prior to cell seeding, as previously reported [39]. Briefly, 5.0×10^4 cells were seeded on control (TCPS) or micropatterned substrates in a 24-well plate. To induce cell differentiation on the TCPS substrate for the immunostaining experiment, cells were grown to confluence, and cell culture was shifted to DMEM supplemented with 2% horse serum (Thermo Fisher Scientific Inc., Massachusetts, USA). Differentiation medium was changed every day during 6 days of cell culture. Samples were incubated for 3, 5 and 7 days at 37 °C in an atmosphere of 95% air and 5% CO_2 for immunostaining and mRNA gene expression analysis. The numbers of viable cells were counted using an automated cell counter (TC 20TM, Bio-Rad Laboratories, Inc., Philadelphia, PA, USA) after treatment with a 0.4% trypan blue solution. Cell behaviors and morphological changes were observed with a phase-contrast microscope (Leica DMI 4000B microscope, Wetzlar, Germany).

3.4.4 Quantification of mRNA by real-time quantitative polymerase chain reaction (RT-PCR)

Extraction of total RNA was performed using ISOGEN (Nippon Gene Co., Ltd., Toyama, Japan) according to the manufacturer's instructions. cDNA templates were synthesized from 20 ng of total RNA and were reverse transcribed using PrimeScriptase RTase (Takara Bio Inc., Shiga, Japan), followed by triplicate polymerase chain reaction (PCR) reactions in 10 µL of SYBR Green Master Mix (Applied Biosystems™, Life Technologies, New York, NY, USA), containing 10 µM of forward and reverse primers. The primer sequences for each gene (Table 2) were designed by the primer 3 plus software and the NCBI PubMed primer blast software. Amplification and quantification of mRNA were performed at 95 °C for 20 s, followed by 40 cycles of 3 s at 95 °C and 30 s at 60 °C. After amplification, a melting curve analysis was carried out to verify the specificity of amplification products. The relative expression levels of target genes were normalized by subtracting the corresponding *GAPDH* and β-*actin* threshold cycle (C_T) values and using the $\Delta\Delta C_T$ comparative method [40]. PCR products were separated on 2% agarose gels, stained with ethidium bromide and then photographed under UV light to confirm a single amplicon.

3.4.5 Immunostaining of MyHC

After 3, 5 and 7 days of cell culture in either differentiation serum-free or differentiation serum-containing media, C2C12 cells were rinsed with cold PBS and pre-fixed with 4% (*v*/*v*) formaldehyde in the culture medium for 2 min. Then, the medium was replaced with 2% (*v*/*v*) formaldehyde and incubated for 20 min at room temperature (RT). After washing twice with PBS and wash buffer (0.1% BSA in PBS), blocking buffer (PBS/10% normal donkey serum (ab166643)/0.3% Triton® X-100) was added to avoid non-specific staining for 45 min at RT. Cells were then immunostained for myosin by incubation with a mouse monoclonal anti-MyHC antibody (MF-20, diluted in the PBS, 1:100; R & D Systems, Inc., Minneapolis, MN, USA), followed by the secondary antibody, which was visualized with a donkey anti-mouse IgG (H + L) antibody conjugated with Alexa Fluor 594 (NL007, 1:200 dilution; R & D Systems, Inc.), at RT for 1 h. Subsequently, the nuclei were stained with DAPI (1:1000 in PBS; Nissui Pharmaceutical). Fluorescence images at different magnifications were acquired to visualize the myotubes using a confocal microscope (Nikkon ECLIPSE TE2000-U, Nikon Corporation*).*

Table 2. List of primers used for validation of gene expression using quantitative real-time RT-PCR.

Target gene	Forward sequencing primer (5' to 3')	Reverse sequencing primer (5' to 3')	Product length (bp)	Accession number
GLUT4	GTAACTTCATTGTCGGCATGG	AGCTGAGATCTGGTCAAACG	155	NM_009204
MyHC-1	GTCCAAGTTCCGCAAGGT	CCACCTAAAGGGCTGTTG	205	NM_080728
MyHC-2a	TGACCTTGAGCTGACACTGG	CGGTGCCACAGGCAAACTG	194	NM_001039545.2
MyHC-2b	CGGTGCCACAGGCAAACTG	AGAAGCATCTCAATAAGCTCTGGTT	150	NM_010855.3
GAPDH	CCGTGTTCCTACCCCCAATG	AAGCCCAGCTCTCCCCATA	82	NM_008084.3
β-*actin*	GATTACTGCTCTGGCTCCTAG	GACTCATCGTACTCCTGCTTG	147	NM_007393.5

3.5 Results and discussion

3.5.1 Effects of topographical features and chitooligomers on myotube formation

I successfully fabricated a synergistic combination of topographical characteristics and GlcNAc6 oligomers self-assembled in two different geometries, as depicted in Figure 3-3, according to my previous report [39]. Here, C2C12 cells were cultured on GlcNAc6-SAMs or GlcNAc6-free substrate, to confirm the hypothesis that immobilized GlcNAc6 oligomers promote myoblast fusion and to demonstrate direct myotube formation in a culture system without any replenishment of differentiation medium. I found that the myoblasts started to fuse together on GlcNAc6-SAM patterns after five days of culture (Fig. 3-4a) and subsequently promoted unidirectional cell orientation, as well as actin alignments after seven days of culture (Fig. 3-4b). In contrast, myocytes and undifferentiated C2C12 cells were observed on GlcNAc6-free patterns, the GlcNAc6-SAM non-pattern and control tissue culture polystyrene (TCPS) substrates. This result suggests that physical structures of the underlying GlcNAc6-SAM substrates can influence the clustering of integrins and other adhesion molecules, which in turn activate singling pathways that ultimately govern cell behavior. It is possible that such an interaction occurs at the interface of GlcNAc6 oligomers and integrin-based adhesion complexes, which are a prerequisite for myotube formation during the first phase of myoblasts fusion.

To gain more insights into the influence of topography-mediated myoblast differentiation on myotube functions, I first evaluated the mRNA expression levels of *GLUT4* and *MyHC* isoforms, which have a significant role in the indirect physiochemical mechanism of the spontaneous contractions of differentiated myoblasts. At this stage, experiments were conducted at day 7 after the initial cell seeding, according to the late stage differentiation of C2C12 cells. GlcNAc6-SAM-fixed patterns demonstrated a statistically-significant higher expression of the *GLUT4* and *MyHC* genes, compared to that on the GlcNAc6-SAM non-pattern or GlcNAc6-free patterns (Fig. 3-4c–e). This indicated that primary myotubes preferentially form themselves on GlcNAc6-SAM substrates. These results are consistent with my prior finding that clustered carbohydrate patterns regulated more effectively myoblast behavior than carbohydrate-free substrates [39]. Topographical features may effectively direct myotube maturation; thus, I examined whether micropatterned GlcNAc6-SAM substrates play a vital role in transcriptional regulation (up- or down-regulation) of the

activation of mechanotransduction signaling, which is involved in subsequent myoblast fusion. The following experiments were undertaken on GlcNAc6-SAMs, which were designed to have the exact dimensions of micropatterned widths of 200, 500 and 1000 μm.

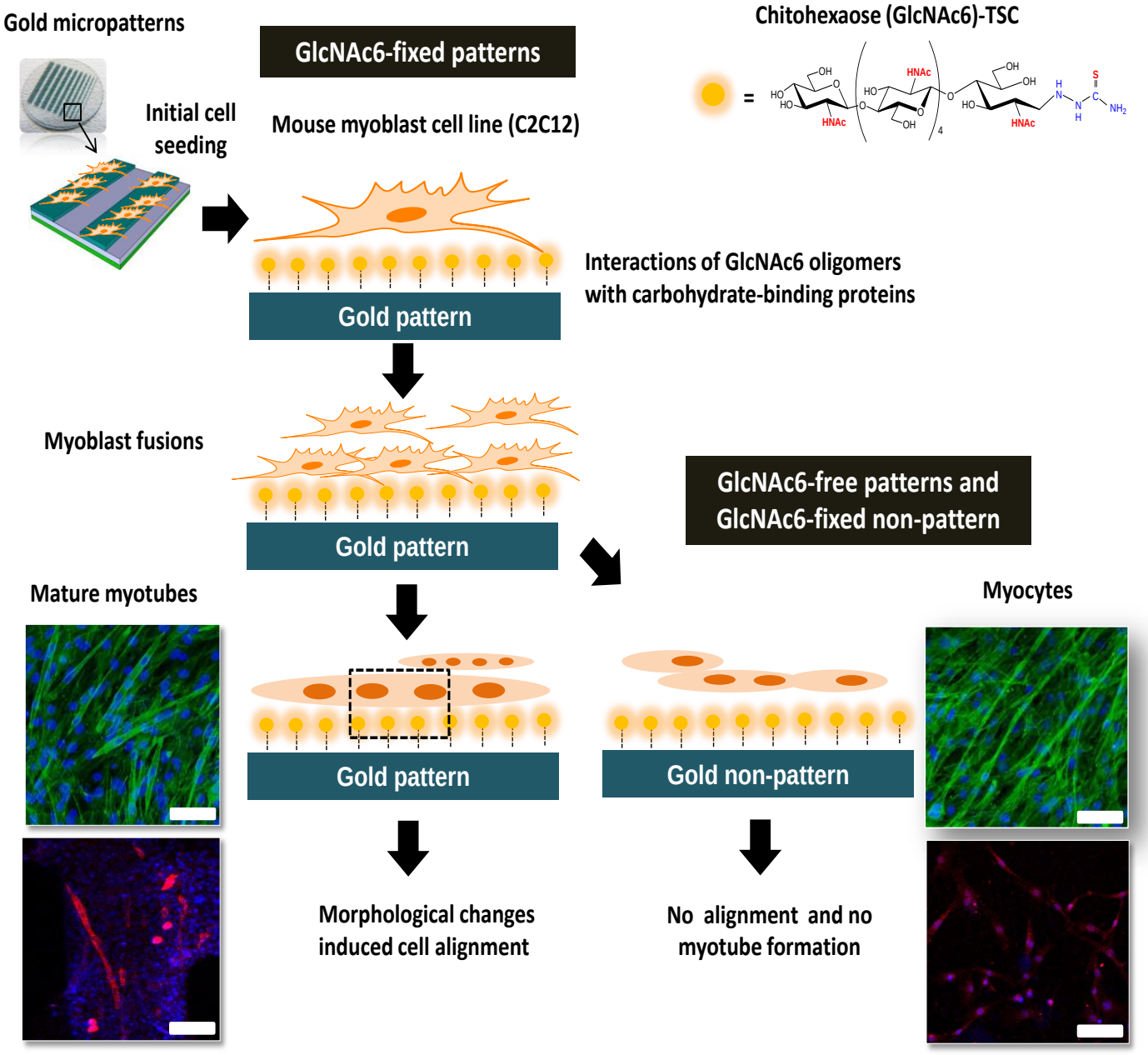

Fig. 3-3 Cont.

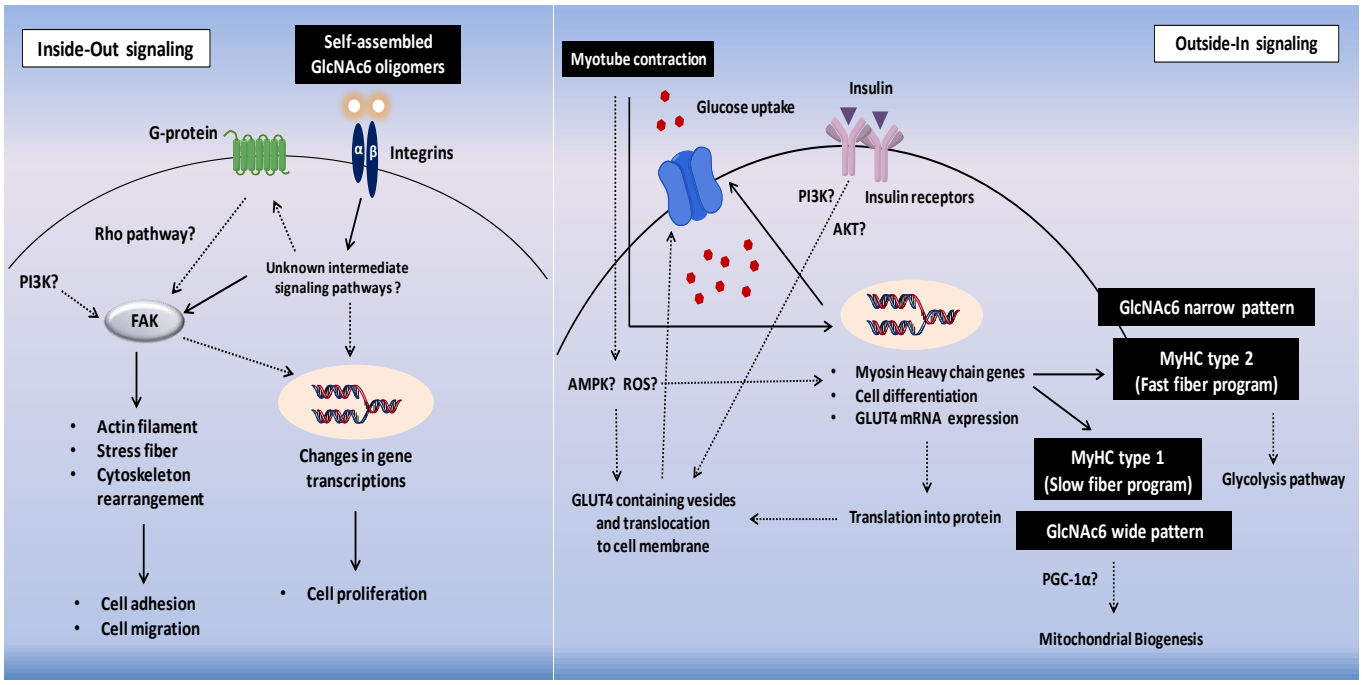

Fig. 3-3 Schematic illustration of differentiation behavior and myoblast fusion on microscale topographical patterns of hexa-*N*-acetyl-D-glucosamine (GlcNAc6)-self-assembled monolayers (SAMs) and GlcNAc6-free substrates, directing myotube formation and the possible cellular signaling machinery involved in gene regulation and contraction-stimulated glucose uptake through a specific GlcNAc6-receptor interaction on cell surfaces, which denoted in a dashed black box. The main signaling pathways for possible regulation through GlcNAc6 oligomers interacting with glyco-receptor proteins in myoblasts (thick arrows) and the convergence of unknown signaling pathways that induce myoblast fusion (dashed arrows) are depicted. Scale bars represent 200 μm.

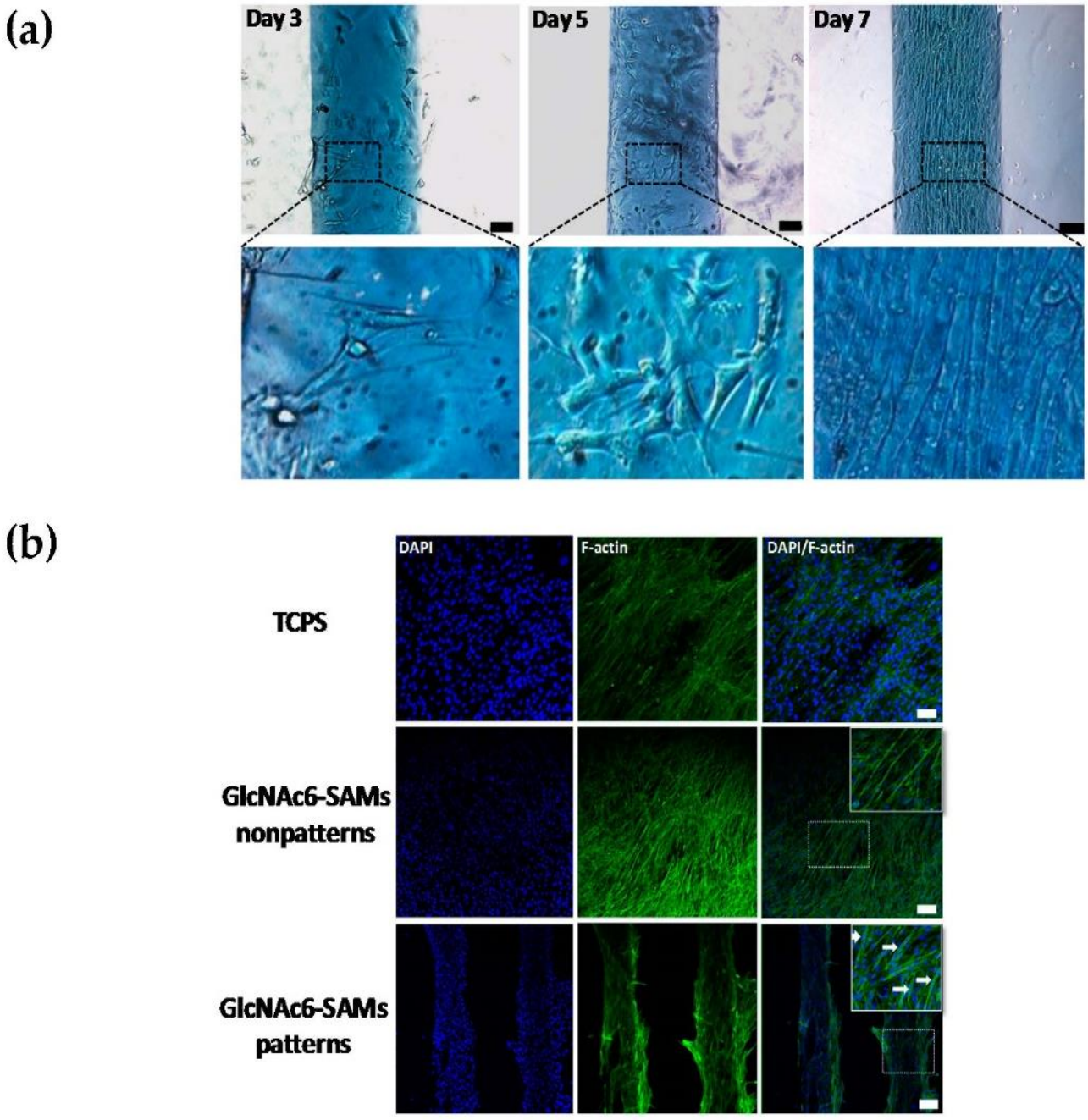
(a)
Day 3
Day 5
Day 7
(b)
DAPI
F-actin
DAPI/F-actin
TCPS
GlcNAc6-SAMs nonpatterns
GlcNAc6-SAMs patterns

Fig. 3-4 Cont.

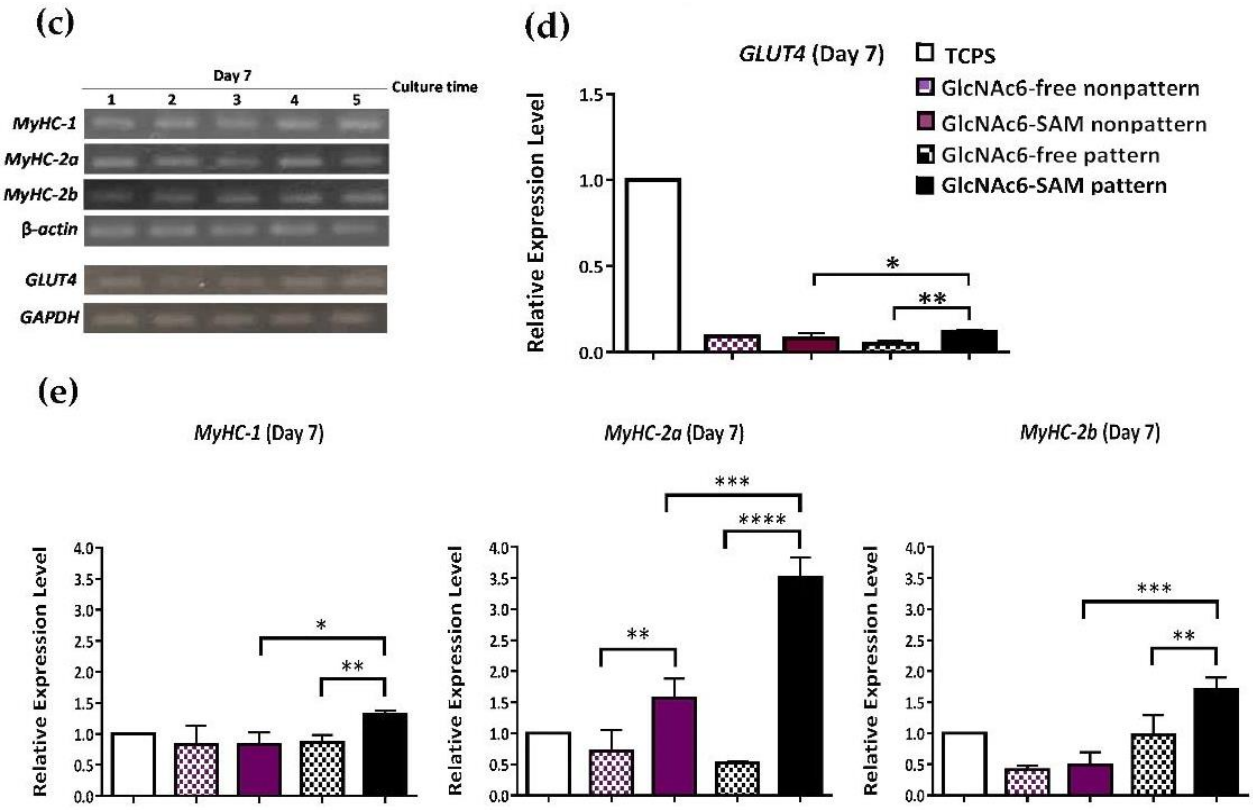

Fig. 3-4 Effects of micropatterns and non-patterns with or without GlcNAc6-SAMs on differentiated C2C12 cells during myotube development. **a**) Myoblast differentiation proceeds in stages from days 3–7 under culture medium without switching to differentiation medium on the GlcNAc6-SAM pattern (1000 μm). **b**) Confocal images of differentiated myoblasts on the GlcNAc6-SAM pattern (500 μm). Actin filaments were stained green, and nuclei were visualized with DAPI (blue) after seven days of culture. Myotubes are labeled with white arrows. Scale bars represent 200 μm **c**–**e**). mRNA expression levels of *GLUT4* and three isoforms of myosin heavy chains (*MyHCs*) in myoblasts after seven days of culture. The expression level was normalized to *GAPDH* and β-*actin* for *GLUT4* and *MyHCs*, respectively. Representative polymerase chain reaction (PCR) products of target genes were determined on 2% agarose gels by ethidium bromide staining. Lane 1: tissue culture polystyrene (TCPS); Lane 2: GlcNAc6-free non-pattern; Lane 3: GlcNAc6-SAM non-pattern; Lane 4: GlcNAc6-free pattern (500 μm); and Lane 5: GlcNAc6-SAM pattern (500 μm). Asterisks signify a significant difference from the appropriate control value. Values are the mean ± SEM, $n = 9$ per each sample; * $p < 0.05$, ** $p < 0.01$, *** $p < 0.001$ and **** $p < 0.0001$.

3.5.2 Early and late stages of myoblast fusion on GlcNAc6-SAM patterns

Myoblast fusion in skeletal muscle is an essential early step indispensable for the generation of multinucleated myofibers during *in vivo* muscle development. MyHC, a motor protein of muscle thick filaments that performs in the generation of mechanical force in skeletal muscle contraction, has fundamental roles in the dynamic regulation of myoblast fusion [10,41]. The biochemical properties of muscle fibers are involved in the speed of contraction and ATPase activity, in which MyHC type 1 (*MyHC-1*) has been shown to be responsible for slow contraction, whereas *MyHC-2* is responsible for fast contraction [42-44]. In this study, I examined whether different geometries of GlcNAc6-SAM micropatterns can directly influence myoblast differentiation and its spontaneous contraction in a differentiation serum-free medium.

This hypothesis was assessed by validation of the gene expression of *MyHCs*, of which three individual isoforms have been identified as *MyHC-1*, *MyHC-2a* and *MyHC-2b*. The different *MyHC* isoforms have very different individual characteristics for defining specific muscle properties in mammalian adult skeletal muscle cells. Comparison of the mRNA expression levels revealed that at three days after cell seeding, there was only a trace amount of *MyHCs* detected (Fig. 3-5a,c). Furthermore, low intensity staining of cells was visualized on substrates (Fig. 3-5b), suggesting that nearly no myoblast fusion occurred.

However, the expression levels of *MyHc-2a* on all GlcNAc6-SAM patterns increased between day 3 and 5 of cell culture by eight-fold on GlcNAc6-SAM with narrow patterns and by five-fold on the wide pattern (Fig. 3-5c,d). Conversely, we observed no changes in the mRNA expression level of MyHC-2b. However, there was a slight increase in MyHC-1 expression on the narrow pattern (200 µm) and wide pattern (1000 µm). These results suggest that cultured myoblasts on GlcNAc6-SAM patterns underwent differentiation with complicated changes in morphology and were subsequently able to drastically transform. Interestingly, the initial stage of myoblast-induced cell fusion seems likely to depend on *MyHc-2a* gene expression. This is because *MyHc-2a* more involves the translation of biochemical signaling pathways into forces that move cells and thus activates actin polymerization, whereas *MyHc-2b* shows the retraction prevents over-elongation of myoblasts [45]. The expression level of *MyHC-1* on the wider pattern (1000 µm) was higher than that on the narrow patterns between day 5 and 7 of cell culture; however, the level of *MyHC-2b* expression did not significantly change during myoblast development (Fig. 3-5c–e). This indicated

that cultured myoblasts on the wider pattern may have a high possibility to convert themselves to cardiomyocyte-like cells. Conversely, the narrow patterns showed higher expression of *MyHC-2b* and consistently altered in the expression levels of both *MyHC* type 2 isoforms (Fig. 3-5d,e). This implied that narrow patterns preferentially upregulated the expression of *MyHC* type 2 upon cell commitment and induced drastic downregulation of *MyHC* type 1 with time, due to the rapid significant increase in myoblast fusion, which later transformed into myotubes. This suggests that the onset of cell cycle withdrawal can be greatly accelerated by narrower patterns and demonstrated an early differentiation phase. Furthermore, the effects of narrow dimensions on end-to-end alignment of myoblasts are a synergistic factor for enhancing fusion and differentiation into myotubes, because myoblasts are polarized cells, and the decrease in the width of the topographical features increased the migration rate, resulting in enhanced recognition and adhesion of myoblasts prior to fusion [46]. However, it has been reported that myoblasts were not able to fuse on narrow substrates despite cells being highly aligned in one direction and exhibiting lateral contacts with neighboring cells [47]. Because of these discrepancies, I confirmed that GlcNAc6-SAMs play a key role in myoblast fusion through aligned assembly of myoblasts to promote the subsequent fusion and differentiation into multinucleated myotubes.

To compare the morphological changes of myotubes in the late stage of muscle differentiation, herein, myoblasts were cultured in differentiation serum-free and differentiation serum-containing media. Immunostaining at day 7 confirmed that the myoblasts were completely transformed into myotubes by fusion on GlcNAc6-SAM patterns under differentiation serum-free conditions, showing the long and thin appearance of myotubes. By contrast, control TCPS substrate promoted thicker myotubes with numerous branched structures under differentiation serum-containing conditions, when compared to those of GlcNAc6-SAM patterns (Fig. 3-5b). This indicated that more mature myotubes were found on the control substrate, due to the effect of differentiation media. However, these results revealed that GlcNAc6 oligomer-fixed geometries enhanced the fusion efficiency of myoblasts and greatly influenced the regulation of myotube formation without requiring any differentiation medium during cell culture, eventually leading to muscle contraction.

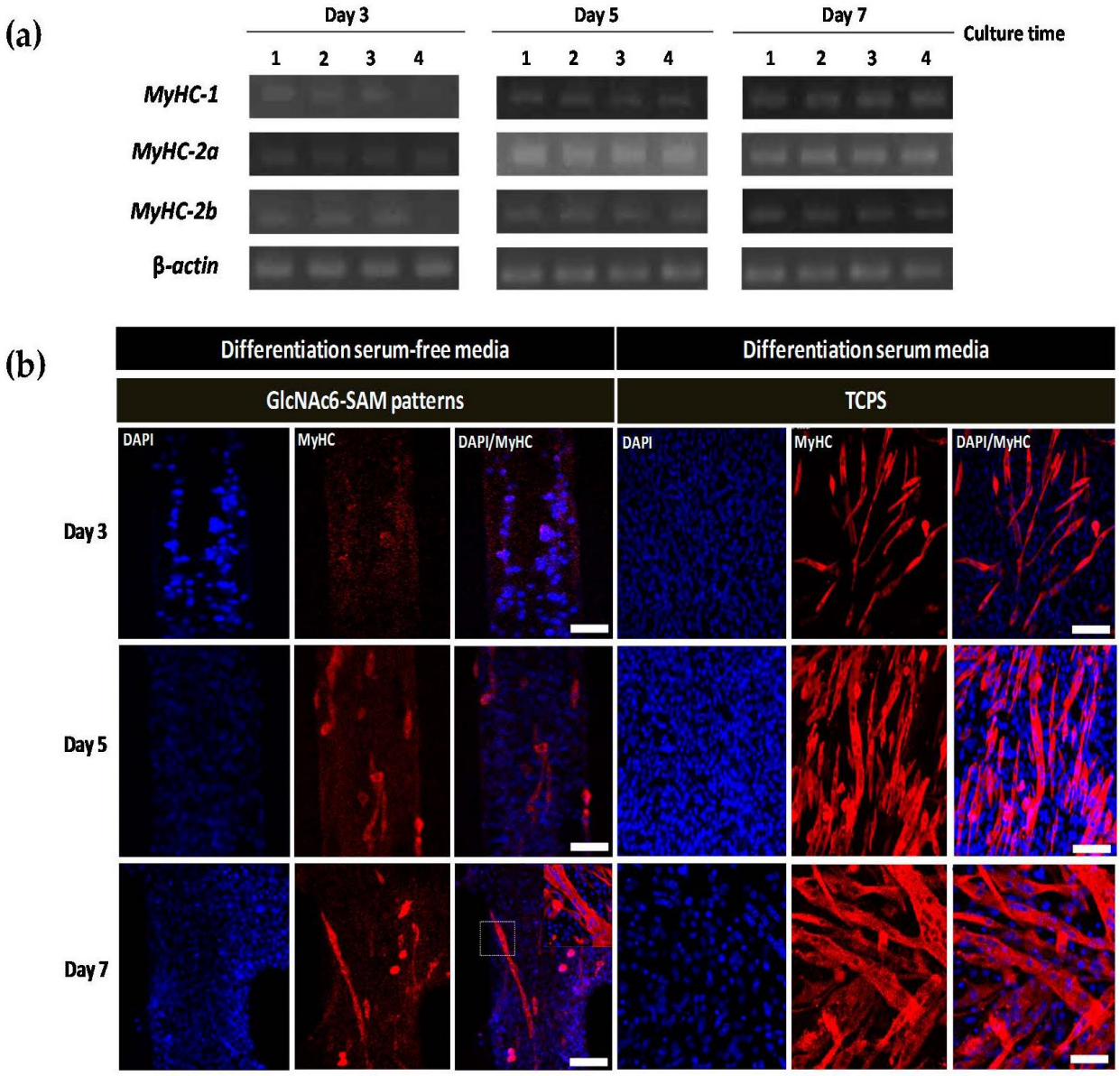
(a)
Day 3
Day 5
Day 7
Culture time
1 2 3 4
1 2 3 4
1 2 3 4
MyHC-1
MyHC-2a
MyHC-2b
β-actin
(b)
Differentiation serum-free media
Differentiation serum media
GlcNAc6-SAM patterns
TCPS
DAPI
MyHC
DAPI/MyHC
DAPI
MyHC
DAPI/MyHC
Day 3
Day 5
Day 7

Fig. 3-5 Cont.

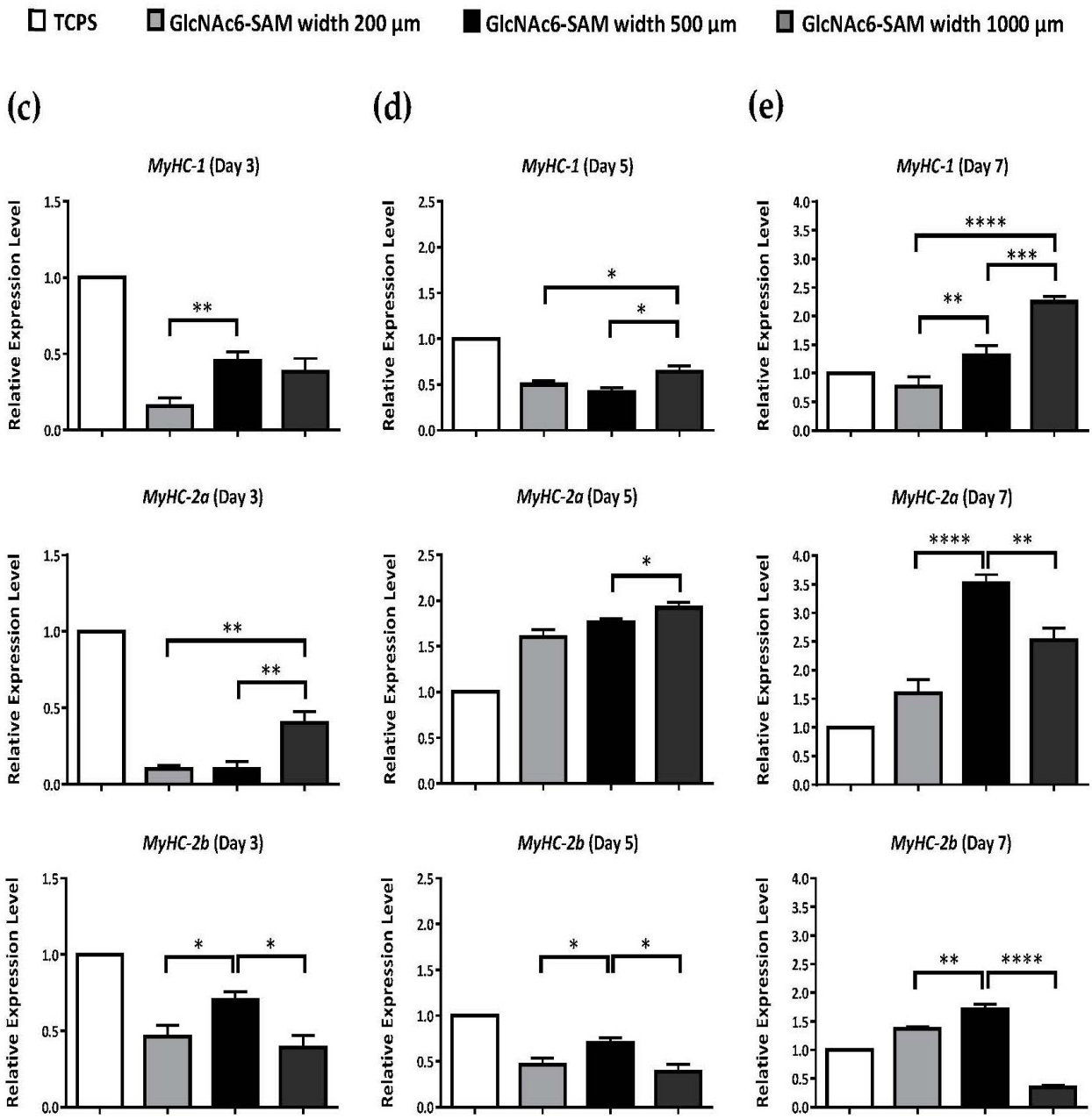

Fig. 3-5 Effects of micropatterned GlcNAc6-SAMs on myosin heavy chain (MyHC) expression in differentiated C2C12 cells at different culture time points in a differentiation serum-free medium. **a)** Representative quantitative real-time PCR products of *MyHC*s. The mRNA levels were normalized to β-*actin*. Lane 1: tissue culture polystyrene (TCPS); Lane 2: GlcNAc6-SAM pattern (200 µm); Lane 3: GlcNAc6-SAM pattern (500 µm); Lane 4: GlcNAc6-SAM pattern (1000 µm). **b)** Immunocytochemical staining of MyHCs on narrow patterns and control TCPS substrate in the absence and

presence of differentiation serum media, respectively. Myoblast fusion and myotube formation were found on GlcNAc6-SAM patterns after day 5 and 7 of culture, respectively. A close-up image of multinucleated myotubes is shown in the inset panel. At day 7, myotubes cultured on the GlcNAc6-SAM patterns under differentiation serum-free conditions demonstrated long and thin morphology when compared to those on the TCPS substrate under differentiation serum-containing conditions, which promoted the formation of thicker myotubes with numerous branched structures. Shown are confocal images of differentiated cells stained with anti-MyHC antibody to monitor myotube formation (red). DAPI was used to visualize nuclei (blue). Scale bars represent 200 μm. **c**–**e**) Individual *MyHC* mRNA expression profiles on various geometries. Values are the mean ± SEM, $n = 9$ per each sample. * $p < 0.05$, ** $p < 0.01$, *** $p < 0.001$ and **** $p < 0.0001$.

3.6 Summary

During *in vitro* differentiation, the biophysical cues of topographical features alter and regulate a variety of cellular processes. Many researches have given important evidence regarding the mechanisms and biomolecules that mediate myoblast fusion in skeletal muscle [48-50]. However, a complete understanding of the precise mechanisms that lead to the activation and recruitment, governing the fusion process, still remains enigmatic. Here, I determined the effects of GlcNAc6-SAM patterns on the mRNA expression of *MyHC* isoforms. MyHCs are the main determinants of the contractile properties of adult mammalian skeletal muscles, which have been associated with the stage of myotube formation [51,52]. Results showed that GlcNAc6 oligomers play a predominant role in the transition of primitive myoblasts into myotubes by concomitant drastic reorganization of actin filaments and the contractile capabilities of cells. A significant difference in the morphological changes of cells on GlcNAc6-SAM patterns was observed after 3–7 days of initial seeding. The initial formation of nascent myotubes, which is referred to as the second stage of myoblast fusion, was found at day 5. Subsequently, myoblasts were fused with nascent myotubes into multinucleated myotubes along with high spatial regulation of aligned myoblasts at day 7. In addition, the type of *MyHC* isoform expressed was predominantly dependent on the width of the GlcNAc6-SAM patterns. Narrow patterns tended to regulate *MyHC* type 2, whereas *MyHC* type 1 was profoundly expressed on the wide pattern. Based on these findings, I conclude that GlcNAc6-SAM patterns play a pivotal role by being an intermediate regulator in modulating myoblast fusion.

References

1. Tortorella, L.L.; Pilch, P.F. C2C12 myocytes lack an insulin-responsive vesicular compartment despite dexamethasone-induced GLUT4 expression. *Am. J. Physiol. Endocrinol. Metab.* **2002**, *283*, E514–E524.
2. Hindi, S.M.; Tajrishi, M.M.; Kumar, A. Signaling mechanisms in mammalian myoblast fusion. *Sci. Signal.* **2013**, *6*, re2, doi:10.1126/scisignal.2003832.
3. Kim, J.H.; Jin, P.; Duan, R.; Chen, E.H. Mechanisms of myoblast fusion during muscle development. *Curr. Opin. Genet. Dev.* **2015**, *32*, 162–170.
4. Luo, W.; Li, E.; Nie, Q.; Zhang, X. Myomaker, regulated by MYOD, MYOG and miR-140-3P, promotes chicken myoblast fusion. *Int. J. Mol. Sci.* **2015**, *16*, 26186–26201.
5. Rochlin, K.; Yu, S.; Roy, S.; Baylies, M.K. Myoblast fusion: When it takes more to make one. *Dev. Biol.* **2010**, *341*, 66–83.
6. Stern-Straeter, J.; Bran, G.; Riedel, F.; Sauter, A.; Hörmann, K.; Goessler, U.R. Characterization of human myoblast cultures for tissue engineering. *Int. J. Mol. Med.* **2008**, *21*, 49–56.
7. Stern-Straeter, J.; Riedel, F.; Bran, G.; Hörmann, K.; Goessler, U.R. Advances in skeletal muscle tissue engineering. *In Vivo* **2007**, *21*, 435–444.
8. Stevenson, E.J.; Koncarevic, A.; Giresi, P.G.; Jackman, R.W.; Kandarian, S.C. Transcriptional profile of a myotube starvation model of atrophy. *J. Appl. Physiol.* **2005**, *98*, 1396–1406.
9. Franke, J.; Abs, V.; Zizzadoro, C.; Abraham, G. Comparative study of the effects of fetal bovine serum *versus* horse serum on growth and differentiation of primary equine bronchial fibroblasts. *BMC Vet. Res.* **2014**, *10*, 119, doi:10.1186/1746-6148-10-119.
10. Das, M.; Rumsey, J.W.; Bhargava, N.; Stancescu, M.; Hickman, J.J. Skeletal muscle tissue engineering: A maturation model promoting long-term survival of myotubes, structural development of the excitation-contraction coupling apparatus and neonatal myosin heavy chain expression. *Biomaterials* **2009**, *30*, 5392–5402.
11. Stevenson, E.J.; Giresi, P.G.; Koncarevic, A.; Kandarian, S.C. Global analysis of gene expression patterns during disuse atrophy in rat skeletal muscle. *J. Physiol.* **2003**, *551*, 33–48.

12. Laurin, M.; Côté, J. Insights into the biological functions of Dock family guanine nucleotide exchange factors. *Genes Dev.* **2014**, *28*, 533–547.
13. Aguilar, P.S.; Baylies, M.K.; Fleissner, A.; Helming, L.; Inoue, N.; Podbilewicz, B.; Wang, H.; Wong, M. Genetic basis of cell-cell fusion mechanisms. *Trends Genet.* **2013**, *29*, 427–437.
14. Braun, T.; Gautel, M. Transcriptional mechanisms regulating skeletal muscle differentiation, growth and homeostasis. *Nat. Rev. Mol. Cell Biol.* **2011**, *12*, 349–361.
15. Zhang, Q.; Shi, X.E.; Song, C.; Sun, S.; Yang, G.; Li, X. BAMBI promotes C2C12 myogenic differentiation by enhancing Wnt/β-catenin signaling. *Int. J. Mol. Sci.* **2015**, *16*, 17734–17745.
16. Lam, M.T.; Sim, S.; Zhu, X.; Takayama, S. The effect of continuous wavy micropatterns on silicone substrates on the alignment of skeletal muscle myoblasts and myotubes. *Biomaterials* **2006**, *27*, 4340–4347.
17. Hosseini, V.; Ahadian, S.; Ostrovidov, S.; Camci-Unal, G.; Chen, S.; Kaji, H.; Ramalingam, M.; Khademhosseini, A. Engineered contractile skeletal muscle tissue on a microgrooved methacrylated gelatin substrate. *Tissue Eng. Part A* **2012**, *18*, 2453–2465.
18. Engler, A.J.; Griffin, M.A.; Sen, S.; Bönnemann, C.G.; Sweeney, H.L.; Discher, D.E. Myotubes differentiate optimally on substrates with tissue-like stiffness: Pathological implications for soft or stiff microenvironments. *J. Cell Biol.* **2004**, *166*, 877–887.
19. Boontheekul, T.; Hill, E.E.; Kong, H.J.; Mooney, D.J. Regulating myoblast phenotype through controlled gel stiffness and degradation. *Tissue Eng.* **2007**, *13*, 1431–1442.
20. Zatti, S.; Zoso, A.; Serena, E.; Luni, C.; Cimetta, E.; Elvassore, N. Micropatterning topology on soft substrates affects myoblast proliferation and differentiation. *Langmuir* **2012**, *28*, 2718–2726.
21. Huang, N.F.; Patel, S.; Thakar, R.G.; Wu, J.; Hsiao, B.S.; Chu, B.; Lee, R.J.; Li, S. Myotube assembly on nanofibrous and micropatterned polymers. *Nano Lett.* **2006**, *6*, 537–542.
22. Tran, T.H.; Shi, X.; Zaia, J.; Ai, X. Heparan sulfate 6-*O*-endosulfatases (Sulfs) coordinate the Wnt signaling pathways to regulate myoblast fusion during skeletal muscle regeneration. *J. Biol. Chem.* **2012**, *287*, 32651–32664.
23. Karagounis, L. G.; Hawley, J. A. Skeletal muscle: Increasing the size of the locomotor cell. *Int. J. Biochem. Cell Biol.* **2010**, *42*, 1376–1379.

24. Zierath, J. R.; Hawley, J. A. Skeletal muscle fiber type: Influence on contractile and metabolic properties. *PLoS Biol.* **2004**, *2*, e348.
25. Wang, Y. X.; Zhang, C. L.; Yu, R. T.; Cho, H. K.; Nelson, M. C.; Bayuga-Ocampo, C. R.; Ham, J.; Kang, H.; Evans, R. M. Regulation of muscle fiber type and running endurance by PPAR δ. *PLoS Biol.* 2004, *2*, e294.
26. Schiaffino, S.; Reggiani, C. Fiber types in mammalian skeletal muscles. *Physiol. Rev.* **2011**, *91*, 1447–1531.
27. Liu, Y.; Shen, T.; Randall, W. R.; Schneider, M. F. Signaling pathways in activity-dependent fiber type plasticity in adult skeletal muscle. *J. Muscle Res. Cell Motil.* **2005**, *26*, 13–21.
28. Bassel-Duby, R.; Olson, E. N. Signaling pathways in skeletal muscle remodeling. *Annu. Rev. Biochem.* **2006**, *75*, 19–37
29. Schiaffino, S. Fibre types in skeletal muscle: A personal account. *Acta Physiol.* **2010**, *199*, 451–463.
30. Spangenburg, E. E.; Booth, F. W. Molecular regulation of individual skeletal muscle fibre types. *Acta Physiol. Scand.* **2003**, *178*, 413–424.
31. Derave, W.; Ai, H.; Ihlemann, J.; Witters, L.A.; Kristiansen, S.; Richter, E.A.; Ploug, T. Dissociation of AMP-activated protein kinase slow-twitch muscle. *Diabetes* **2000**, *49*, 1281–1287.
32. Sandström, M.E.; Zhang, S.J.; Westerblad, H.; Katz, A. Mechanical load plays little role in contraction-mediated glucose transport in mouse skeletal muscle. *J. Physiol.* **2007**, *579*, 527–534.
33. Sakiyama, K.; Abe, S.; Tamatsu, Y.; Ide, Y.; Akiyama, K.S.; Be, S.A.; Amatsu, Y.T.; De, Y.I. Effects of stretching stress on the muscle contraction proteins of skeletal muscle myoblasts. *Biomed. Res.* **2005**, *26*, 61–68.
34. Chen, J.; Wang, D. Z. MicroRNAs in cardiovascular development. *J. Mol. Cell. Cardiol.* **2012**, *52*, 949–957.
35. Chakkalakal, J. V.; Kuang, S.; Buffelli, M.; Lichtman, J. W.; Sanes, J. R. Mouse transgenic lines that selectively label type I, type IIa, and types IIX+B skeletal muscle fibers. *Genesis* **2012**, *50*, 50–58.

36. Vicente-Manzanares, M.; Ma, X.; Adelstein, R.S.; Horwitz, A. R. Non-muscle myosin II takes centre stage in cell adhesion and migration. *Nat. Rev. Mol. Cell Biol.* **2009**, *10*, 778–790.
37. Vicente-Manzanares, M.; Koach, M. A.; Whitmore, L.; Lamers, M. L.; Horwitz, A. F. Segregation and activation of myosin IIB creates a rear in migrating cells. *J. Cell Biol.* **2008**, *183*, 543–554.
38. Parsons, J. T.; Horwitz, A. R.; Schwartz, M. a Cell adhesion: integrating cytoskeletal dynamics and cellular tension. *Nat. Rev. Mol. Cell Biol.* **2010**, *11*, 633–643.
39. Poosala, P.; Kitaoka, T. Chitooligomer-immobilized biointerfaces with micropatterned geometries for unidirectional alignment of myoblast cells. *Biomolecules* **2016**, *6*, 1–13.
40. Livak, K.J.; Schmittgen, T.D. Analysis of relative gene expression data using real-time quantitative PCR and the $2^{-\Delta\Delta C}{}_{\mathrm{T}}$ method. *Methods* **2001**, *25*, 402–408.
41. Torgan, C.E.; Daniels, M.P. Regulation of myosin heavy chain expression during rat skeletal muscle development *in vitro*. *Mol. Biol. Cell* **2001**, *12*, 1499–1508.
42. Staron, R.S.; Johnson, P. Myosin polymorphism and differential expression in adult human skeletal muscle. *Comp. Biochem. Physiol. B.* **1993**, *106*, 463–475.
43. Allen, D.L.; Leinwand, L.A. Postnatal myosin heavy chain isoform expression in normal mice and mice null for IIb or IId myosin heavy chains. *Dev. Biol.* **2001**, *229*, 383–395.
44. Lu, B.D.; Allen, D.L.; Leinwand, L.A.; Lyons, G.E. Spatial and temporal changes in myosin heavy chain gene expression in skeletal muscle development. *Dev. Biol.* **1999**, *216*, 312–326.
45. Swailes, N. T.; Colegrave, M.; Knight, P. J.; Peckham, M. Non-muscle myosins 2A and 2B drive changes in cell morphology that occur as myoblasts align and fuse. *J Cell Sci* **2006**, *119*, 3561–3570.
46. Langhammer, G.C.; Kutzing, K.M.; Luo, V.; Zahn, D.J.; Firestein, L.B. A Topographically modified substrate-embedded MEA for directed myotube formation at electrode contact sites. *Ann. Biomed. Eng*. **2013**, *41*, 408–420.
47. Clark, P.; Dunn, G.A.; Knibbs, A.; Peckham, M. Alignment of myoblasts on ultrafine gratings inhibits fusion *in vitro*. *Int. J. Biochem. Cell Biol.* **2002**, *34*, 816–825.
48. Millay, D.P.; O'Rourke, J.R.; Sutherland, L.B.; Bezprozvannaya, S.; Shelton, J.M.; Bassel-Duby, R.; Olson, E.N. Myomaker is a membrane activator of myoblast fusion and muscle formation. *Nature* **2013**, *499*, 301–305.

49. Gruenbaum-Cohen, Y.; Harel, I.; Umansky, K.B.; Tzahor, E.; Snapper, S.B.; Shilo, B.Z.; Schejter, E.D. The actin regulator N-WASp is required for muscle-cell fusion in mice. *Proc. Natl. Acad. Sci. USA* **2012**, *109*, 11211–11216.
50. Nowak, S.J.; Nahirney, P.C.; Hadjantonakis, A.K.; Baylies, M.K. Nap1-mediated actin remodeling is essential for mammalian myoblast fusion. *J. Cell Sci.* **2009**, *122*, 3282–3293.
51. Sebastian, S.; Goulding, L.; Kuchipudi, S.V; Chang, K. Extended 2D myotube culture recapitulates postnatal fibre type plasticity. *BMC Cell Biol.* **2015**, *16*, 1–10.
52. Miller, J.B.; Crow, M.T.; Stockdale, F.E. Slow and fast myosin heavy chain content defines three types of myotubes in early muscle cell cultures. *J. Cell Biol.* **1985**, *101*, 1643–1650.

Chapter 4

Chapter 4

Activation of Rho pathway

Rho family proteins are known to regulate the formation of distinct actin filament-based structures in several adherent cell types. In myoblast C2C12 cells, Rho pathway mediates the formation of stress fibers and focal adhesions, which is a key to modulate the myoblast fusion during myogenesis [1-5]. Therefore, this chapter will report the effect of clustering GlcNAc6 on the regulation of Rho pathway using quantitative real-time PCR.

4.1 Rho signaling pathway

Rho signaling pathway belongs to the Rho family of guanosine triphosphatases (GTPases). The Rho GTPases family plays crucial roles in the regulation of a wide range of cellular processes and the activation of downstream kinases, which make an impact on cellular mechanisms [6-10]. The classification of Rho GTPase family in mammalian cells has been classified into three subfamilies as Rho (RhoA, RhoB and RhoC), Rac (Rac1, Rac2 and Rac3) and CDC42 (Cell Division Cycle-42). The Rho is activated by a variety of extracellular, transmembrane and intracellular signaling molecules such as binary molecular switches for cycling between an active guanosine triphosphate (GTP)-bound state and an inactivate guanosine diphosphate (GDP)-bound state [11,12]. These processes are regulated by Guanine nucleotide exchange factors (GEFs) and GTPase activating proteins (GAPs) [13]. Activation of Rho pathway is associated with multiple specific downstream effectors, resulting in the regulation of the actin cytoskeleton assembly and organization, including cell proliferation, differentiation, and apoptosis as shown in Figure 4-1. In addition, the aforementioned effects, the Rho activation would consequently have been introduced with the contractile activity of cells through contraction-stimulated glucose uptake, possibly

through the correlation between the parallel orientation of myoblast and its rearrangement of actin filaments [14,15]. Furthermore, RhoA is one of the best-characterized members of the Rho family of GTPases as important regulators of myogenesis [16-18] and influences the trafficking of glucose transporter 4 (GLUT4) - a major glucose transporter, which has been identified and predominantly expressed in C2C12 myoblasts [19].

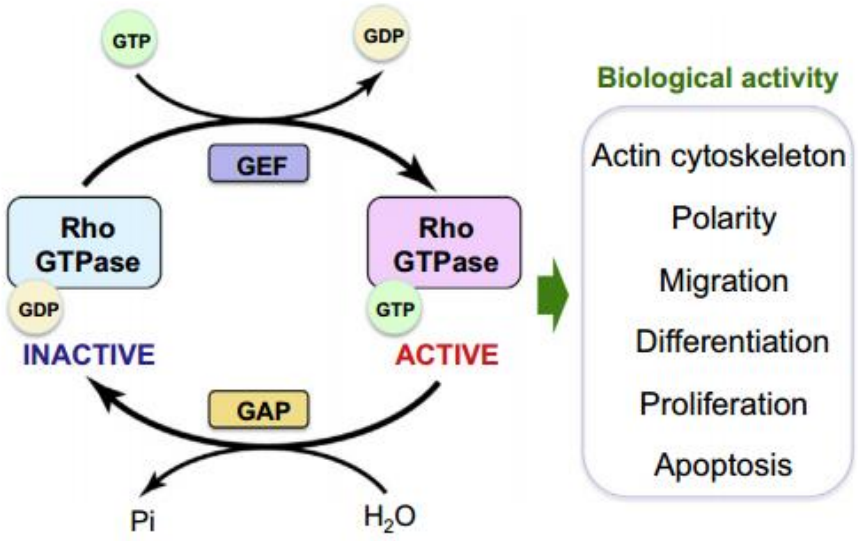

Fig. 4-1 Schematic representation of the Rho GTPases regulation and signaling functions. Upon activation by various stimuli, activated Rho GTPases transiently interact with multiple effector proteins to transduce signals for various cell functions. (Melendez, J.; Grogg, M.; Zheng, Y. Signaling role of Cdc42 in regulating mammalian physiology. *J. Biol. Chem.* **2011**, *286*, 2375–2381)

4.2 RhoA pathway roles in regulating cytoskeleton reorganization and stress fiber formation

Cells receive extracellular stimuli in various ways including interacting with cell-surface receptors as well as adhesive interactions with the extracellular matrix to form cell–cell adhesions. These stimuli act to generate changes in the actin cytoskeleton at specific sites primarily through Rho proteins [21]. Once activated, Rho GTPases bind to a variety of effectors, including protein kinases and some actin-binding proteins. These directly or indirectly affect the local assembly or disassembly of F-actin [22]. RhoA acts to initiate protrusive events in the lamellipodial region, a flat sheet-like region of a dense network of actin filament, and undergoes retrograde flow towards the cell body. Subsequently actomyosin stress fibers, which are stiff actin bundles associated with myosin-based contractility that terminate in focal adhesions, can be arranged orthogonal to the cell edge as depicted in Figure 4-2

In addition, RhoA signaling not only is modulated by cell-ECM adhesion, but also acts as an important regulator of adhesion. Adhesion to the ECM involves numerous interrelated processes including integrin binding to form large structures known as focal adhesions. A recent study has shown that GTPase RhoA-activated cells have highly activated focal adhesion and actin organization on the micropatterned substrate compared to cells cultured on the planar substrate *via* the RhoA-ROCK-MLCK (myosin II) pathway [23]. This suggested that the formation and maturation of focal adhesion, focal adhesion kinase (FAK) phosphorylation and polymerization of the actin cytoskeleton were all affected by the topography. Besides, it has been reported that RhoA-ROCK mediated cytoskeletal tension appears to limit the degree to which cells spread and is critical for focal adhesion maturation and signaling, and ROCK-generated tension which shows the feedback to regulate RhoA [24-27]. The possible existence of that feedback effects and presumably the feedforward regulatory loops would play a significant role in how cells adaptively alter adhesion, morphology, and mechanics in response to their ECM environment.

As mentioned above, although RhoA was initially shown to have a role in cytoskeletal remodeling, it is also well-known that RhoA are involved in several other cellular processes such as membrane trafficking, transcriptional activation and cell growth control including cellular motility [29,30]. The signal transduction pathways mediating these biological phenomena appear to be complex and interwoven as shown in Figure 4-3. However, understanding the signaling

pathways and the function of Rho family members *in vitro* on glyco-substrate remain unclear. It will be a major challenge in the future to establish studies related to their physiological relevance and to dissect the diverse downstream signaling pathways of Rho GTPases.

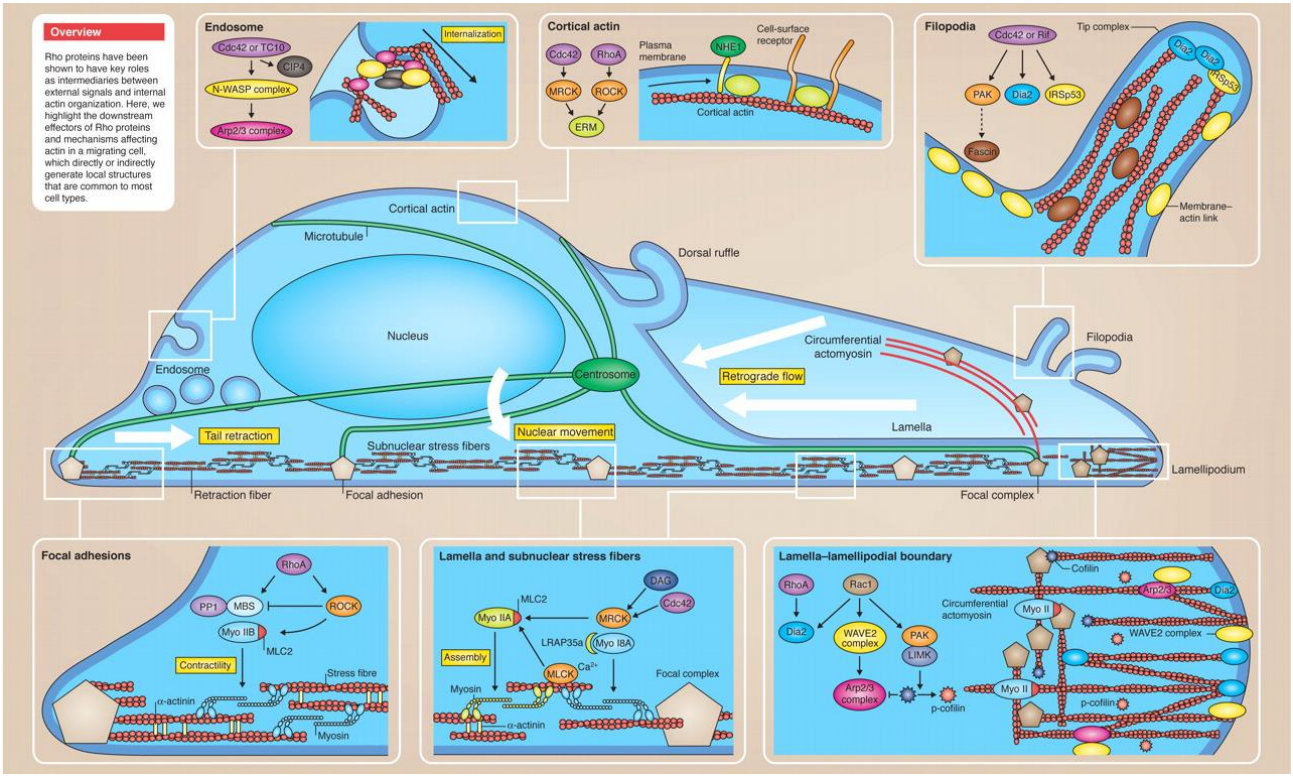

Fig. 4-2 Rho GTPases and their role in organizing the actin cytoskeleton. (Sit, S.-T.; Manser, E. Rho GTPases and their role in organizing the actin cytoskeleton. *J. Cell Sci.* **2011**, *124*, 679–683)

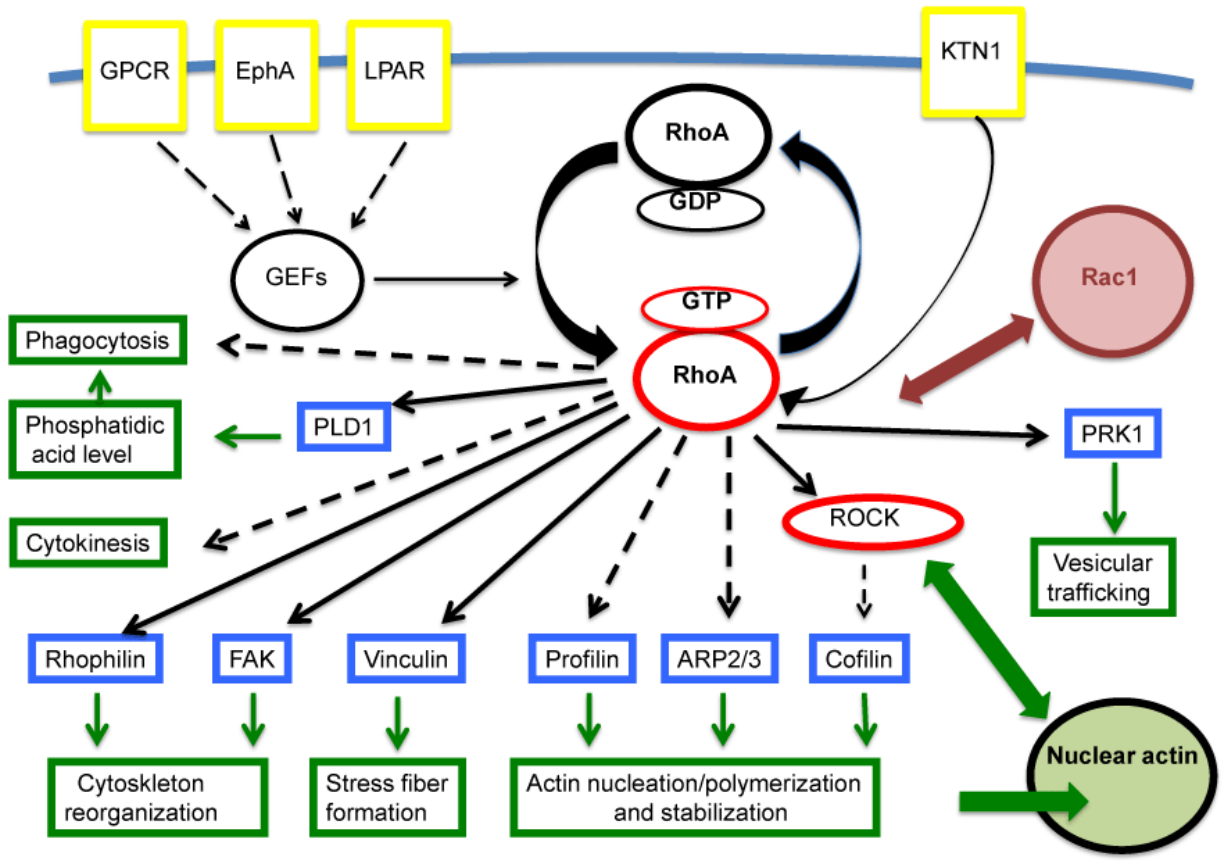

Fig. 4-3 RhoA pathway roles in actin cytoskeleton-related cell functions. The RhoA switch between inactive RhoA-GDP and active RhoA-GTP form is induced by various extracellular signals and receptors (yellow boxes) acting indirectly *via* GEFs. Activated RhoA regulates various cellular processes (green boxes) though proteins (blue boxes) and ROCK kinase effectors. (Kloc, M.; Li, X. C.; Ghobrial, R. M. RhoA Cytoskeletal Pathway to Transplantation. *J. Immunol. Clin. Res.* **2014**, *2*, 25–27)

4.3 Materials and Method

4.3.1 Materials

Please see in the chapter 2, section 2.4.1

4.3.2 Cell Culture Assay

Please see in the chapter 3, section 3.4.3

4.3.3 RhoA activation assay

The RhoA expression in C2C12 cells was assessed by the following manufacturer's instructions. In brief, C2C12 cells were grown to confluence on control and GlcNAc6-SAMs with and without patterns for 7 days, the medium was replaced with DMEM supplemented with 1% FBS and cultured for 24 h, and serum-starved for 24 h. 1µg/ml of RhoA activator II (CN03; Cytoskeleton, Denver, Colorado, USA) in warm DMEM was applied and then incubated for 3 h at 37 °C and 5% CO_2. The mechanism of Rho Activator II started when it enters into the cell and activates Rho GTPase isoforms by deamidating glutamine-63, which is located at the switch II region of these GTPases. This modification converts glutamine-63 to glutamate, which blocks intrinsic and GAP stimulated GTPase activity resulting in constitutively active Rho. This Rho Activator II robustly increases the level of GTP bound RhoA.

4.3.4 Real time quantitative PCR

Total RNA was isolated from cell preparations using ISOGEN (*Nippon Gene* Co., Ltd., Toyama, Japan) according to the manufacturer's instructions. The purity and concentration of each RNA preparation was assessed using a NanoDrop™ 1000 spectrophotometer and Experion (Bio-Rad Laboratories Inc., Hercules, CA, USA), consisting of a 20 ng cDNA template, 10 µM of forward and reverse primers, and fast in 10 µL of SYBR Green Master Mix (Applied Biosystems™, Life Technologies, New York, NY, USA). The primer sequences of each gene *RhoA* and *GAPDH* were designed by the primer 3 plus software and blasted in the NCBI PubMed primer blast software. 5′ CCGTGTTCCTACCCCCAATG 3′ and reverse primer: 5′ AAGCCC AGCTCTCCCCATA 3′ for *GAPDH*, and forward primer: 5′ GCCTCTCTCTTATCCAGACACC 3′ and reverse primer: 5′GACAGAAA TGCTTGACTTCTGGAG for *RhoA*. Amplification and

quantification of mRNA were performed at 95 °C for 20 s, followed by 3 s at 95 °C, and 30 s at 60 °C for 40 cycles.

4.3.5 Statistical analysis

Bioassay data of individual samples were separately analyzed in triplicate using GraphPad Prism Version 6.0 (GraphPad Software, Inc., La Jolla, CA, USA). Data are expressed as the mean ± SEM. Statistical differences between two groups were evaluated using an independent *t*-test. Statistical significance is indicated by *p*-values of: * $p < 0.05$, ** $p < 0.01$, *** $p < 0.001$ and **** $p < 0.0001$.

4.4 Results and Discussion

4.4.1 Topographical features of GlcNAc6-SAMs activate RhoA

RhoA is an integral part of the skeletal muscle differentiation pathway and plays an obligatory role during myogenic induction through muscle-regulatory factors (MRFs), thereby promoting myogenin expression and subsequent differentiation in myoblast cell lines. Additionally, RhoA controls a variety of cytoskeleton-dependent cell functions such as actin cytoskeleton organization, microtubule dynamics, membrane transport, cell polarity, and transcriptional activity [32-34].

The role of GlcNAc6-SAM substrates on expression and activation of RhoA during myoblast differentiation was determined. Since C2C12 cells reached confluence and were well aligned along the entire substrates, we compared the relative mRNA levels at day 7 of culture between two groups of samples with absence and presence of RhoA activator as described in unstimulated and stimulated cells, respectively. At the beginning, we investigated Rho activation on two different geometries, denoted as micropatterned and non-patterned with and without GlcNAc6-SAMs on substrates. *RhoA* has been identified in either unstimulated or stimulated C2C12 cells. Interestingly, mRNA expression levels of *RhoA* in stimulated cells are extremely low, as compared to control (TCPS) and unstimulated cells on overall substrates (Fig. 4-4). Despite this finding is still enigmatic in this stage, however, there is a possibility that the overexpression of constitutively active *RhoA* gene by activator might induce actin depolymerization, leading to prevent the formation of F-actin fibers and also reduce attachment of the cells to substrate. We next further examined *RhoA* expression on restriction patterns which were characterized by determining in widths of 200, 500 and 1000 μm of GlcNAc6-SAMs. The predominant effect of *RhoA* expression was found on GlcNAc6-SAM narrow pattern, having a 500 μm width in unstimulated cells (Fig. 4-5). This indicated that GlcNAc6 residues would act to accelerate the activity of G-proteins by increasing the conversion of GEF bound to GTP in exchange cycles, which can then active a new GTPase. This result leads to an increase the level of active Rho GTPase. It seems likely that the acceleration of Rho GTPase, which is regulated by GlcNAc6 residues would undergo faster than that of the Rho activator. Furthermore, toprographic micropatterns regulate cytoskeleton rearrangement *via* cell tension signaling cascades would play

a vital role in activation of *RhoA* according to reported data which involved in the alignment of actin filament (chapter 2, section 2.5.3).

In addition, the intensities of PCR bands in unstimulated cells were stronger than those of others have been shown for the stimulated cells on any different types of substrates. Taken together, these data indicated that the interaction with GlcNAc6-SAMs is very important for altering Rho activation *in vitro* and concomitantly leading to myotube formation while being conducted for myogenesis induction. Nevertheless, further investigations are required to gain a better understanding how GlcNAc6 residues can activate *Rho* gene expression and allow the cells to compensate for the inhibition of actin stress fiber formation independently from Rho Activators. The Rho-associated kinase ROCK (Rho/ROCK) signaling would be a great candidate to elucidate the intracellular mechanisms which regulate the crosstalk between myoblast proliferation and differentiation during myogenesis. Because ROCK has been identified as a direct effector of RhoA in myoblast fusion and demonstrated as major downstream targets to control cellular functions [35-37].

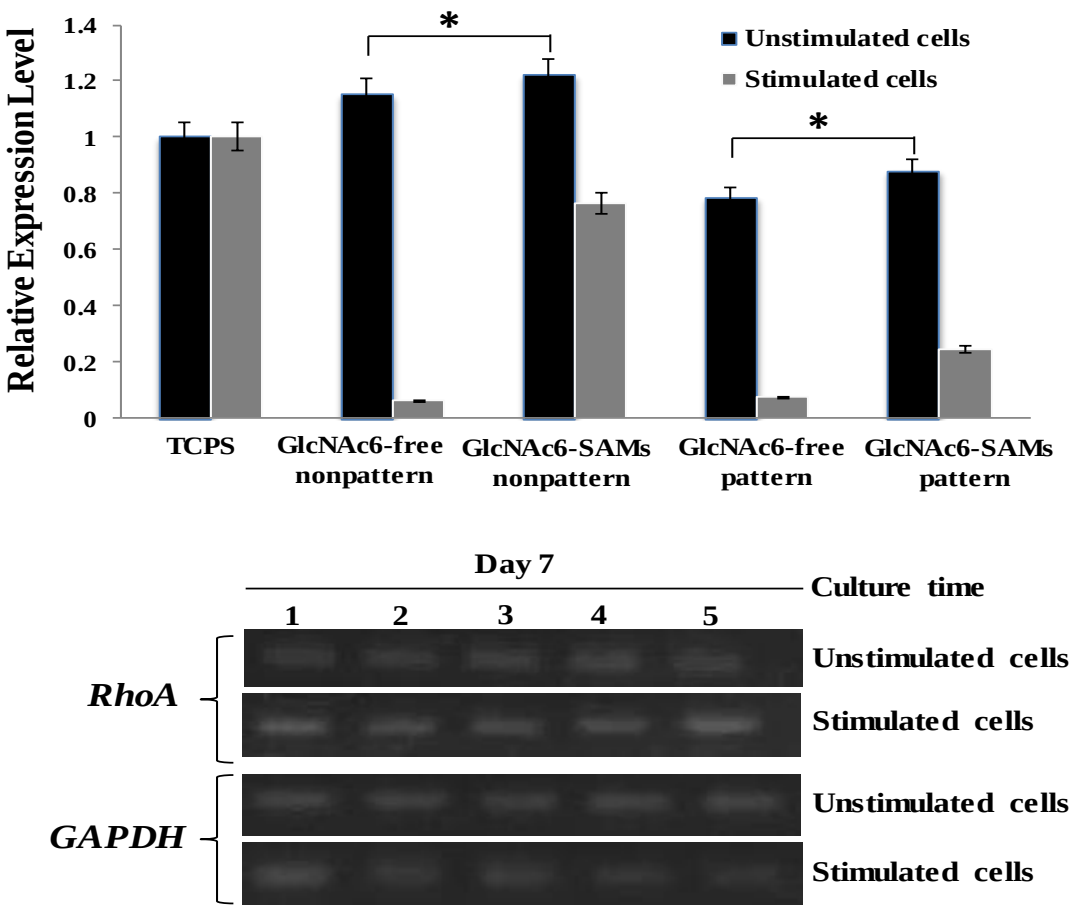

Fig. 4-4 Clustered carbohydrates and geometric patterns induced *RhoA* expressions. Comparison of an individual mRNA expression profile in unstimulated and stimulated myoblast C2C12 cells on the different substrates. PCR products were detected on a 2% agarose gel by ethidium bromide staining. Band intensities are presented as normalized values to GAPDH. Lane 1: TCPS, Lane 2: GlcNAc6-free nonpatterns, Lane 3: GlcNAc6-SAM nonpatterns, Lane 4: GlcNAc6-free patterns (500 μm) and Lane 5: GlcNAc6-free patterns (500 μm). Values are means ± standard error of mean. Statistically significant differences (n = 9 per sample); * $p < 0.05$; ** $p < 0.01$; *** $p < 0.001$ and **** $p < 0.0001$, by t-test.

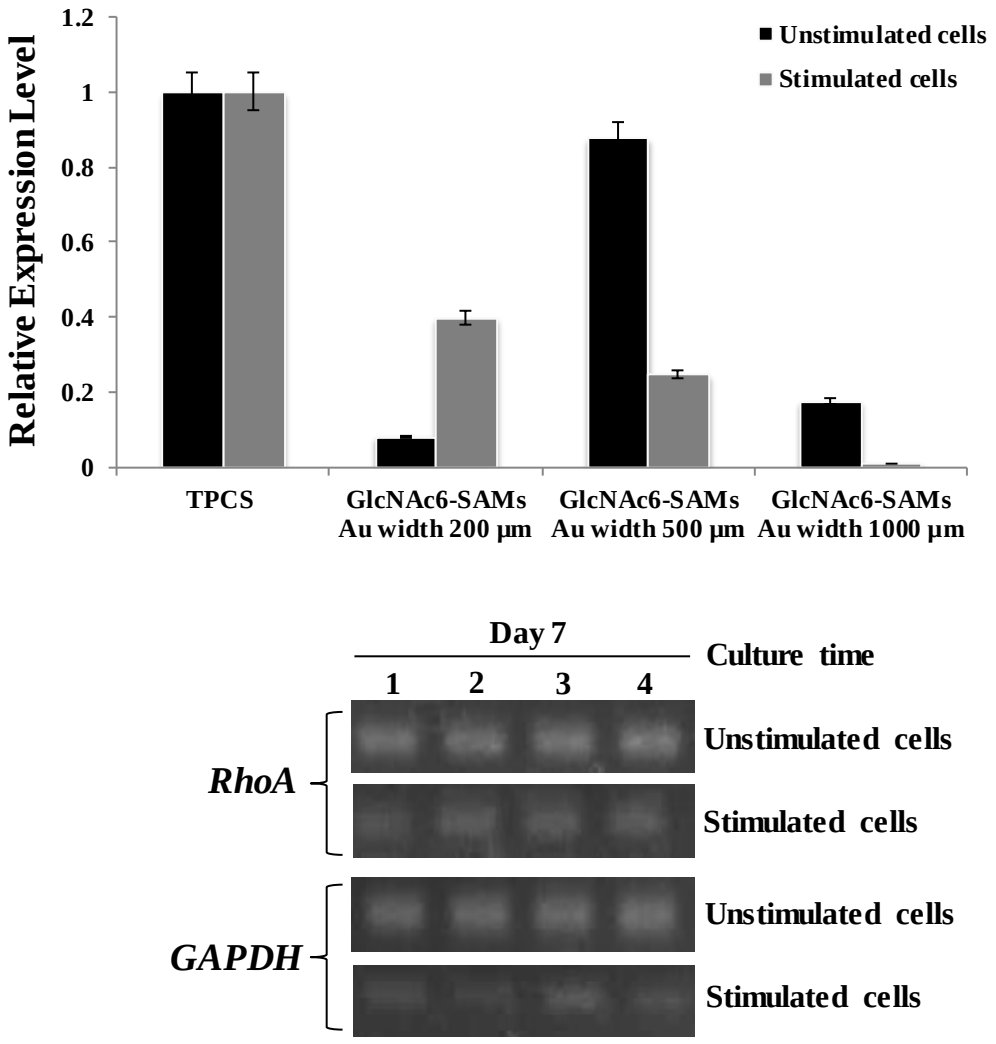

Fig. 4-5 Effect of GlcNAc6-SAM patterns with different geometries on *RhoA* expression. mRNA expression profile in unstimulated and stimulated myoblast C2C12. PCR products and band intensities were normalized to GAPDH. Lane 1: TCPS, Lane 2: GlcNAc6-SAM patterns (200 μm), Lane 3: GlcNAc6-SAM patterns (500 μm), Lane 4: GlcNAc6-SAM patterns (1000 μm).

4.5 Summary

In this work, I believe that Rho-family GTPases play critical roles in a major signaling pathway during myogenesis induction and myoblast fusion. This is because the Rho GTPases make an essential contribution to regulating cell adhesion, migration, cell proliferation and differentiation, particularly in skeletal myogenesis [38-41]. During a multistep process of myoblast fusion, actin cytoskeleton dynamics regulate the organization of the actin filaments, which subsequently control myoblast alignment and elongation. Results revealed that both unstimulated and stimulated cells on GlcNAc6-SAMs substrates showed higher mRNA expression level of *RhoA* than that of on GlcNAc6-free substrates. In addition, the predominant expression level of *RhoA* was found on the GlcNAc6-SAMs patterns, having 500 μm in width size. I anticipated that the direct binding of GlcNAc6 to integrin receptors on the cell surfaces to be an important factor in the modulation of mechanotransduction, which presumably occurs to trigger downstream signal pathways and *RhoA* expression. Subsequently, it acts as the driving force for actin polymerization, leading to changes in cell phenotype and cell behaviors, as well as the cell fate decision.

References

1. Meriane, M.; Roux, P.; Primig, M.; Fort, P.; Gauthier-Rouvière, C. Critical activities of Rac1 and Cdc42Hs in skeletal myogenesis: antagonistic effects of JNK and p38 pathways. *Mol. Biol. Cell* **2000**, *11*, 2513–2528.
2. Charrasse, S.; Meriane, M.; Comunale, F.; Blangy, A.; Gauthier-Rouvière, C. N-cadherin-dependent cell-cell contact regulates Rho GTPases and β-catenin localization in mouse C2C12 myoblasts. *J. Cell Biol.* **2002**, *158*, 953–965.
3. Iwasaki, K.; Hayashi, K.; Fujioka, T.; Sobue, K. Rho/Rho-associated kinase signal regulates myogenic differentiation via myocardin-related transcription factor-A/Smad-dependent transcription of the Id3 gene. *J. Biol. Chem.* **2008**, *283*, 21230–21241.
4. Kang, J. S.; Bae, G. U.; Yi, M. J.; Yang, Y. J.; Oh, J. E.; Takaesu, G.; Yi, T. Z.; Boon, C. L.; Krauss, R. S. A Cdo-Bnip-2-Cdc42 signaling pathway regulates p38 α/β MAPK activity and myogenic differentiation. *J. Cell Biol.* **2008**, *182*, 497–507.
5. Bryan, B. A.; Li, D.; Wu, X.; Liu, M. The Rho family of small GTPases: Crucial regulators of skeletal myogenesis. *Cell. Mol. Life Sci.* **2005**, *62*, 1547–1555.
6. Aznar, S.; Lacal, J. C. Rho signals to cell growth and apoptosis. *Cancer Lett.* **2001**, *165*, 1–10.
7. Olson, M. F.; Ashworth, a; Hall, a An essential role for Rho, Rac, and Cdc42 GTPases in cell cycle progression through G1. *Science* **1995**, *269*, 1270–1272.
8. Yamada, A.; Aiba, A.; Kamijo, R. Rho family small G proteins: Lessons from tissue-specific gene knockout studies. *J. Oral Biosci.* **2014**, *56*, 23–29.
9. Bishop, A. L.; Hall, A. Rho GTPases and their effector proteins. *Biochem. J.* **2000**, *348*, 241–255.
10. Nobes, C. D.; Hall, a Rho, rac, and cdc42 GTPases regulate the assembly of multimolecular focal complexes associated with actin stress fibers, lamellipodia, and filopodia. *Cell* **1995**, *81*, 53–62.
11. Travaglione, S.; Messina, G.; Fabbri, a; Falzano, L.; Giammarioli, a M.; Grossi, M.; Rufini, S.; Fiorentini, C. Cytotoxic necrotizing factor 1 hinders skeletal muscle differentiation in vitro by perturbing the activation/deactivation balance of Rho GTPases. *Cell Death Differ.* **2005**, *12*, 78–86.

12. Fritz, G.; Henninger, C. Rho GTPases: Novel Players in the Regulation of the DNA Damage Response? *Biomolecules* **2015**, *5*, 2417–2434.
13. Etienne-Manneville, S.; Hall, A. Rho GTPases in cell biology. *Nature* **2002**, *420*, 629–635.
14. Fulcher, F. K.; Smith, B. T.; Russ, M.; Patel, Y. M. Dual role for myosin II in GLUT4-mediated glucose uptake in 3T3-L1 adipocytes. *Exp. Cell Res.* **2008**, *314*, 3264–3274.
15. Satoh, T. Molecular mechanisms for the regulation of insulin-stimulated glucose uptake by small guanosine triphosphatases in skeletal muscle and adipocytes. *Int. J. Mol. Sci.* **2014**, *15*, 18677–18692.
16. Bryan, B. A.; Li, D.; Wu, X.; Liu, M. The Rho family of small GTPases: Crucial regulators of skeletal myogenesis. *Cell. Mol. Life Sci.* **2005**, *62*, 1547–1555.
17. Iwasaki, K.; Hayashi, K.; Fujioka, T.; Sobue, K. Rho/Rho-associated kinase signal regulates myogenic differentiation via myocardin-related transcription factor-A/Smad-dependent transcription of the Id3 gene. *J. Biol. Chem.* **2008**, *283*, 21230–21241.
18. Ridley, a J. Rho proteins: linking signaling with membrane trafficking. *Traffic* **2001**, *2*, 303–310.
19. Tortorella, L. L.; Pilch, P. F. C2C12 myocytes lack an insulin-responsive vesicular compartment despite dexamethasone-induced GLUT4 expression. *Am J Physiol Endocrinol Metab* **2002**, *283*, E514–524.
20. Melendez, J.; Grogg, M.; Zheng, Y. Signaling role of Cdc42 in regulating mammalian physiology. *J. Biol. Chem.* **2011**, *286*, 2375–2381.
21. Heasman, S. J.; Ridley, A. J. Mammalian Rho GTPases: new insights into their functions from in vivo studies. *Nat. Rev. Mol. Cell Biol.* **2008**, *9*, 690–701.
22. Zhao, Z.; Manser, E. PAK and other Rho-associated kinases--effectors with surprisingly diverse mechanisms of regulation. *Biochem. J.* **2005**, *386*, 201–214.
23. Seo, C. H.; Furukawa, K.; Montagne, K.; Jeong, H.; Ushida, T. The effect of substrate microtopography on focal adhesion maturation and actin organization via the RhoA/ROCK pathway. *Biomaterials* **2011**, *32*, 9568–9575.
24. Galbraith, C. G.; Yamada, K. M.; Sheetz, M. P. The relationship between force and focal complex development. *J. Cell Biol.* **2002**, *159*, 695–705.
25. Bhadriraju, K.; Yang, M.; Alom Ruiz, S.; Pirone, D.; Tan, J.; Chen, C. S. Activation of ROCK by RhoA is regulated by cell adhesion, shape, and cytoskeletal tension. *Exp. Cell*

Res. **2007**, *313*, 3616–3623.

26. Celeste, M. N.; Dana, M. P.; John, L. T.; Chen, S. C. Vascular endothelial-cadherin regulates cytoskeletal tension, cell spreading, and focal adhesions by stimulating RhoA. *Mol. Biol. Cell* **2004**, *15*, 2943–2953.
27. Truebestein, L.; Elsner, D. J.; Fuchs, E.; Leonard, T. A. A molecular ruler regulates cytoskeletal remodelling by the Rho kinases. *Nat. Commun.* **2015**, *6*, 10029.
28. Sit, S.-T.; Manser, E. Rho GTPases and their role in organizing the actin cytoskeleton. *J. Cell Sci.* **2011**, *124*, 679–683.
29. Hervé, J. C.; Bourmeyster, N. Rho GTPases at the crossroad of signaling networks in mammals. *Small GTPases* **2015**, *6*, 43–48.
30. Van Aelst, L.; D'Souza-Schorey, C. Rho GTPases and signaling networks. *Genes Dev.* **1997**, *11*, 2295–2322.
31. Kloc, M.; Li, X. C.; Ghobrial, R. M. RhoA Cytoskeletal Pathway to Transplantation. *J. Immunol. Clin. Res.* **2014**, *2*, 25–27.
32. Etienne-Manneville, S.; Hall, A. Rho GTPases in cell biology. *Nature* **2002**, *420*, 629–635.
33. Lu, B.D.; Allen, D.L.; Leinwand, L.A.; Lyons, G.E. Spatial and temporal changes in myosin heavy chain gene expression in skeletal muscle development. *Dev. Biol.* **1999**, *216*, 312–326.
34. Millay, D.P.; O'Rourke, J.R.; Sutherland, L.B.; Bezprozvannaya, S.; Shelton, J.M.; Bassel-Duby, R.; Olson, E.N. Myomaker is a membrane activator of myoblast fusion and muscle formation. *Nature* **2013**, *499*, 301–305
35. Castellani, L.; Salvati, E.; Alemà, S.; Falcone, G. Fine regulation of RhoA and Rock is required for skeletal muscle differentiation. *J. Biol. Chem.* **2006**, *281*, 15249–15257.
36. Bishop, A. L.; Hall, A. Rho GTPases and their effector proteins. *Biochem. J.* **2000**, *348*, 241–255.
37. Nishiyama, T.; Kii, I.; Kudo, A. Inactivation of Rho/ROCK signaling is crucial for the nuclear accumulation of FKHR and myoblast fusion. *J. Biol. Chem.* **2004**, *279*, 47311–47319.

38. Meriane, M.; Roux, P.; Primig, M.; Fort, P.; Gauthier-Rouvière, C. Critical activities of Rac1 and Cdc42Hs in skeletal myogenesis: Antagonistic effects of JNK and p38 pathways. *Mol. Biol. Cell* **2000**, *11*, 2513–2528.
39. Hakeda-Suzuki, S.; Ng, J.; Tzu, J.; Dietzl, G.; Sun, Y.; Harms, M.; Nardine, T.; Luo, L.; Dickson, B.J. Rac function and regulation during Drosophila development. *Nature* **2002**, *416*, 438–442.
40. Castellani, L.; Salvati, E.; Alemà, S.; Falcone, G. Fine regulation of RhoA and Rock is required for skeletal muscle differentiation. *J. Biol. Chem.* **2006**, *281*, 15249–15257.
41. Charrasse, S.; Comunale, F.; Fortier, M.; Portales-Casamar, E.; Debant, A.; Gauthier-Rouvière, C. M-cadherin activates Rac1 GTPase through the Rho-GEF Trio during myoblast fusion. *Mol. Biol. Cell* **2007**, *18*, 1734–1743.

Chapter 5

Chapter 5

GLUT4 and Glucose uptake

The activities of glucose transporter type 4 (GLUT4) are known to be regulated by a variety of mechanisms and one of them is transcriptional regulation. Understanding the molecular mechanisms governing GLUT4 gene expression is critical because it has been implicated in the control of glucose uptake in cells. In addition, there is a complex interplay between the mechanisms involved in *GLUT4* gene regulation and GLUT4 translocation in order to promote contraction-induced glucose transport activity [1-3]. In this chapter, characteristics of spontaneous contraction in mouse myoblast cells (C2C12) on carbohydrate-functionalized surface geometries will be discussed.

5.1 Glucose transporters type 4 (GLUT4)

Glucose transporters are a wide group of membrane proteins that facilitate the transport of glucose over a plasma membrane. Skeletal muscles contain at least three different isoforms of the glucose transporter. The glucose transporter type 4 isoform (GLUT4) belongs to the glucose transporter family which is mainly expressed in the skeletal muscle, adipose tissue, and heart [4,5]. GLUT4 is tissue-specific and subjected to metabolic control. The major mechanism responsible for glucose uptake in muscle is associated with the insulin-stimulated translocation of GLUT4 by the intracellular vesicles carrying GLUT4 and delivery it from a storage site to the plasma membrane [6]. This process is regulated by a cascade of signal transduction, which is initiated by the binding of insulin to insulin receptor on plasma membranes (The mechanism regulates GLUT4 will report in section 5.2). In addition, the level expression of GLUT4 has also

been associated with skeletal muscle fiber types and the level of glucose transport. Slow twitch fibers show a higher expression of GLUT4 as compared to fast twitch fibers [7,8]. Furthermore, the disruption of GLUT4 expression has been extensively associated with pathologies of impaired glucose uptake and insulin resistance such as type 2 diabetes and obesity [9]. This indicates that the regulation of GLUT4 in skeletal muscle would be useful in clinical and therapeutic application, especially in various metabolic disorders characterized by skeletal muscle insulin resistance.

5.2 Mechanism regulates GLUT4 translocation and glucose uptake

In muscle, several transcription factors and molecular signaling mechanisms are involved in regulating *GLUT4* gene expression and its translocation. The convergence of signaling pathways initiated by insulin and exercise (e.g. muscle contraction) has shown remarkable stimulation of GLUT4 translocation [10,11] as shown in Figure 5-1. In insulin-stimulated translocation of GLUT4, phosphatidylinositol 3-kinase (PI3K), insulin receptor substrate (IRS)-1 and Akt kinase are involved in transmitting signals for the translocation of GLUT4, resulting in uptake of glucose into the cells [12,13]. In contrast, studies have been reported that contractions cause the translocation of GLUT4 through a variety of upstream signaling pathway that ultimately leads to GLUT4 translocation such as AMPK, Ca^{2+}, and NOS including GTPases and cytoskeletal components [14-16] (Fig. 5-2).

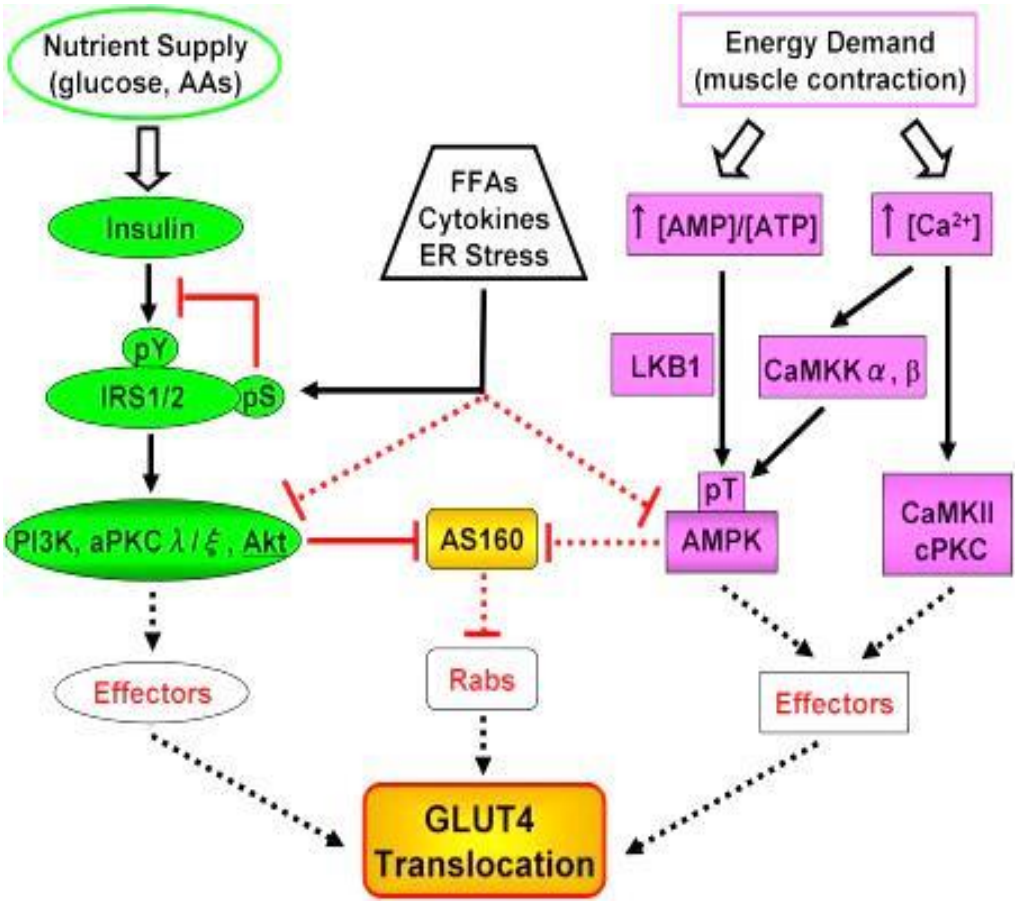

Fig. 5-1 Convergence of signaling pathways initiated by insulin and exercise leading to GLUT4 translocation. (Huang, S.; Czech, M. P. The GLUT4 Glucose Transporter. *Cell Metab.* **2007**, *5*, 237–252)

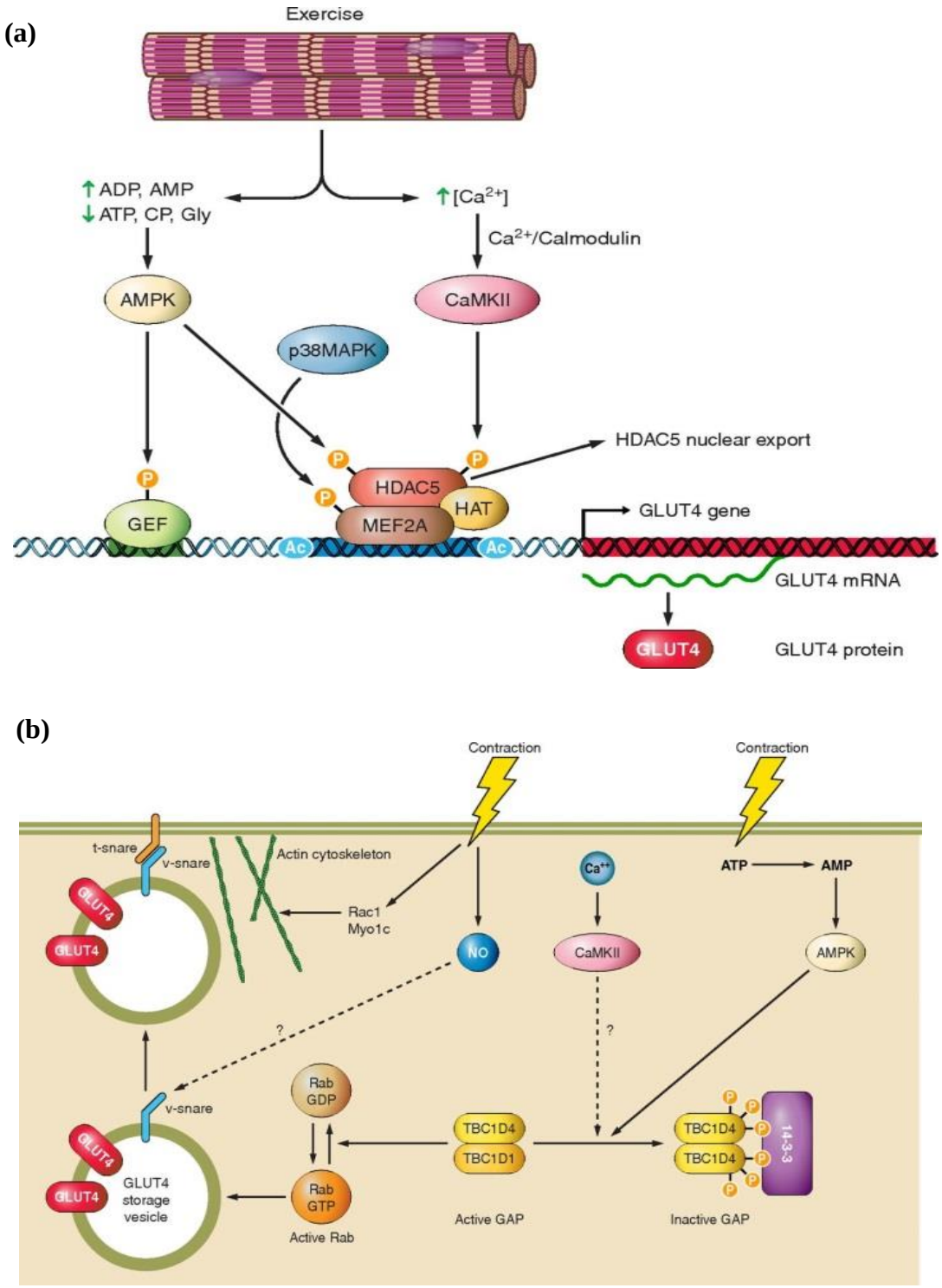

Fig. 5-2 Schematic of molecular signaling involved in **a)** contraction-induced *GLUT4* gene activation and **b)** GLUT4 translocation to the surface membrane. (Richter, E. a; Hargreaves, M. Exercise, GLUT4, and skeletal muscle glucose uptake. *Physiol. Rev.* **2013**, *93*, 993–1017)

5.3Materials and Method

5.3.1 Materials

Please see in the chapter 2, section 2.4.1

5.3.2 Cell culture assay

Please see in the chapter 3, section 3.4.3

5.3.3 Quantification of GLUT4 mRNA by real-time quantitative polymerase chain reaction (RT-PCR)

Please see in the chapter 3, section 3.4.4

5.3.4 Glucose uptake assay

The glucose uptake assay was carried out through measurement of the transport of accumulated 2-deoxy-D-glucose-6-phosphate (2-DG6P), which is proportional to 2-DG (or glucose) uptake by cells. C2C12 cells were cultured in 24-well plates for 5 or 7 days. After a 12-h serum starvation in DMEM, differentiated C2C12 cells were thoroughly rinsed three times with PBS, followed by incubation with Krebs-Ringer-Phosphate-HEPES (KRPH) buffer containing 2% bovine serum albumin (BSA) (KRPH: 20 mM Hepes, 5 mM KH_2PO_4, 1 mM $MgSO_4$, 1 mM $CaCl_2$, 136 mM NaCl, 4.7 mM KCl, pH 7.4) for 40 min. Then, the cells were stimulated with or without 1 μM insulin for 20 min in the presence of 10 mM 2-DG. The amount of glucose in the lysate was quantified using the Glucose-Uptake assay kit (ab136955, Abcam Inc., Cambridge, U.K.), and the absorbance values of samples were measured at 412 nm on an EnSight Multimode Plate Reader (PerkinElmer Inc., Waltham, MA, USA).

5.3.5 Statistical Analysis

Bioassay data of individual samples were separately analyzed in triplicate using GraphPad Prism Version 6.0 (GraphPad Software, Inc., La Jolla, CA, USA). Data are expressed as the mean ± SEM. Statistical differences between two groups were evaluated using an independent *t*-test. Statistical significance is indicated by *p*-values of: * $p < 0.05$, ** $p < 0.01$, *** $p < 0.001$ and **** $p < 0.0001$.

5.4 Results and Discussion

5.4.1 Hexa-*N*-acetyl-D-glucosamine (GlcNAc6)-self-assembled monolayers (SAMs) regulate glucose transporter type 4 (GLUT4) mRNA expression

GLUT4 expression is highly regulated in muscle cells. The translocation of GLUT4 to the plasma membrane surface is activated independently by an insulin-stimulated signaling pathway or cell contraction [19,20]. In this study, I investigated the mRNA expression level of *GLUT4* at 5 and 7 days of culture on designated GlcNAc6-SAM patterns with different widths. *GLUT4* was extremely high detected at day 5 on the GlcNAc6-SAM pattern (500 μm; Fig. 5-3a). Furthermore, the expression levels on patterns of 200 and 1000 μm were slightly higher than those on the control substrates. Nevertheless, *GLUT4* expression was substantially reduced at day 7, and the amount of mRNA was hardly detected. Interestingly, elevation in glucose uptake and reduction in *GLUT4* mRNA levels at day 7 seem plausible with regard to changes in *MyHC* type 2 expression, which is possibly relevant to fast-twitch muscle fibers. I speculated that GlcNAc6 oligomers on patterns induced conformational changes in the cross-bridge action where myosin-binding sites on actin molecules result in enhanced myosin ATP concentration and contraction velocity. An increase in contraction speed is presumably responsible for releasing intracellular *GLUT4* vesicles through depletion of *GLUT4* mRNA levels, leading to increased regulation of GLUT4 translocation and trafficking to the cell membrane to facilitate glucose transport [21–23]. This implies that metabolic feedback signals and mechanical stress-activated signals are sufficient to elicit the full contraction glucose transport response during cell contraction [24].

Besides, I found that the role of glucose uptake into cells depended on the width of the patterns. Particularly, the GlcNAc6-SAM pattern with a 500-μm width showed significantly higher 2-DG uptake than that of other substrates and the control. Furthermore, I compared the 2-DG uptake in the presence or absence of insulin in myoblasts on GlcNAc6-SAM patterns. Insulin stimulates glucose uptake in muscle cells through activation of the translocation of GLUT4-containing vesicles from the cytosol to the plasma membrane through a protein phosphorylation cascade [25,26]. Results showed that the narrow micropatterns improved the glucose uptake (Fig. 5-3a,b). This indicated that GlcNAc6-SAM patterns directly stimulated glucose transport through

an unknown mechanism, which is different from insulin-independent pathways during cell-induced contraction. Taken together, these findings suggest that the established GlcNAc6-SAM patterns have a strong influence on inducing myoblast differentiation into myotubes without using any differentiation medium.

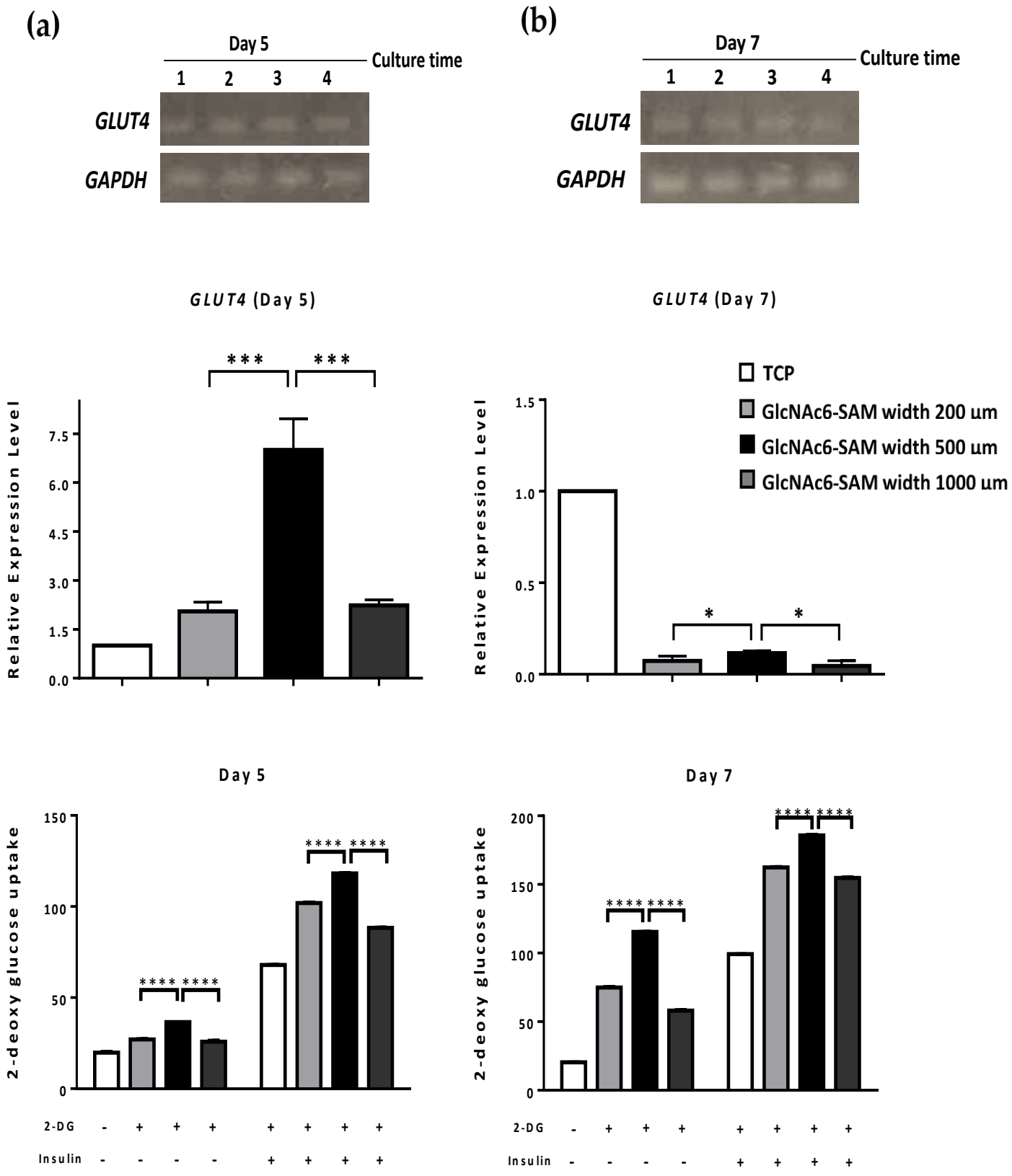
(a)
Day 5
Culture time
1 2 3 4
GLUT4
GAPDH
(b)
Day 7
Culture time
1 2 3 4
GLUT4
GAPDH
GLUT4 (Day 5)
Relative Expression Level
***
***
GLUT4 (Day 7)
TCP
GlcNAc6-SAM width 200 um
GlcNAc6-SAM width 500 um
GlcNAc6-SAM width 1000 um
Relative Expression Level
*
*
Day 5
2-deoxy glucose uptake
****
****
****
****
2-DG
Insulin
Day 7
2-deoxy glucose uptake
****
****
****
****
2-DG
Insulin

Fig. 5-3 Micropatterned GlcNAc6-SAMs induce *GLUT4* mRNA expression in differentiated C2C12 cells through contraction-dependent glucose uptake. Myoblasts were stimulated with (+) or without (-) 1 µM insulin, and glucose uptake rates were measured. Data were obtained after **a**) five days and **b**) seven days. Results are presented as the mean ± standard error of the mean (SEM) from triplicate measurements and are representative of three independent experiments. Lane 1: tissue culture polystyrene (TCPS); Lane 2: GlcNAc6-SAM pattern (200 µm); Lane 3: GlcNAc6-SAM pattern (500 µm); Lane 4: GlcNAc6-SAM pattern (1000 µm). Values were analyzed by the *t*-test, * $p < 0.05$, *** $p < 0.001$ and **** $p < 0.0001$.

5.5 Summary

Glucose transporters type 4 (GLUT4) is identified as the key glucose transporter isoform responsible for insulin- and contraction-stimulated glucose transport in skeletal muscle. In this study, the presence of spontaneous contractile activity in cultured myotubes on GlcNAc6-SAM patterns was confirmed through *GLUT4* mRNA expression and glucose uptake. I highlighted the synergistic effect of combining microscale topographical patterns and surface chemical functionality using chitooligomers with bioactive motifs on the development of structured myoblast cultures under differentiation medium-free conditions. Data clearly demonstrated that carbohydrate-functionalized micropatterns induced transcriptional activation of *GLUT4* genes, which results in the regulation of numerous downstream signaling pathways related to myoblast fusion and myotube contractions. In addition, I found that the molecular mechanisms controlling muscle plasticity are highly dependent on narrow GlcNAc6-SAM patterns during the fusion process. Interestingly, the 500-µm narrow pattern manipulated myoblast fusion more effectively compared with the 200-µm pattern, as determined by the glucose uptake rate and the mRNA expression level of MyHCs. This indicated that the predominant factor in manipulating myoblast fusion on narrow patterns was driven by the GlcNAc6-mediated contraction and presumably the activation of Rho family proteins.

References

1. Birnbaum, M. J. Identification of a novel gene encoding an insulin-responsive glucose transporter protein. *Cell* **1989**, *57*, 305–315.
2. Charron, M. J.; Brosius, F. C.; Alper, S. L.; Lodish, H. F. A glucose transport protein expressed predominately in insulin-responsive tissues. *Proc. Natl. Acad. Sci. U. S. A.* **1989**, *86*, 25352–25359.
3. James, D. E.; Strube, M.; Muecdler, M.; Mueckler, M. Molecular cloning and characterization of an insulin-regulatable glucose transporter. *Nature* 1989, *338*, 83–87.
4. Im, S.-S.; Kwon, S.-K.; Kim, T.-H.; Kim, H.-I.; Ahn, Y.-H. Regulation of glucose transporter type 4 isoform gene expression in muscle and adipocytes. *IUBMB Life* **2007**, *59*, 134–145.
5. Kahn, B. B. Glucose transport: pivotal step in insulin action. *Diabetes* **1996**, *45*, 1644–1654.
6. Shepherd, P. R.; Kahn, B. B. Glucose transporters and insulin action–implications for insulin resistance and diabetes mellitus. *N. Engl. J. Med*. **1999**, *341*, 248–257.
7. Daugaard, J. R. J. R.; Richter, E. A. E. A. Relationship between muscle fibre composition, glucose transporter protein 4 and exercise training: possible consequences in non-insulin-dependent diabetes mellitus. *Acta Physiol. Scand.* **2001**, *171*, 267–276.
8. Albers, P. H.; Pedersen, A. J. T.; Birk, J. B.; Kristensen, D. E.; Vind, B. F.; Baba, O.; Nohr, J.; Hojlund, K.; Wojtaszewski, J. F. P. Human muscle fiber type-specific insulin signaling: Impact of obesity and type 2 diabetes. *Diabetes* **2015**, *64*, 485–497.
9. Karnieli, E.; Armoni, M. Transcriptional regulation of the insulin-responsive glucose transporter GLUT4 gene: from physiology to pathology. *Am. J. Physiol. Endocrinol. Metab.* **2008**, *295*, E38–E45.
10. Herman, M. A.; Kahn, B. B. Glucose transport and sensing in the maintenance of glucose homeostasis and metabolic harmony. *J. Clin. Invest.* **2006**, *116*, 1767–1775.
11. Rose, A. J.; Richter, E. a Skeletal muscle glucose uptake during exercise: how is it regulated? *Physiology (Bethesda).* **2005**, *20*, 260–270.
12. Vanhaesebroeck, B.; Alessi, D. R. The PI3K-PDK1 connection: more than just a road to PKB. *Biochem. J.* **2000**, *346 Pt 3*, 561–576.
13. Sarbassov, D. D.; Guertin, D. a; Ali, S. M.; Sabatini, D. M. Phosphorylation and

regulation of Akt/PKB by the rictor-mTOR complex. *Science* **2005**, *307*, 1098–1101.

14. Coderre, L.; Kandror, K. V; Vallega, G.; Pilch, P. F. Identification and characterization of an exercise-sensitive pool of glucose transporters in skeletal muscle. *J.Biol.Chem.* **1995**, *270*, 27584–27588.
15. Douen, A. G.; Ramlal, T.; Rastogi, S.; Rilan, P. J.; Cartee, G. D.; Vranie, M.; Holloszy, J. O.; Klip Exercise induces the recruitment of the "Insulin-responsive Glucose Transporter." *J. Biol. Chem.* **1990**, *265*, 13427–13430.
16. Lemieux, K.; Han, X. X.; Dombrowski, L.; Bonen, A.; Marette, A. The transferrin receptor defines two distinct contraction-responsive GLUT4 vesicle populations in skeletal muscle. *Diabetes* **2000**, *49*, 183–189.
17. Huang, S.; Czech, M. P. The GLUT4 Glucose Transporter. *Cell Metab.* **2007**, *5*, 237–252.
18. Richter, E. a; Hargreaves, M. Exercise, GLUT4, and skeletal muscle glucose uptake. *Physiol. Rev.* **2013**, *93*, 993–1017.
19. Manabe, Y.; Miyatake, S.; Takagi, M.; Nakamura, M.; Okeda, A.; Nakano, T.; Hirshman, M.F.; Goodyear, L.J.; Fujii, N.L. Characterization of an acute muscle contraction model using cultured C2C12 myotubes. *PLoS ONE* **2012**, *7*, e52592.
20. Michael, L.F.; Wu, Z.; Cheatham, R.B.; Puigserver, P.; Adelmant, G.; Lehman, J.J.; Kelly, D.P.; Spiegelman, B.M. Restoration of insulin-sensitive glucose transporter (*GLUT4*) gene expression in muscle cells by the transcriptional coactivator PGC-1. *Proc. Natl. Acad. Sci. USA* **2001**, *98*, 3820–3825.
21. Jensen, T.E.; Sylow, L.; Rose, A.J.; Madsen, A.B.; Angin, Y.; Maarbjerg, S.J.; Richter, E.A. Contraction-stimulated glucose transport in muscle is controlled by AMPK and mechanical stress but not sarcoplasmatic reticulum Ca^{2+} release. *Mol. Metab.* **2014**, *3*, 742–753.
22. Mu, J.; Brozinick, J.T.; Valladares, O.; Bucan, M.; Birnbaum, M.J. A role for AMP-activated protein kinase in contraction- and hypoxia-regulated glucose transport in skeletal muscle. *Mol. Cell* **2001**, *7*, 1085–1094.
23. Merry, T.L.; McConell, G.K. Skeletal muscle glucose uptake during exercise: A focus on reactive oxygen species and nitric oxide signaling. *IUBMB Life* **2009**, *61*, 479–484.
24. Ihlemann, J.; Ploug, T.; Hellsten, Y.; Galbo, H. Effect of tension on contraction-induced glucose transport in rat skeletal muscle. *Am. J. Physiol.* **1999**, *277*, E208–E214

25. Leney, S.E.; Tavaré, J.M. The molecular basis of insulin-stimulated glucose uptake: Signalling, trafficking and potential drug targets. *J. Endocrinol.* **2009**, *203*, 1–18.
26. Leto, D.; Saltiel, A.R. Regulation of glucose transport by insulin: Traffic control of GLUT4. *Nat. Rev. Mol. Cell Biol.* **2012**, *13*, 383–396.

Chapter 6

Chapter 6

General conclusions

This dissertation presents a novel strategy to develop a carbohydrate-based micropatterning technique which serves as a powerful tool for regulating cell behavior and cell fate. In this study, chitooligomers were successfully immobilized on the gold surface to form self-assembled monolayers (SAMs), and played an important role in controlling the cell adhesion and cellular alignment as well as cell fusion through the molecular recognition of clustered GlcNAc residues. Glyco-SAMs were formed on transparent Au micropatterns through site-selective S-derivatization of sugar reducing end groups with thiosemicarbazide (TSC). The determination of the chemical compositions on the glyco-SAM surfaces (e.g. carbon, oxygen and nitrogen) was investigated by XPS characterization. The data suggested that the elemental compositions remain unchanged over time, indicating the stability of chitooligomer-SAMs *via* covalent immobilization on nano-flat Au surfaces. The QCM measurement combined with XPS data was exploited in order to examine the adsorption of carbohydrate-TSC molecules on the Au surface. The results suggested that the carbohydrate molecules were successfully accumulated with high density on the Au surface.

Glyco-SAMs with comb-like micropatterns of different sizes in width affected biological behavior of mouse-derived myoblast C2C12 cells such as cell morphology, proliferation, differentiation and elongation, leading to unidirectional cellular alignment along the micropatterned lines. Such alignments occurred after seven days in culture adopting an appearance similar to muscle cells *in vivo*. The long-range self-organization of these myoblasts is required to organize muscle architecture aligned with neighboring tissues through contact guidance in order to exhibit proper muscle function. Based on these results, the underlying effects of microtopographical patterns consisting of non-reducing ends of GlcNAc6 oligomers

provide crucial insights into regulation of myoblast morphology and function, possibly involving carbohydrate-protein interactions. The integrin/FAK signaling pathway would play an essential role to promote actin filament formation, which has been shown to be required for myoblast differentiation, especially for cell migration and myotube formation through cell fusion.

Additionally, micropattern geometries of GlcNAc6-SAMs regulated myoblast fusion without adding any differentiation culture medium and demonstrated spontaneous contraction through various transient activations of fusion-related target genes. These results affected individual facets of myoblast behaviors and exhibited increased the level of fusion of mononucleated myoblasts into myotubes and alignment towards a preferential direction, as well as high expression of genes that involved in muscle contraction. Interestingly, these distinctive responses were predominantly associated with narrow patterns of GlcNAc6-SAMs. Based on these findings, I concluded that GlcNAc6 residues mediated fusion machinery during muscle development in a differentiation serum-free culture system. The architectural design of carbohydrate-based micropatterns *via* vectorial chain immobilization is expected to provide a new approach in a variety of applications, which opens up new doors for a novel concept in the development of the advanced biomedical engineering and regenerative medicine. For instance, the ability to control the direction of cell differentiation *in vitro* by changing the width of carbohydrate micorpatterns. However, further investigation is required, to identify the functions downstream of small Rho GTPases, which generally promote actin polymerization and drive the formation of actomyosin filament bundles, including the associated regulators that are involved in contraction. Metabolic markers, such as AMP-activated protein kinase, reactive oxygen species and mitochondrial biogenesis, also need to be investigated, to obtain a better understanding of the convergence of multiple signaling pathways that lead to the activation of the signaling mechanisms of myoblast fusion on geometrical carbohydrate micropatterns.

Future perspectives

Cell alignment widely exists in native tissues, playing a critical role in cell behaviors and providing necessary structure and physical properties for maintaining tissue functions. Although current studies have provided knowledge and valuable insight into engineering cell alignment through various approaches including mechanical loading, topographical patterning, surface chemical treatment and electrical stimulation, there are still several challenges that need to be addressed in the future. The studies in this dissertation have highlighted a simple and direct method to control the alignment and fusion of mouse-derived myoblast C2C12 cells through 2D micropatterning of glyco-decorated scaffolds, demonstrating that cells with the intrinsic potential to form aligned and differentiated into myotube-like morphology. In addition, controlled cellular alignment and cell behaviors were done without the need for any additional differentiation serum media. Thus, the combination of microengineering with glycan is applicable to be used as a model for investigating cellular events and elucidating the underlying molecular mechanism which is responsible for inducing cell function *in vitro*, including the possibility of creating tissue constructs with microscale control of 3D cellular alignment.

However, the future works should be more focused on realistic substrates with higher degree of biomimetic relevance to impose multidirectional cues within cellular microenvironment. Such novel substrates will enable addressing issues on how cells globally integrate biophysical signals from their surrounding microenvironment. Furthermore, another big challenge is that how to induce the alignment of different cell types (e.g. cardiac, nerve and epithelial cells) on glyco-SAM patterns and constructing them as *in vitro* disease models for high-throughput applications. These challenges with the advances in carbohydrate micropatterns would be an important step forward in cell biology, tissue engineering and regenerative medicine in the near future.

Publication lists

Poosala, P.; Kitaoka, T. Chitooligomer-Immobilized Biointerfaces with Micropatterned Geometries for Unidirectional Alignment of Myoblast Cells. *Biomolecules* **2016**, *6*, 12.

Poosala, P.; Ichinose, H.; Kitaoka, T. Spatial Geometries of Self-Assembled Chitohexaose Monolayers Regulate Myoblast Fusion. *Int. J. Mol. Sci.* **2016**, *17*, 68 6.